

# Chapter 3

## Cellular Neural Networks for Seismic Horizon Linking

### 3.1 Introduction

Seismic horizon linking is an important task in geophysical data processing. In this thesis, we design the algorithm based on cellular neural networks to link seismic horizons.

Linking seismic horizons can help us to recognize the geological structure underground. Several researchers had proposed the different methods of the detection of seismic horizons: Keskes had used the concept of ordering and the use of graphs to represent the spatial relation among objects extracted from seismic data in his horizon detection procedure [1]-[3]; Lu had used dynamic programming of string matching in the seismic skeletonization [4]; Cheng and Lu had used the binary consistency checking scheme and applied to seismic horizon detection [5]; Huang had used the branch and bound search to automatic linking process of seismic horizons [6].

### 3.2 The Brief Introduction of Gathering Seismic Data

The geophysical prospecting methods can help us to study and analyze the stratum structure [7]. The geophysical techniques most widely employed are the seismic, gravity, magnetic and electrical methods. Seismic and gravity prospecting are mainly tools for oil exploration; electrical methods are mainly used for mineral exploration. Magnetic methods are employed for both oil exploration and mineral exploration. Generally speaking, gravity prospecting offers the worse analysis of stratum. Electrical methods and magnetic methods are simple and convenient to do and with low costs, but they can't detect the deeper stratum.

Seismic reflection method is one kind geophysical prospecting method that has better analysis ability. It has already been applied to oil exploration for decades. The past twenty years, seismic reflection method was often used to study shallow stratum, which include the detection of groundwater, engineering foundation investigation, ..., etc.. The basic principle of seismic reflection method is summarized below.

Seismic reflection method is utilizing the artificial seismic source on the earth's surface to produce seismic wave. Seismic wave would be transmitted underground. If seismic wave reaches an interface between two formations having different velocity, it would reflect to the surface. And then seismic wave would be received by receivers on the ground, as Fig. 3.1 shows [7]. Then we can use computers to process these signals and enable these data to depict the structure of stratum.

The seismic wave is not reflected in accordance with the ideal horizontal stratum, so receivers receive not only one kind signal. The signal may include noise which is produced by seismic source, such as air wave, surface wave, refracted wave, ..., etc.. There are noises produced by environment at the same time, such as noises produced by cars or airplanes. In order to reduce these noises, we choose appropriate distance between seismic source and receivers according to the characteristic of each kind wave. In order to overcome the influence of noises, we adopt the technique of common depth point (CDP). CDP can raise signal-to-noise ratio. Its cardinal principle is summing multiple reflection signals which have the same reflection point and are in phase after proper travel-time correction. The summing of multiple reflection signals can increase the energy of reflection signals. And ambient noise not in phase would be canceled. So we can get higher signal-to-noise ratio. After removing noise, we find all traces of the same reflection; this is CDP gather, as Fig. 3.2 shows [7]. Besides travel-time correction, the other correction, called normal moveout (NMO), depends on depth (record time) to the reflecting horizon. NMO is defined as the increase in reflection time due to an increase in distance from source to receiver for a horizontal reflecting interface in a homogeneous medium of constant velocity. This correction converts a trace of offset distance into a zero-offset trace. Finally we stack these continuous CDP traces and then get the needed stratum section.

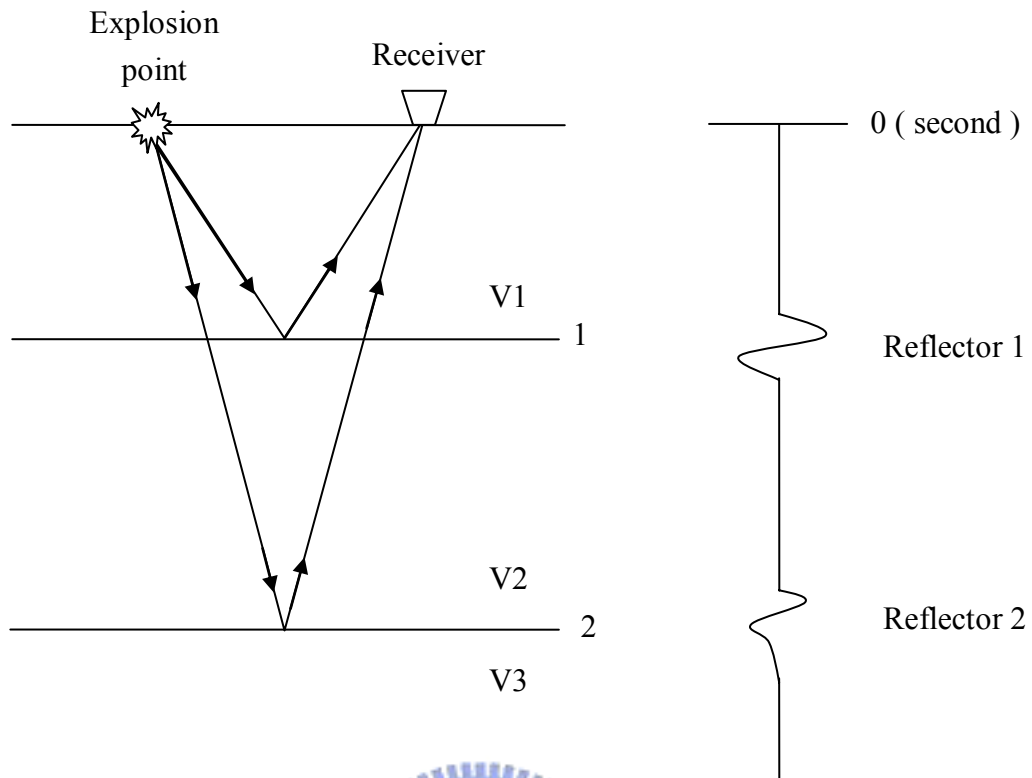


Fig. 3.1 The basic model of seismic source and receivers.

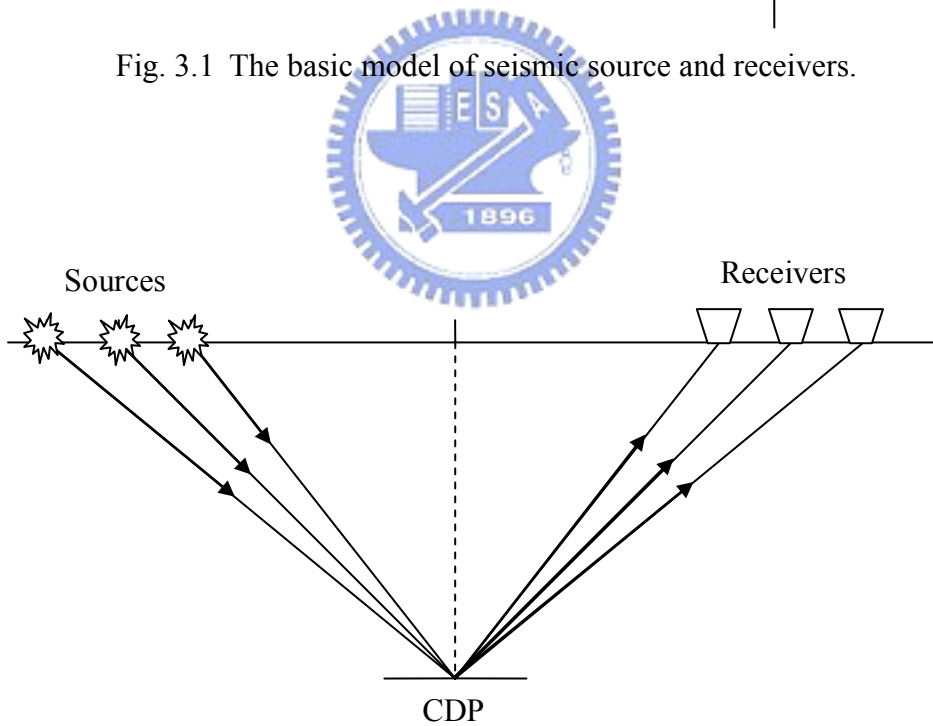


Fig. 3.2 Concept of CDP (Common Depth Point).

### 3.3 The Preprocessing of Seismic Data

The seismogram is generated from geologic model, and it is composed by many seismic traces. Every trace contains many peaks. We can extract horizons from peak data. So before linking seismic horizons, we have to preprocess the seismograms to get peak data. The seismogram passes through preprocessing in Fig. 3.3, which includes envelope, thresholding, peaking, and the compression in the vertical time-axis direction.

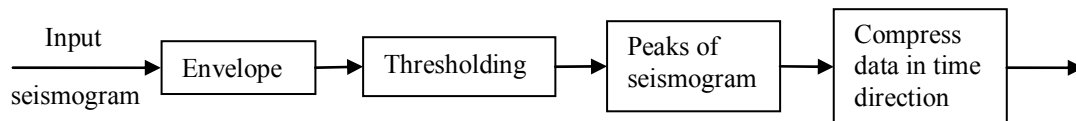
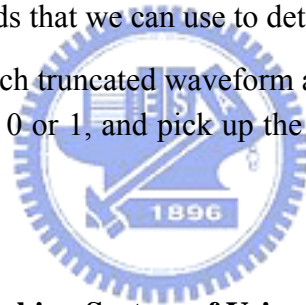


Fig. 3.3 The preprocessing steps of seismic data.

Envelope describes the outer shape of the wavelet. After thresholding, the value 1 represents the peak; the value 0 represents the nonpeak, one peak represents a wavelet. There are two methods that we can use to detect peaks on every trace [6]:

- (a) Locate the maximum of each truncated waveform as the peak.
- (b) Threshold the envelope to 0 or 1, and pick up the middle point at each interval as the peak.



### 3.4 The Seismic Horizon Linking System of Using Cellular Neural Networks

We use cellular neural networks to deal with the linking of seismic horizons [8]. Fig. 3.4 shows the block diagram of seismic horizon linking system.

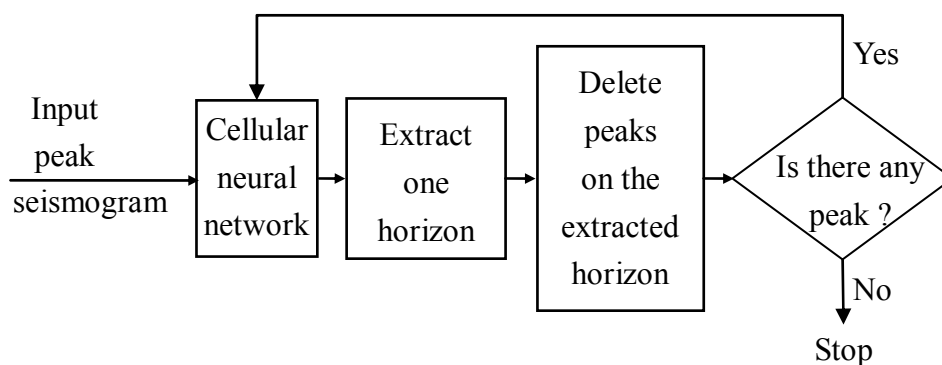


Fig. 3.4 The seismic horizon linking system.

Preprocessing the seismogram at first, and then the result is like Fig. 3.5:

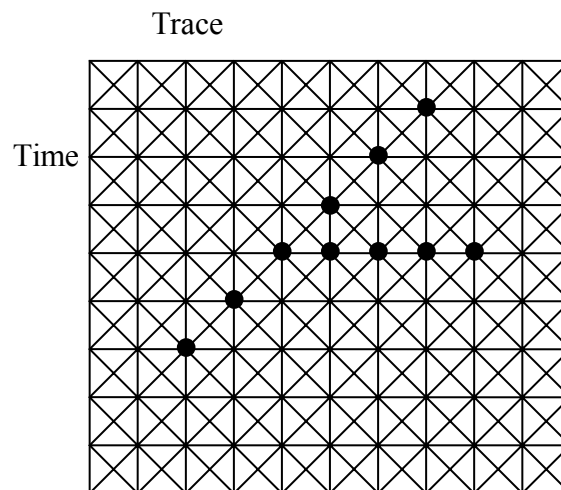


Fig. 3.5 Peak data.

The black points in Fig. 3.5 represent peaks. We scan the seismogram from top to bottom and then left to right until finding the first peak. This peak is regarded as the starting point of the first horizon, and set the input and output of this cell as 1. The inputs of cells of other peaks are 1, and these cells' outputs are 0. The inputs and outputs of cells of nonpeaks all are 0. Only the output value of every cell can be changed. The input of every cell is fixed. The input of a cell of a peak is 1, and the input of a cell of nonpeak is 0. Then we calculate  $A(i, j; k, l)$ . The detail of the computing technique will be introduced after here. We continue calculating the next state values of all cells, and then calculate the outputs of all cells. Then we calculate  $A(i, j; k, l)$  again, and then continue calculating the state values and outputs of all cells. We continue calculating so until the output values of all cells are no longer changed, then a horizon has been detected. Then we delete the peaks on the detected horizon. And then we check for there is any peak in the seismogram. If there is any peak in the seismogram, then we continue detecting the next horizon. Otherwise, it shows that all horizons have already been detected, and then output all detected horizons.

### Network Training

**Input:** The coordinate and input of each cell

**Output:**  $A(i, j; k, l)$

Step 1: According to the constraints of horizon linking, set up the energy equation.

Step 2: Compare the energy equation that is set up in Step 1 and the standard energy equation of a cellular neural network, then  $A(i, j; k, l)$  can be calculated. The standard energy equation of a cellular neural network is derived as follows.

$$E = -0.5 \sum_i \sum_j \sum_k \sum_l A(i, j; k, l) Y_{i,j} Y_{k,l} + 0.5 \sum_i \sum_j Y_{i,j}^2 - \sum_i \sum_j \sum_k \sum_l B(i, j; k, l) Y_{i,j} U_{k,l} - \sum_i \sum_j I Y_{i,j}$$

where  $Y_{i,j}$  is the output of cell  $C_{ij}$ ,  $Y_{k,l}$  is the output of cell  $C_{kl}$ , and  $U_{k,l}$  is the input of cell  $C_{kl}$ . Here we define that the extra input  $I = 0$  and  $B(i, j; k, l) = 0$ .

The following is the details of Step 1 and Step 2 respectively:

**Step 1: Set up the energy equation.**

We have to analyze the distribution situations of cells at first, namely analyze the situations of cells on the same horizon and not on the same horizon. And then we set up the energy equation according to various kinds of distribution situation. Let the energy of cells on the same horizon be decreased, because this kind of distribution situation is wanted by us. Let the energy of cells not on the same horizon be increased, because this kind of distribution situation is avoided by us.

**Analysis of distribution situations of cells:**

Under the situation of neighborhood radius  $r = 1$ , the distribution situation of the center cell and its neighboring cells is a  $3 \times 3$  space. We call this space as a window, as Fig. 3.6 shows, the coordinate of center cell is  $(i, j)$ .

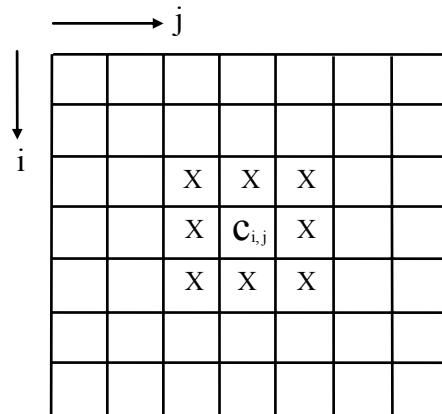


Fig. 3.6 Neighborhood radius  $r = 1$ , the distribution situation of the center cell and its neighboring cells.

We define four local distribution situations. The first kind of distribution situation is shown in Fig. 3.7. In a  $3 \times 3$  window, center cell is a peak and the outputs of center cell and its one of six neighboring cells are 1. Center cell  $C_{ij}$  is a peak, so its input  $U_{i,j} = 1$ . There are six kinds of cases, and these cases are listed in Table 3.1. Because center cell  $C_{ij}$  and its neighboring cell with output value 1 are very possible on the same horizon, so this kind of distribution situation is a situation that we want. So the cell energy equation  $E_1$  of this kind distribution will be decreased.

$$E_1 = -0.5a_1 \sum_i \sum_j (Y_{i,j} Y_{i,j+1} U_{i,j} + Y_{i,j} Y_{i-1,j+1} U_{i,j} + Y_{i,j} Y_{i-1,j-1} U_{i,j} + Y_{i,j} Y_{i,j-1} U_{i,j} + Y_{i,j} Y_{i+1,j-1} U_{i,j} + Y_{i,j} Y_{i+1,j+1} U_{i,j})$$

where  $a_1$  is a positive constant.

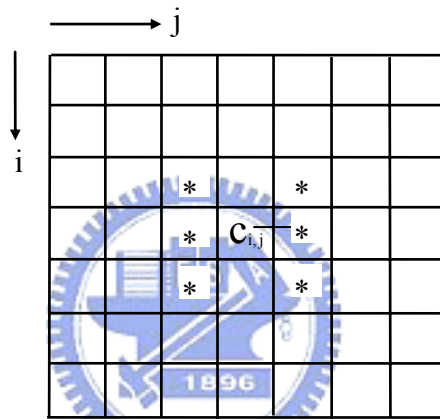


Fig. 3.7 The first kind distribution: the outputs of center cell and its one of six neighboring cells are 1.

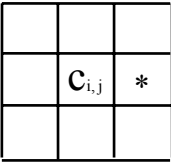
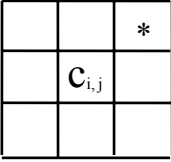
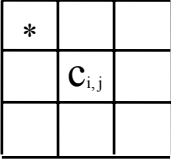

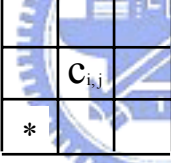
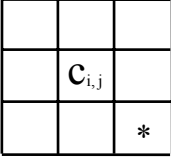
	The cells with output value 1 at the same time	Coordinate	
Case 1		(i, j)	(i, j+1)
Case 2		(i, j)	(i-1, j+1)
Case 3		(i, j)	(i-1, j-1)
Case 4		(i, j)	(i, j-1)
Case 5		(i, j)	(i+1, j-1)
Case 6		(i, j)	(i+1, j+1)

Table 3.1 The coordinates of the first kind of distribution situation.

The second distribution situation is that the center column of a  $7 \times 7$  window has at least two cells with output value 1 and these cells except center cell are peaks. As Fig. 3.8 shows, there are cells and the center cell  $C_{ij}$  in the same column of a  $7 \times 7$  window. The coordinates of these cells are shown in Table 3.2. This kind of distribution situation is not a situation that we want. When we link the seismic horizons, only link a horizon at one time, so center cell and cells in the same column can't exist with output value 1 at the same time. So if appearing this situation, the cell energy equation  $E_2$  of this kind distribution will be increased.



$$E_2 = 0.5a_2 \sum_i \sum_j \sum_{k \neq i, |k-i| \leq 3} Y_{i,j} Y_{k,j} U_{k,j}$$

where  $a_2$  is a positive constant.

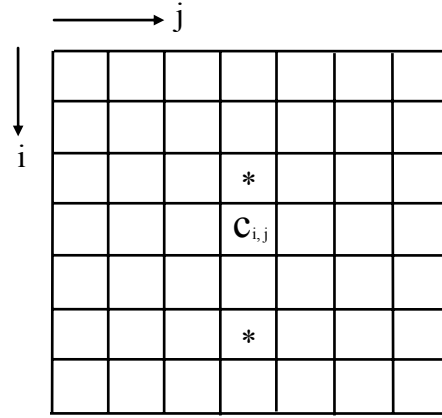


Fig. 3.8 The second kind distribution: at least two cells with output value 1 in the same column.

	The cells with output value 1 at the same time	Coordinate	
Case 1	Center cell and upper cells	(i, j)	$\{(k, j) \mid i-3 \leq k < i\}$
Case 2	Center cell and lower cells	(i, j)	$\{(k, j) \mid i+3 \geq k > i\}$

Table 3.2 The coordinates of the second kind of distribution situation.

The third distribution situation is that the output of center cell  $C_{ij}$  is 1 and there are cells with output value 1 and input value 1 in the neighboring columns of center cell in a  $7 \times 7$  window, and the distance between one of these cells and center cell is greater than 1, as Fig. 3.9 shows. The coordinates of these cells are shown in Table 3.3. Because these cells don't belong to the horizon which contains center cell, so this kind of distribution situation is not a situation that we want too. So the cell energy equation  $E_3$  of this kind distribution will be increased.

$$E_3 = 0.5a_3 \sum_i \sum_j \sum_{1 < |k-i| \leq 3} (Y_{i,j} Y_{k,j+1} U_{k,j+1} + Y_{i,j} Y_{k,j-1} U_{k,j-1})$$

where  $a_3$  is a positive constant.

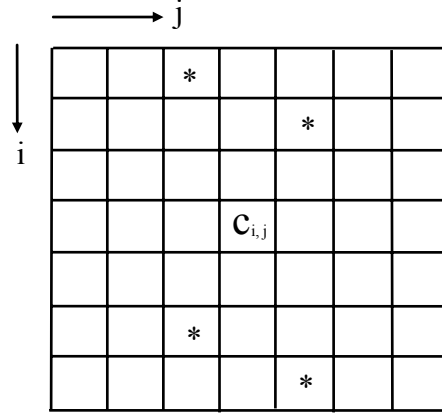


Fig. 3.9 The third kind distribution: the output of center cell  $C_{ij}$  is 1 and there are cells with output value 1 and input value 1 in the neighboring columns of center cell, and the distance between one of these cells and center cell is greater than 1.

	The cells with output value 1 at the same time	Coordinate	
Case 1	Center cell and upper-right cells	(i, j)	$\{(k, j+1) \mid i-3 \leq k < i-1\}$
Case 2	Center cell and lower-right cells	(i, j)	$\{(k, j+1) \mid i+3 \geq k > i+1\}$
Case 3	Center cell and upper-left cells	(i, j)	$\{(k, j-1) \mid i-3 \leq k < i-1\}$
Case 4	Center cell and lower-left cells	(i, j)	$\{(k, j-1) \mid i+3 \geq k > i+1\}$

Table 3.3 The coordinates of the third kind of distribution situation.

The fourth distribution situation is that the center cell is not a peak and the output of center cell is 1 and a cell with output value 1 and input value 1 in the left neighboring column of center cell and a cell is a peak in the right neighboring column of center cell in a  $3 \times 3$  window, as Fig. 3.10 shows. There are five kinds of cases, and these cases are listed in Table 3.4. Because center cell, the cell with output value 1 in the left neighboring column of center cell and a cell being a peak in the right neighboring column of center cell are very possible on the same horizon, so this kind of distribution situation is a situation that we want. So the cell energy equation  $E_4$  of this kind distribution will be decreased.

$$\begin{aligned}
 E_4 = & -0.5a_4 \sum_i \sum_j (Y_{i,j} Y_{i+1,j-1} U_{i+1,j-1} U_{i-1,j+1} (1 - U_{i,j}) + Y_{i,j} Y_{i,j-1} U_{i,j-1} U_{i,j+1} (1 - U_{i,j}) \\
 & + Y_{i,j} Y_{i-1,j-1} U_{i-1,j-1} U_{i+1,j+1} (1 - U_{i,j}) + Y_{i,j} Y_{i,j-1} U_{i,j-1} U_{i-1,j+1} (1 - U_{i,j}) \\
 & + Y_{i,j} Y_{i,j-1} U_{i,j-1} U_{i+1,j+1} (1 - U_{i,j}))
 \end{aligned}$$

where  $a_4$  is a positive constant.

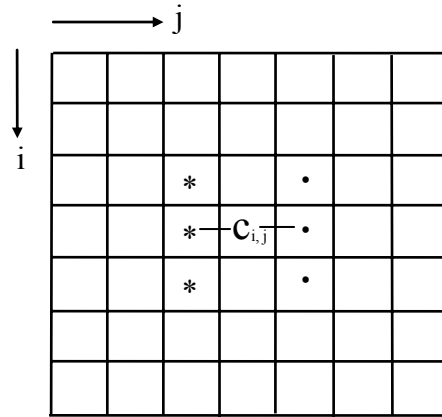


Fig. 3.10 The fourth kind distribution: the center cell is not a peak and the output of center cell is 1 and a cell with output value 1 and input value 1 in the left neighboring column of center cell and a cell is a peak in the right neighboring column of center cell in a  $3 \times 3$  window.

	The cells with output value 1 at the same time and the cell with input value 1	Coordinate		
		Cells with output value 1		Cell with input value 1
Case 1		(i, j)	(i+1, j-1)	(i-1, j+1)
Case 2		(i, j)	(i, j-1)	(i, j+1)
Case 3		(i, j)	(i-1, j-1)	(i+1, j+1)
Case 4		(i, j)	(i, j-1)	(i-1, j+1)
Case 5		(i, j)	(i, j-1)	(i+1, j+1)

Table 3.4 The coordinates of the fourth kind of distribution situation.

As soon as we sum energy equation  $E_1$ ,  $E_2$ ,  $E_3$  and  $E_4$ , we set up our energy equation  $E = E_1 + E_2 + E_3 + E_4$ .

$$\begin{aligned}
E &= E_1 + E_2 + E_3 + E_4 \\
&= -0.5a_1 \sum_i \sum_j (Y_{i,j} Y_{i,j+1} U_{i,j} + Y_{i,j} Y_{i-1,j+1} U_{i,j} + Y_{i,j} Y_{i-1,j-1} U_{i,j} \\
&\quad + Y_{i,j} Y_{i,j-1} U_{i,j} + Y_{i,j} Y_{i+1,j-1} U_{i,j} + Y_{i,j} Y_{i+1,j+1} U_{i,j}) \\
&\quad + 0.5a_2 \sum_i \sum_j \sum_{k \neq i, |k-i| \leq 3} Y_{i,j} Y_{k,j} U_{k,j} \\
&\quad + 0.5a_3 \sum_i \sum_j \sum_{l < |k-i| \leq 3} (Y_{i,j} Y_{k,j+1} U_{k,j+1} + Y_{i,j} Y_{k,j-1} U_{k,j-1}) \\
&\quad - 0.5a_4 \sum_i \sum_j (Y_{i,j} Y_{i+1,j-1} U_{i+1,j-1} U_{i-1,j+1} (1 - U_{i,j}) + Y_{i,j} Y_{i,j-1} U_{i,j-1} U_{i,j+1} (1 - U_{i,j}) \\
&\quad + Y_{i,j} Y_{i-1,j-1} U_{i-1,j-1} U_{i+1,j+1} (1 - U_{i,j}) + Y_{i,j} Y_{i,j-1} U_{i,j-1} U_{i-1,j+1} (1 - U_{i,j}) \\
&\quad + Y_{i,j} Y_{i,j-1} U_{i,j-1} U_{i+1,j+1} (1 - U_{i,j})) \tag{3-1}
\end{aligned}$$

## Step 2: Compare energy equations and calculate $A(i, j; k, l)$ .

After we set up energy equation  $E$ , we compare  $E$  with the standard energy equation of a cellular neural network, then we can get  $A(i, j; k, l)$ . We have known that the standard energy equation of a cellular neural network as Equation (3-2) lists.

$$\begin{aligned}
E_{\text{standard}} &= -0.5 \sum_i \sum_j \sum_k \sum_l A(i, j; k, l) Y_{i,j} Y_{k,l} + 0.5 \sum_i \sum_j Y_{i,j}^2 \\
&\quad - \sum_i \sum_j \sum_k \sum_l B(i, j; k, l) Y_{i,j} U_{k,l} - \sum_i \sum_j I Y_{i,j} \\
&= -0.5 \sum_i \sum_j \sum_{k \neq i} \sum_{l \neq j} A(i, j; k, l) Y_{i,j} Y_{k,l} - 0.5 \sum_i \sum_j [A(i, j; i, j) - 1] Y_{i,j}^2 \\
&\quad - \sum_i \sum_j \sum_k \sum_l B(i, j; k, l) Y_{i,j} U_{k,l} - \sum_i \sum_j I Y_{i,j} \tag{3-2}
\end{aligned}$$

We illustrate how to compare the energy equations with examples at first, then calculate  $A(i, j; k, l)$  of seismic horizon linking algorithm in this thesis. We suppose that there is a energy equation  $E_{\text{case1}}$ . We compare it with the Equation (3-2), then we can get  $A_{\text{case1}}(i, j; k, l)$ .

Compare  $E_{\text{case1}}$  with  $E_{\text{standard}}$  :

$$\begin{aligned}
E_{\text{case1}} &= -0.5a_1 \sum_i \sum_j Y_{i,j} Y_{i-1,j} \\
E_{\text{standard}} &= -0.5 \sum_i \sum_j \sum_{k \neq i} \sum_{l \neq j} A(i, j; k, l) Y_{i,j} Y_{k,l} - 0.5 \sum_i \sum_j [A(i, j; i, j) - 1] Y_{i,j}^2 \\
&\quad - \sum_i \sum_j \sum_k \sum_l B(i, j; k, l) Y_{i,j} U_{k,l} - \sum_i \sum_j I Y_{i,j}
\end{aligned}$$

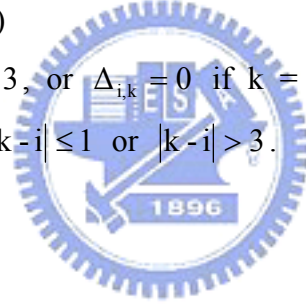
We get:

$$A_{\text{case1}}(i, j; k, l) = a_1 (\delta(i-1, k) \delta(j, l)) + \delta(i, k) \delta(j, l)$$

We use the same comparing technique to compare the energy equation  $E = E_1 + E_2 + E_3 + E_4$  with the Equation (3-2), then we can get  $A(i, j; k, l)$ , as the following Equation (3-3) shows. If  $p = q$ ,  $\delta(p, q) = 1$ . Otherwise, if  $p \neq q$ ,  $\delta(p, q) = 0$ .

$$\begin{aligned}
A(i, j; k, l) = & a_1 (\delta(i, k)\delta(j+1, l)U_{i,j} + \delta(i-1, k)\delta(j+1, l)U_{i,j} \\
& + \delta(i-1, k)\delta(j-1, l)U_{i,j} + \delta(i, k)\delta(j-1, l)U_{i,j} \\
& + \delta(i+1, k)\delta(j-1, l)U_{i,j} + \delta(i+1, k)\delta(j+1, l)U_{i,j}) \\
& - a_2 \Delta_{i,k} \delta(j, l)U_{k,j} \\
& - a_3 (\Delta'_{i,k} \delta(j+1, l)U_{k,j+1} + \Delta'_{i,k} \delta(j-1, l)U_{k,j-1}) \\
& + a_4 (\delta(i+1, k)\delta(j-1, l)U_{i+1,j-1} U_{i-1,j+1} (1 - U_{i,j}) \\
& + \delta(i, k)\delta(j-1, l)U_{i,j-1} U_{i,j+1} (1 - U_{i,j}) \\
& + \delta(i-1, k)\delta(j-1, l)U_{i-1,j-1} U_{i+1,j+1} (1 - U_{i,j}) \\
& + \delta(i, k)\delta(j-1, l)U_{i,j-1} U_{i-1,j+1} (1 - U_{i,j}) \\
& + \delta(i, k)\delta(j-1, l)U_{i,j-1} U_{i+1,j+1} (1 - U_{i,j})) \\
& + \delta(i, k)\delta(j, l)
\end{aligned} \tag{3-3}$$

where  $\Delta_{i,k} = 1$  if  $0 < |k - i| \leq 3$ , or  $\Delta_{i,k} = 0$  if  $k = i$  or  $|k - i| > 3$ , and  $\Delta'_{i,k} = 1$  if  $1 < |k - i| \leq 3$ , or  $\Delta'_{i,k} = 0$  if  $|k - i| \leq 1$  or  $|k - i| > 3$ .



### Stability of the system

The state equation of the cell at location  $(i, j)$  is as the following.

$$X_{i,j} = \sum_k \sum_l A(i, j; k, l) Y_{k,l} + \sum_k \sum_l B(i, j; k, l) U_{k,l} + I$$

The output function is as the following.

$$Y_{i,j} = f(X_{i,j}) = \begin{cases} 1, & \text{if } X_{i,j} > 0 \\ 0, & \text{if } X_{i,j} \leq 0 \end{cases}$$

The energy equation of the system is as the following.

$$\begin{aligned}
E &= -0.5 \sum_i \sum_j \sum_k \sum_l A(i, j; k, l) Y_{i,j} Y_{k,l} + 0.5 \sum_i \sum_j Y_{i,j}^2 \\
&\quad - \sum_i \sum_j \sum_k \sum_l B(i, j; k, l) Y_{i,j} U_{k,l} - \sum_i \sum_j I Y_{i,j} \\
&= -0.5 \sum_i \sum_j \sum_{k \neq i} \sum_{l \neq j} A(i, j; k, l) Y_{i,j} Y_{k,l} - 0.5 \sum_i \sum_j [A(i, j; i, j) - 1] Y_{i,j}^2 \\
&\quad - \sum_i \sum_j \sum_k \sum_l B(i, j; k, l) Y_{i,j} U_{k,l} - \sum_i \sum_j I Y_{i,j}
\end{aligned}$$

From Equation (3-3), we know  $A(i, j; i, j) = 1$ , so

$$\begin{aligned}
E &= -0.5 \sum_i \sum_j \sum_{k \neq i} \sum_{l \neq j} A(i, j; k, l) Y_{i,j} Y_{k,l} - \sum_i \sum_j \sum_k \sum_l B(i, j; k, l) Y_{i,j} U_{k,l} \\
&\quad - \sum_i \sum_j I Y_{i,j}
\end{aligned}$$

From the condition  $A(i, j; k, l) = A(k, l; i, j)$ , we get

$$\Delta E = - \left( \sum_{k \neq i} \sum_{l \neq j} A(i, j; k, l) Y_{k,l} + \sum_k \sum_l B(i, j; k, l) U_{k,l} + I \right) \Delta Y_{i,j}$$

If  $\sum_{k \neq i} \sum_{l \neq j} A(i, j; k, l) Y_{k,l} + \sum_k \sum_l B(i, j; k, l) U_{k,l} + I < 0$ , then there are three cases:

(1)  $\sum_k \sum_l A(i, j; k, l) Y_{k,l} + \sum_k \sum_l B(i, j; k, l) U_{k,l} + I < 0$ , then the output of cell  $C_{ij}$  is

0. And  $\Delta Y_{i,j} \leq 0$ , so  $\Delta E \leq 0$ .

(2)  $\sum_k \sum_l A(i, j; k, l) Y_{k,l} + \sum_k \sum_l B(i, j; k, l) U_{k,l} + I = 0$ ,  $Y_{i,j} = 1$ , then the output of

cell  $C_{ij}$  is 0. And  $\Delta Y_{i,j} < 0$ , so  $\Delta E < 0$ .

(3)  $\sum_k \sum_l A(i, j; k, l) Y_{k,l} + \sum_k \sum_l B(i, j; k, l) U_{k,l} + I > 0$ ,  $Y_{i,j} = 1$ , then the output of

cell  $C_{ij}$  is 1. And  $\Delta Y_{i,j} = 0$ , so  $\Delta E = 0$ .

If  $\sum_{k \neq i} \sum_{l \neq j} A(i, j; k, l) Y_{k,l} + \sum_k \sum_l B(i, j; k, l) U_{k,l} + I = 0$ , then there are two cases:

(1)  $\sum_k \sum_l A(i, j; k, l) Y_{k,l} + \sum_k \sum_l B(i, j; k, l) U_{k,l} + I = 0$ ,  $Y_{i,j} = 0$ , then the output of

cell  $C_{ij}$  is 0. And  $\Delta Y_{i,j} = 0$ , so  $\Delta E = 0$ .

(2)  $\sum_k \sum_l A(i, j; k, l) Y_{k,l} + \sum_k \sum_l B(i, j; k, l) U_{k,l} + I > 0$ ,  $Y_{i,j} = 1$ , then the output of

cell  $C_{ij}$  is 1. And  $\Delta Y_{i,j} = 0$ , so  $\Delta E = 0$ .

If  $\sum_{k \neq i} \sum_{l \neq j} A(i, j; k, l) Y_{k,l} + \sum_k \sum_l B(i, j; k, l) U_{k,l} + I > 0$ , then

$\sum_k \sum_l A(i, j; k, l) Y_{k,l} + \sum_k \sum_l B(i, j; k, l) U_{k,l} + I > 0$ , so the output of cell  $C_{ij}$  is 1.

And  $\Delta Y_{i,j} \geq 0$ , so  $\Delta E \leq 0$ .

### Present Linking Direction

When we start linking a horizon, we scan peak data from top to bottom and then left to right until find the first peak. The first peak must be the left most peak. It is regarded as the starting point of the horizon. Because only the output of the cell of the first peak is 1, the outputs of other cells are 0 at the beginning. So only the outputs of the cells of the peaks and the cells according with the fourth distribution situation near the first peak will be changed from 0 to 1, the outputs of other cells will not be changed; they are still 0 after the second iteration. Because the first peak is the left most peak, so the cells with output value 1 are in the right neighboring column of the first peak after the second iteration. And then the outputs of cells of the peaks and the cells according with the fourth distribution situation in the next right neighboring column possibly will be changed from 0 to 1. The outputs of the cells of the peaks in the left neighboring column will not be changed from 0 to 1. Because it will cause more than one cell with output value 1 in the left neighboring column, it will violate the constraint of the second distribution situation. So the direction of outputs of cells changed from 0 to 1 is from left to right, namely the linking direction is from left to right. But if it meets the situation like Fig. 3.11(a), then it will have a problem. The star symbol “ \* “ in Fig. 3.11 represents the cell of one peak with output value 1; the solid dot “ • “ represents the cell of one peak with output value 0. After the next iteration, two cells with output value 0 are influenced by the cell with output value 1, and then the outputs of these two cells are changed to 1, as Fig. 3.11(b) shows. After the next iteration again, these two cells are influenced each other according to the constraint of the second distribution situation, and then the outputs of these two cells are changed to 0, as Fig. 3.11(c) shows. After the next iteration again, it is changed to

the situation of Fig. 3.11(b) again. The output changing situation of these two cells will circulate as so, the procedure will be unable to stop.



Fig. 3.11 (a) One situation of linking process; (b) The situation of (a) after the next iteration; (c) The situation of (b) after the next iteration.

So we have to add the consideration of directionality. According to the direction of peak linking, we modify the constraints of the second and third distribution situations for some peaks. Because the direction of peak linking is right, so we only need to consider the linking directions of upper-right, lower-right and right. If the linking direction is upper-right at present, and we meet the situations as Fig. 3.12(a) and (b) respectively, then make it link the peak in upper-right side, namely let it turn into the situations of Fig. 3.12(d) and (e) respectively. If we meet the situation as Fig. 3.12(c), then make it link the peak in right-side, namely let it turn into the situation of Fig. 3.12(f). If the linking direction is lower-right at present, and we meet the situations as Fig. 3.12(a), (b) and (c) respectively, then make it link the peak in lower-right side, right side and lower-right side respectively, namely let it turn into the situations of Fig. 3.12(g), (h) and (i) respectively. If the linking direction is right at present, and we meet the situation as Fig. 3.12(a), then we have to decide which peak is linked according to the previous linking direction. If the previous linking direction is upper-right, then the peak in upper-right side is linked, namely let it turn into the situation of Fig. 3.12(d). Otherwise, the peak in lower-right side is linked, namely let it turn into the situation of Fig. 3.12(g). If the linking direction is right at present, and we meet the situations as Fig. 3.12(b) and (c) respectively, then make it link the peak in right side, namely let it turn into the situations of Fig. 3.12(h) and (f) respectively.



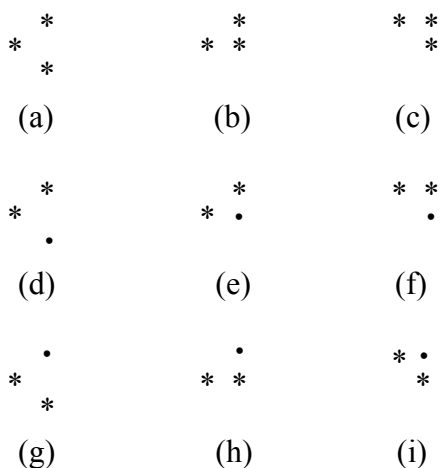


Fig. 3.12 (a) The first situation which is needed to consider for horizon linking; (b) The second situation which is needed to consider for horizon linking; (c) The third situation which is needed to consider for horizon linking; (d) The first linking result; (e) The second linking result; (f) The third linking result; (g) The fourth linking result; (h) The fifth linking result; (i) The sixth linking result.

We determine that the present linking direction is the last linking direction at present. After determining the present linking direction, we determine the present peak. Present peak is the most recently linked peak, namely the peak that its output value is changed from 0 to 1 recently and it is already confirmed belonging to the horizon which is linked at present. According to the present linking direction and the present peak, we modify the constraints of the second and third distribution situations for the peaks in the right neighboring column of present peak. If the present linking direction is upper-right, then the lower peaks of the peaks in the right neighboring column of present peak can not influence the upper peaks of the peaks in the right neighboring column of present peak for the second and third distribution situations. So the output of the cell of the upper peak is still 1. The lower peak is influenced by the upper peak, and its output is changed from 1 to 0, so Fig. 3.12(a), (b) and (c) will be turned into Fig. 3.12(d), (e) and (f) respectively. The same, if the present linking direction is lower-right, then the upper peaks of the peaks in the right neighboring column of present peak can not influence the lower peaks of the peaks in the right neighboring column of present peak for the second and third distribution situations. So Fig. 3.12(a), (b) and (c) will be turned into Fig. 3.12(g), (h) and (i) respectively. If the present linking direction is right and the peak in right-side of present peak exists, then the peaks in the right neighboring column of present peak and above the present peak can not influence the lower peaks of the peaks in the right neighboring column of present peak for the second and third distribution situations, and the peaks in the right neighboring column of present peak and below the present peak can not

influence the upper peaks of the peaks in the right neighboring column of present peak for the second and third distribution situations, and the peak in right-side of present peak can influence the upper and lower peaks of the peaks in the right neighboring column of present peak for the second and third distribution situations. So Fig. 3.12(b) and (c) will be turned into Fig. 3.12(h) and (f) respectively. If the present linking direction is right and the peak in right-side of present peak doesn't exist, then we determine the present linking direction according to the previous linking direction. At the initial, we assume that present linking direction is upper-right. Most  $A(i, j; k, l)$  are calculated by the Equation (3-3). Just only when the two peaks lying in the coordinate  $(i, j)$  and  $(k, l)$  are in the right neighboring column of present peak and the distribution of these two peaks accords with the second or third distribution situation, we need to change the value of  $A(i, j; k, l)$  to 0 according to the present linking direction.

**Algorithm 3.1:** Horizon linking of seismic patterns

**Input:** Seismic patterns

**Output:** Horizons of seismic patterns

Step (1) Set up the initial condition of the network.

Scan peak data from top to bottom and then left to right until finding the first peak. The cell's input and output value of the first peak is 1. The cell of the first peak is regarded as the starting point of the first horizon. The input values of the cells of other peaks are 1, and the output values of the cells of other peaks are all 0. The input and output values of the cells of nonpeak are all 0.

Step (2) Calculate  $A(i, j; k, l)$ .

$A(i, j; k, l)$  are calculated via comparing the energy equation  $E$  and the standard energy equation of a cellular neural network, such as the Equation (3-3) lists,  $i$  and  $j$  in Equation (3-3) represent the coordinate of center cell of a window;  $k$  and  $l$  represent the coordinates of neighboring cells of center cell of a window. And according to the present linking direction and the present peak, change the value of  $A(i, j; k, l)$  to 0, where the two peaks lying in the coordinate  $(i, j)$  and  $(k, l)$  are in the right neighboring column of present peak and the distribution of these two peaks accords with the second or third distribution situation.

Step (3) Calculate the state value of every cell.

$$X_{ij} = \sum_{|k-i| \leq 3} \sum_{|l-j| \leq 3} A(i, j; k, l) Y_{kl}$$

$X_{ij}$  represents the state value of cell  $C_{ij}$ ;  $Y_{kl}$  represents the output of cell  $C_{kl}$ .

Step (4) Calculate the output of every cell.

We use hardlimiter activation function to calculate the output of each cell. It is different to the standard output function of cellular neural networks.

$$Y_{ij} = \begin{cases} 1, & \text{if } X_{ij} > 0 \\ 0, & \text{if } X_{ij} \leq 0 \end{cases}$$

$Y_{ij}$  represents the output of cell  $C_{ij}$ .

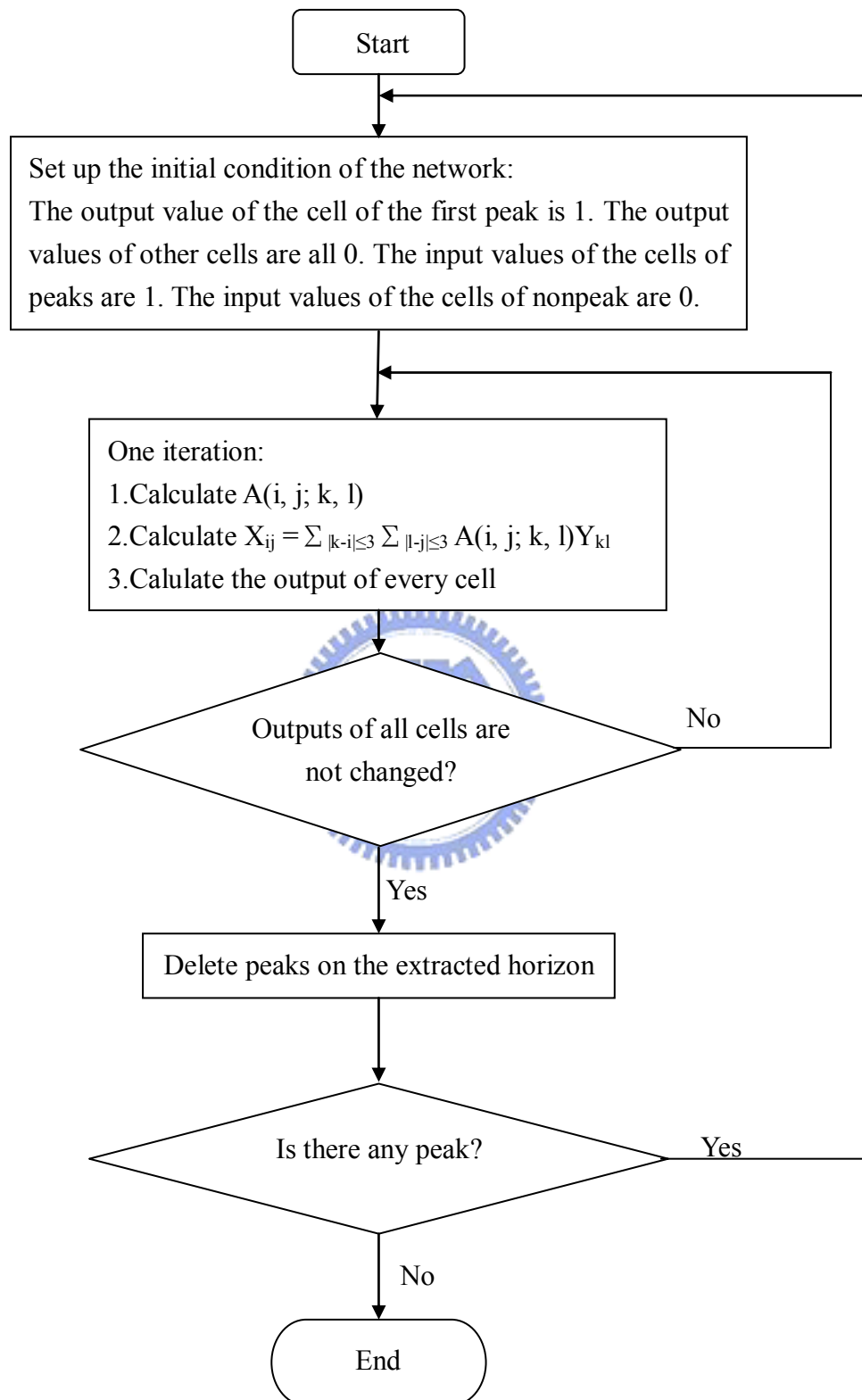
Step (5) Repeat Step (2), (3) and (4) until finish linking a horizon.

When the output values of all cells are no longer changed, it represents that we finish linking a horizon.

Step (6) Delete peaks on the extracted horizon, namely delete peaks with output value 1.

Step (7) Check whether there is any peak. If there is any peak, then repeat Step (1) to (6) until there is no peak.

**The flowchart of Algorithm 3.1:**



## Compare with typical image processing method

In image processing, the typical neighborhood processing can use the so-called mask operation. The principle of mask operation is making the value of a pixel be equal to a function of itself and neighboring pixels.

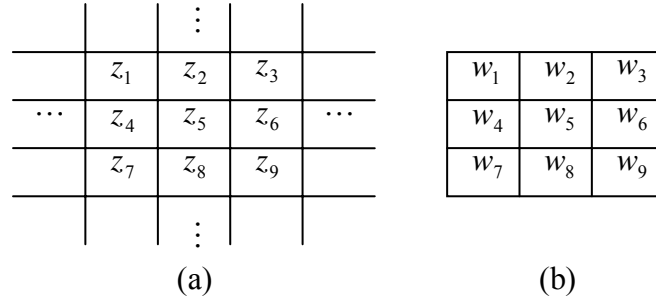


Fig. 3.13 (a) Sub image of an image; (b) A  $3 \times 3$  mask.

From Fig. 3.13, the summation of each pixel value  $z_i$  multiplies the corresponding mask coefficient  $w_i$ ,  $i = 1, 2, \dots, 9$  is

$$z = w_1 z_1 + w_2 z_2 + \dots + w_9 z_9 = \sum_{i=1}^9 w_i z_i$$

The new value of  $z_5$  is  $z$ .

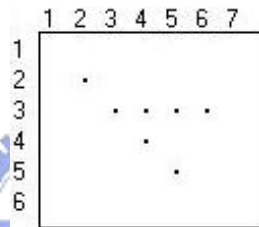
In general, this kind of mask is a space-invariant template. Our algorithm uses a space-variant template. We can design a  $7 \times 7$  mask:

0	0	$-a_3$	$-a_2$	$-a_3$	0	0
0	0	$-a_3$	$-a_2$	$-a_3$	0	0
0	0	$a_1$	$-a_2$	$a_1$	0	0
0	0	$a_1$	1	$a_1$	0	0
0	0	$a_1$	$-a_2$	$a_1$	0	0
0	0	$-a_3$	$-a_2$	$-a_3$	0	0
0	0	$-a_3$	$-a_2$	$-a_3$	0	0

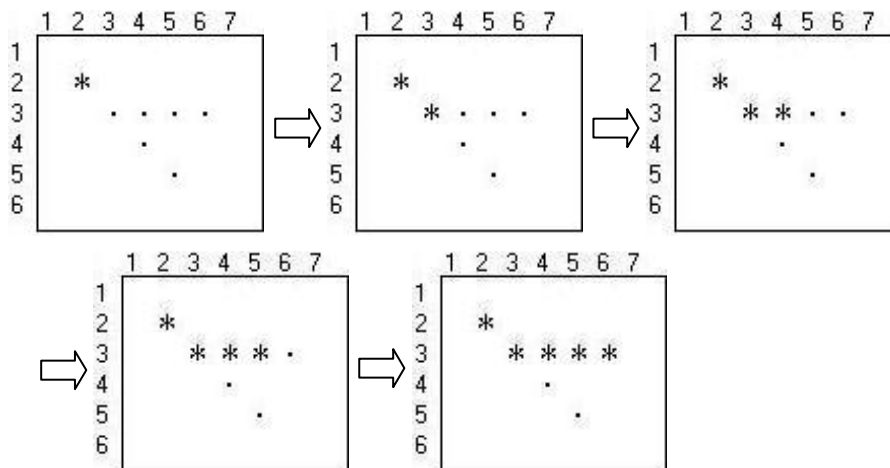
This mask is equivalent to the CNN model which contains the first, second, and third constraints. If  $a_1 = 1$ , and  $a_2 = a_3 = 5$ , then the  $7 \times 7$  mask is shown as the following.

0	0	-5	-5	-5	0	0
0	0	-5	-5	-5	0	0
0	0	1	-5	1	0	0
0	0	1	1	1	0	0
0	0	1	-5	1	0	0
0	0	-5	-5	-5	0	0
0	0	-5	-5	-5	0	0

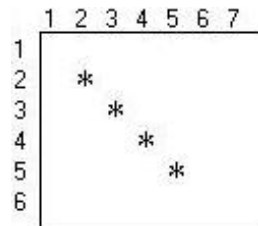
We can input seismic data from top to bottom, then left to right. If the peak is present, then use the above mask to calculate the sum, and then input to the CNN output function to calculate the output of the peak. The different order of inputting seismic data can cause the different result. For example, the seismic data is shown in the following:



And we input seismic data from top to bottom, then left to right. Then the result is shown in the following:



The first extracted horizon is not correct. The correct horizon is shown in the following:



So we should input seismic data from bottom to top, then left to right for this seismic data. Since the order of inputting seismic data will affect the linking result. So we should not use this type of calculation. We can use that type of calculation used in the CNN model. We can also apply the technique of present linking direction to the masks of peaks in the right neighboring column of present peak. Therefore the masks of peaks in the right neighboring column of present peak are different. If the location of present peak is  $(i, j)$ , and the present linking direction is upper-right, then we can set the mask of the peak at location  $(i-1, j+1)$  as the following.

0	0	-5	-5	-5	0	0
0	0	-5	-5	-5	0	0
0	0	1	-5	1	0	0
0	0	1	1	1	0	0
0	0	1	0	1	0	0
0	0	0	0	0	0	0
0	0	0	0	0	0	0

If the location of present peak is  $(i, j)$ , and the present linking direction is lower-right, then we can set the mask of the peak at location  $(i+1, j+1)$  as the following.

0	0	0	0	0	0	0
0	0	0	0	0	0	0
0	0	1	0	1	0	0
0	0	1	1	1	0	0
0	0	1	-5	1	0	0
0	0	-5	-5	-5	0	0
0	0	-5	-5	-5	0	0

If the location of present peak is  $(i, j)$ , the present linking direction is right, and the peak located in  $(i, j+1)$  exists, then we can set the mask of the peak at location  $(i, j+1)$

as the following.

0	0	0	0	0	0	0
0	0	0	0	0	0	0
0	0	1	0	1	0	0
0	0	1	1	1	0	0
0	0	1	0	1	0	0
0	0	0	0	0	0	0
0	0	0	0	0	0	0

And we can set the mask of the peak at location  $(i-1, j+1)$  as the following.

0	0	0	0	0	0	0
0	0	0	0	0	0	0
0	0	1	0	1	0	0
0	0	1	1	1	0	0
0	0	1	-5	1	0	0
0	0	0	0	0	0	0
0	0	0	0	0	0	0

The mask of the peak at location  $(i+1, j+1)$  can be set as the following.

0	0	0	0	0	0	0
0	0	0	0	0	0	0
0	0	1	-5	1	0	0
0	0	1	1	1	0	0
0	0	1	0	1	0	0
0	0	0	0	0	0	0
0	0	0	0	0	0	0

We can use these masks on corresponding peaks to calculate the state value of each peak. And then calculate the output value of each peak by the same output function used in CNN model. Repeat these calculations until the output value of each peak is no more changed. The process of calculation is much different to general image processing. In general image processing, the calculation is pixel by pixel and the new value of each pixel is got directly without using output function. And the calculation is completed after one iteration. The template used in CNN model is space-variant and time-variant. Only the masks of peaks in the right neighboring column of present peak



are different among all masks used above. Other masks are the same. Since present peak is changed iteration by iteration and present linking direction may be changed iteration by iteration. So the masks of peaks in the right neighboring column of present peak are time-variant. This image processing method is similar to the CNN model used in this thesis.

### 3.5 Example

We use an example to explain the process of seismic horizon linking. The size of the input data is  $6 \times 7$ , as Fig. 3.14 shows. We set  $a_1 = 1$ ,  $a_2 = a_3 = 5$ ,  $a_4 = 1$ .  $a_2$  and  $a_3$  are both greater than  $a_1$  and  $a_4$ . This causes the effects of the second and third constraints to be far more than the effect of the first and fourth constraint. Then the second and third distribution situations will certainly not appear in linked horizons.

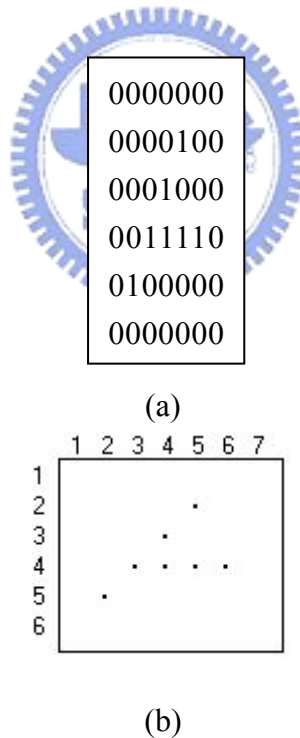
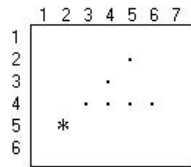


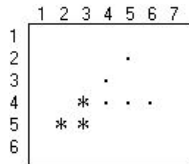
Fig. 3.14 (a) The simulated seismic peak data, (b) The peaks in (a) are shown as solid dots.

The process of seismic horizon linking:

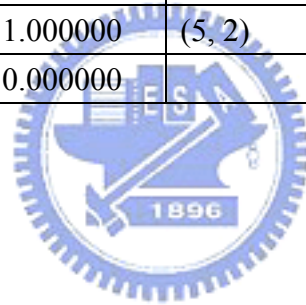
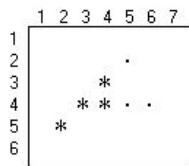
Set up the initial condition of the network:



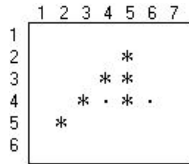
Iteration	Present peak	Present linking direction	Energy
1	(5, 2)	Upper-right	0
Cell	State value	Output value	
(2, 5)	0.000000	0.000000	
(3, 4)	0.000000	0.000000	
(4, 3)	0.000000	0.000000	
(4, 4)	0.000000	0.000000	
(4, 5)	0.000000	0.000000	
(4, 6)	0.000000	0.000000	
(5, 2)	1.000000	1.000000	
(5, 3)	0.000000	0.000000	
(3, 5)	0.000000	0.000000	



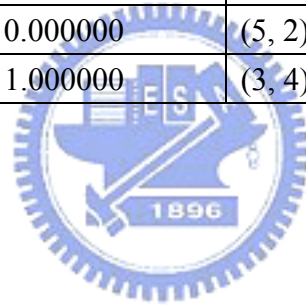
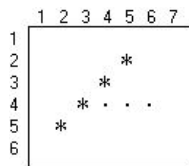
Iteration	Present peak	Present linking direction	Energy
2	(5, 2)	Upper-right	0.5
Cell	State value	Output value	Neighboring cells which influence center cell
(2, 5)	0.000000	0.000000	
(3, 4)	0.000000	0.000000	
(4, 3)	1.000000	1.000000	(5, 2)
(4, 4)	0.000000	0.000000	
(4, 5)	0.000000	0.000000	
(4, 6)	0.000000	0.000000	
(5, 2)	1.000000	1.000000	(5, 2)
(5, 3)	1.000000	1.000000	(5, 2)
(3, 5)	0.000000	0.000000	



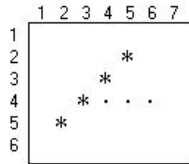
Iteration	Present peak	Present linking direction	Energy
3	(4, 3)	Upper-right	2
Cell	State value	Output value	Neighboring cells which influence center cell
(2, 5)	0.000000	0.000000	
(3, 4)	1.000000	1.000000	(4, 3)
(4, 3)	2.000000	1.000000	(4, 3), (5, 2)
(4, 4)	2.000000	1.000000	(4, 3), (5, 3)
(4, 5)	0.000000	0.000000	
(4, 6)	0.000000	0.000000	
(5, 2)	3.000000	1.000000	(5, 2), (4, 3)
(5, 3)	-3.000000	0.000000	(5, 2), (5, 3), (4, 3)
(3, 5)	0.000000	0.000000	



Iteration	Present peak	Present linking direction	Energy
4	(3, 4)	Upper-right	5
Cell	State value	Output value	Neighboring cells which influence center cell
(2, 5)	1.000000	1.000000	(3, 4)
(3, 4)	2.000000	1.000000	(3, 4), (4, 3)
(4, 3)	4.000000	1.000000	(3, 4), (4, 3), (4, 4), (5, 2)
(4, 4)	-3.000000	0.000000	(4, 3), (4, 4), (3, 4)
(4, 5)	2.000000	1.000000	(3, 4), (4, 4)
(4, 6)	0.000000	0.000000	
(5, 2)	2.000000	1.000000	(5, 2), (4, 3)
(5, 3)	-9.000000	0.000000	(5, 2), (4, 3), (3, 4)
(3, 5)	1.000000	1.000000	(3, 4)



Iteration	Present peak	Present linking direction	Energy
5	(2, 5)	Upper-right	-3
Cell	State value	Output value	Neighboring cells which influence center cell
(2, 5)	2.000000	1.000000	(3, 4), (2, 5)
(3, 4)	5.000000	1.000000	(3, 4), (4, 3), (2, 5), (4, 5), (3, 5)
(4, 3)	3.000000	1.000000	(3, 4), (4, 3), (5, 2)
(4, 4)	-7.000000	0.000000	(4, 3), (3, 5), (4, 5), (3, 4), (2, 5)
(4, 5)	-3.000000	0.000000	(3, 4), (4, 5), (2, 5)
(4, 6)	-3.000000	0.000000	(3, 5), (4, 5), (2, 5)
(5, 2)	2.000000	1.000000	(5, 2), (4, 3)
(5, 3)	-9.000000	0.000000	(5, 2), (4, 3), (3, 4)
(3, 5)	-8.000000	0.000000	(3, 4), (3, 5), (2, 5), (4, 5)



Iteration		Present peak	Present linking direction	Energy
6		(2, 5)	Upper-right	-3
Cell	State value	Output value	Neighboring cells which influence center cell	
(2, 5)	2.000000	1.000000	(3, 4), (2, 5)	
(3, 4)	3.000000	1.000000	(3, 4), (4, 3), (2, 5)	
(4, 3)	3.000000	1.000000	(3, 4), (4, 3), (5, 2)	
(4, 4)	-9.000000	0.000000	(4, 3), (3, 4), (2, 5)	
(4, 5)	-4.000000	0.000000	(3, 4), (2, 5)	
(4, 6)	-5.000000	0.000000	(2, 5)	
(5, 2)	2.000000	1.000000	(5, 2), (4, 3)	
(5, 3)	-9.000000	0.000000	(5, 2), (4, 3), (3, 4)	
(3, 5)	-4.000000	0.000000	(3, 4), (2, 5)	

All cells' outputs in Iteration 6 are the same with all cells' outputs in Iteration 5. So the first horizon is extracted. The first horizon is shown in Fig. 3.15. Delete peaks on the extracted horizon. There are still some peaks. So set up the initial condition of the network again.

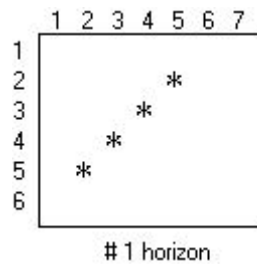


Fig. 3.15 The first extracted horizon.

	1	2	3	4	5	6	7
1							
2							
3							
4			*	.	.		
5							
6							

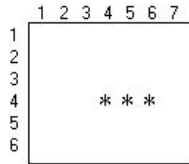
Iteration	Present peak	Present linking direction	Energy
7	(4, 4)	Upper-right	0
Cell	State value	Output value	
(4, 4)	1.000000	1.000000	
(4, 5)	0.000000	0.000000	
(4, 6)	0.000000	0.000000	

	1	2	3	4	5	6	7
1							
2							
3							
4			*	*	.		
5							
6							

Iteration	Present peak	Present linking direction	Energy
8	(4, 5)	Right	-1
Cell	State value	Output value	Neighboring cells which influence center cell
(4, 4)	1.000000	1.000000	(4, 4)
(4, 5)	1.000000	1.000000	(4, 4)
(4, 6)	0.000000	0.000000	

	1	2	3	4	5	6	7
1							
2							
3							
4			*	*	*		
5							
6							

Iteration	Present peak	Present linking direction	Energy
9	(4, 6)	Right	-2
Cell	State value	Output value	Neighboring cells which influence center cell
(4, 4)	2.000000	1.000000	(4, 4), (4, 5)
(4, 5)	2.000000	1.000000	(4, 4), (4, 5)
(4, 6)	1.000000	1.000000	(4, 5)



Iteration	Present peak	Present linking direction	Energy
10	(4, 6)	Right	-2
Cell	State value	Output value	Neighboring cells which influence center cell
(4, 4)	2.000000	1.000000	(4, 4), (4, 5)
(4, 5)	3.000000	1.000000	(4, 4), (4, 5), (4, 6)
(4, 6)	2.000000	1.000000	(4, 5), (4, 6)

All cells' outputs in Iteration 10 are the same with all cells' outputs in Iteration 9. So the second horizon is extracted. The second horizon is shown in Fig. 3.16. Delete peaks on the extracted horizon. There is no peak. So the work of seismic horizon linking is finished.

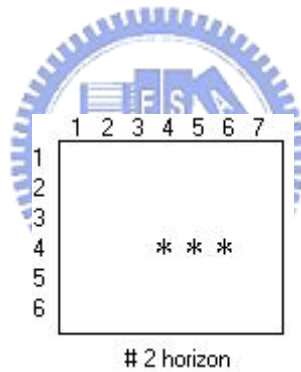
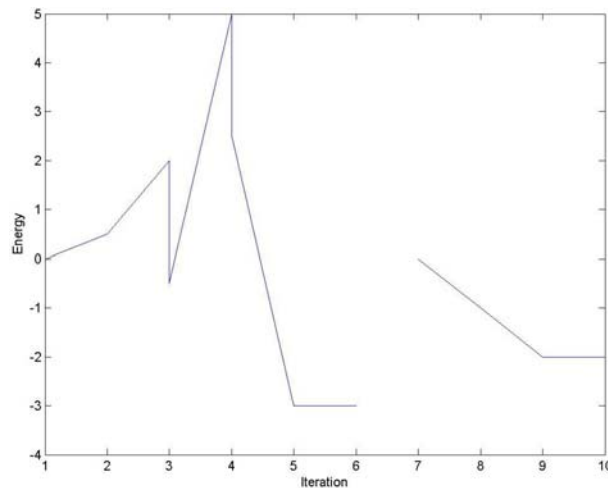
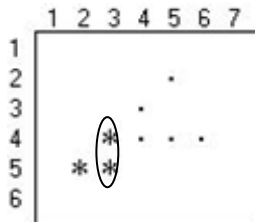


Fig. 3.16 The second extracted horizon.

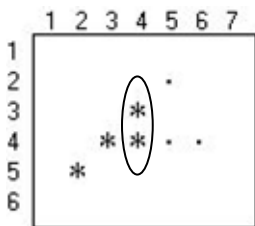
Energy curve:



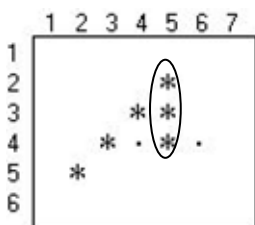
In the above energy curve graph, the curve between Iteration 1 and Iteration 6 is the energy curve when we link the first horizon, and the curve between Iteration 7 and Iteration 10 is the energy curve when we link the second horizon. In the above energy curve graph, there are three line segments which are the cases that energy is raising. The first case of energy rising is between Iteration 1 and Iteration 2, the output of each cell in Iteration 2 is shown in the following figure:



In the above figure, the two cells enclosed by an ellipse accord with the second constraint shown in Fig. 3.8. So the energy is increased. The second case of energy rising is between Iteration 2 and Iteration 3, the output of each cell in Iteration 3 is shown in the following figure:



In the above figure, the two cells enclosed by an ellipse accord with the second constraint shown in Fig. 3.8. So the energy is increased. The third case of energy rising is between Iteration 3 and Iteration 4, the output of each cell in Iteration 4 is shown in the following figure:



In the above figure, the three cells enclosed by an ellipse accord with the second constraint shown in Fig. 3.8. So the energy is increased.  $A(i, j; k, l)$  is not fixed, it is changed whenever the present peak and the present linking direction are changed. This is different from the conventional CNN. So the energy curve is not continuous.



### 3.6 Experimental Results

#### Experiment 1.

The simulated seismic peak data is shown in Fig. 3.17(a), we can show the peaks as solid dots, as Fig. 3.17(b). The size of the input data is  $6 \times 7$ . We set  $a_1 = 1$ ,  $a_2 = a_3 = 5$ ,  $a_4 = 1$ .

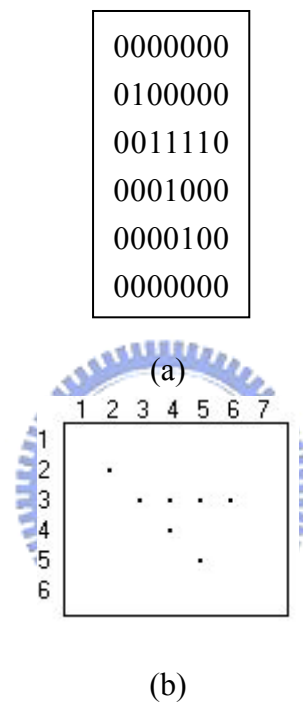


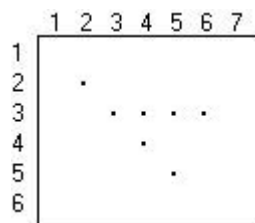
Fig. 3.17 (a) The simulated seismic peak data, (b) The peaks in (a) are shown as solid dots.

Iteration: The numbers of complete surveys.

Present Peak: The coordinate of present peak.

Present Linking Direction: The present linking direction.

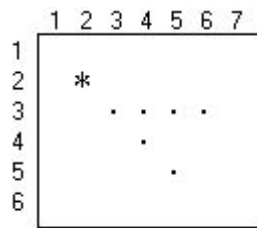
1. Load peak data.



Iteration	
Present Peak	

Present Linking Direction :

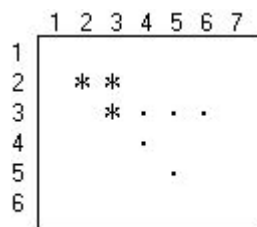
2. Iteration: 1, begin linking the first horizon, set up the initial condition.



Iteration	1
Present Peak	(2, 2)

Present Linking Direction : ↗

3. Iteration: 2

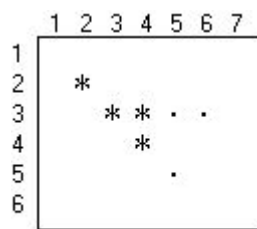


Iteration	2
Present Peak	(2, 2)

Present Linking Direction : ↗



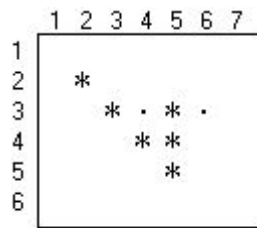
4. Iteration: 3




Iteration	3
Present Peak	(3, 3)

Present Linking Direction : ↘

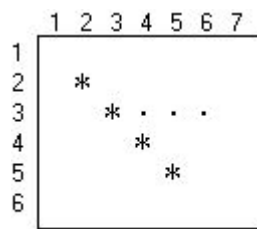
5. Iteration: 4




Iteration	4
Present Peak	(4, 4)

Present Linking Direction : 

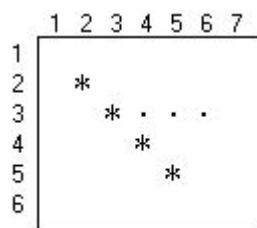
6. Iteration: 5




Iteration	5
Present Peak	(5, 5)

Present Linking Direction : 

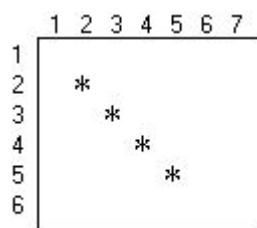
7. Iteration: 6



Iteration	6
Present Peak	(5, 5)

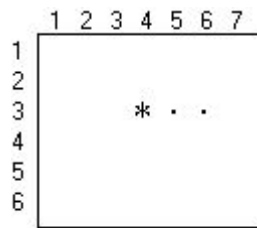
Present Linking Direction : 

8. The first extracted horizon.



# 1 horizon

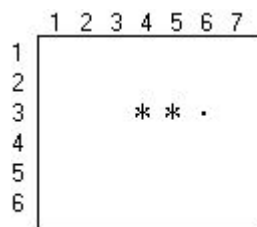
9. Iteration: 7, begin linking the second horizon, set up the initial condition.



Iteration	7
Present Peak	(3, 4)

Present Linking Direction : ↗

10. Iteration: 8

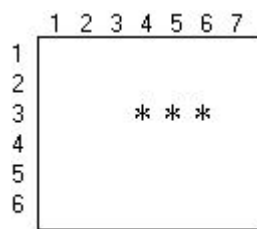


Iteration	8
Present Peak	(3, 5)

Present Linking Direction : →



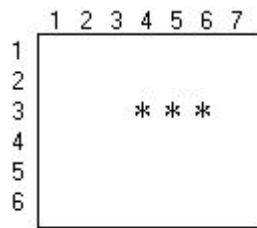
11. Iteration: 9



Iteration	9
Present Peak	(3, 6)

Present Linking Direction : →

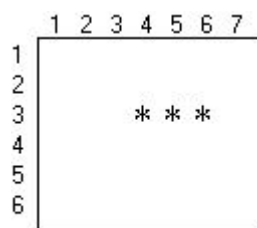
12. Iteration: 10



Iteration	10
Present Peak	(3, 6)

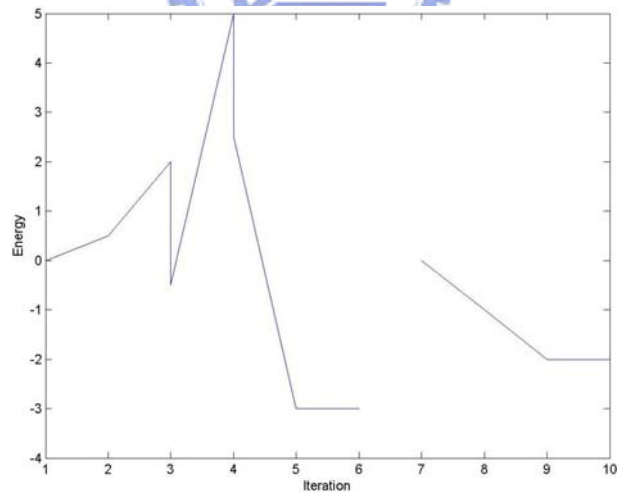
Present Linking Direction : →

13. The second extracted horizon.



# 2 horizon

Energy curve:



## Experiment 2.

The simulated seismic peak data is shown in Fig. 3.18(a), we can show the peaks as solid dots, as Fig. 3.18(b). The simulated peak data contain a broken horizon. The broken horizon contains several broken parts. The size of the input data is  $8 \times 22$ . We set  $a_1 = 1$ ,  $a_2 = a_3 = 5$ ,  $a_4 = 1$ .

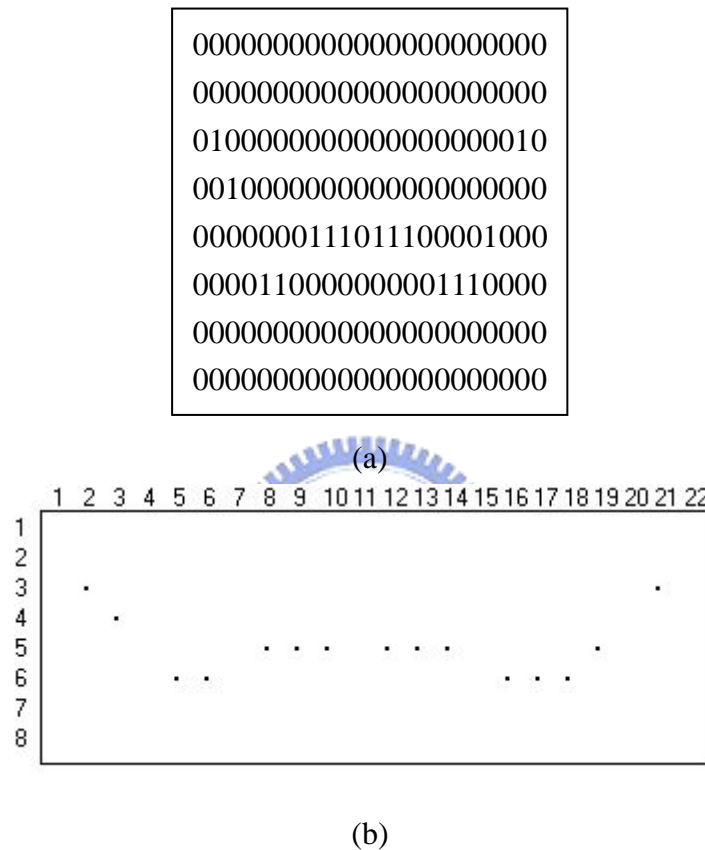
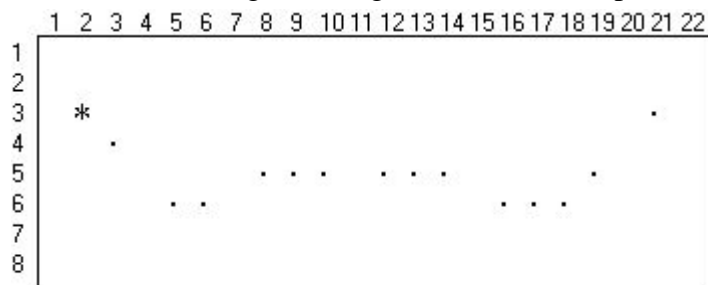


Fig. 3.18 (a) The simulated seismic peak data, (b) The peaks in (a) are shown as solid dots.

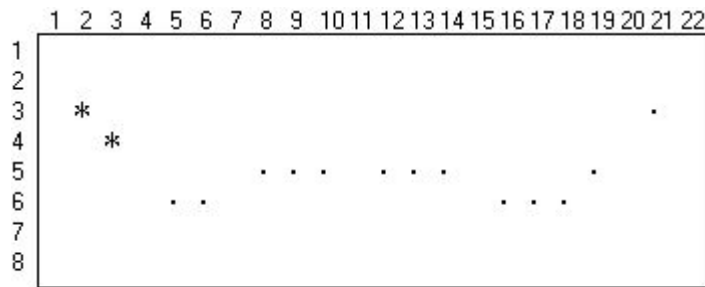
- Iteration: 1, begin linking the horizon, set up the initial condition.



Iteration	1
Present Peak	(3, 2)

Present Linking Direction : ↗

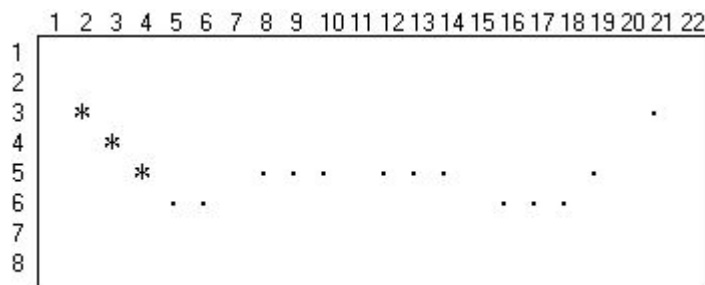
2. Iteration: 2



Iteration	2
Present Peak	(4, 3)

Present Linking Direction :

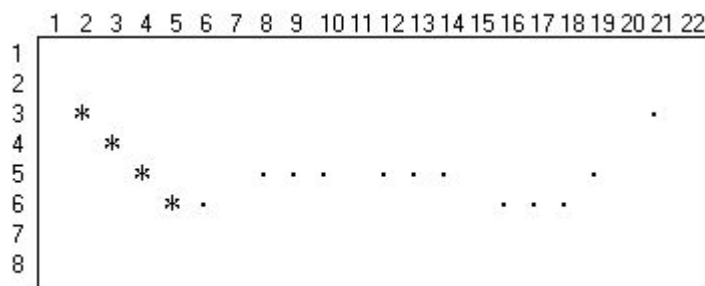
3. Iteration: 3



Iteration	3
Present Peak	(5, 4)

Present Linking Direction :

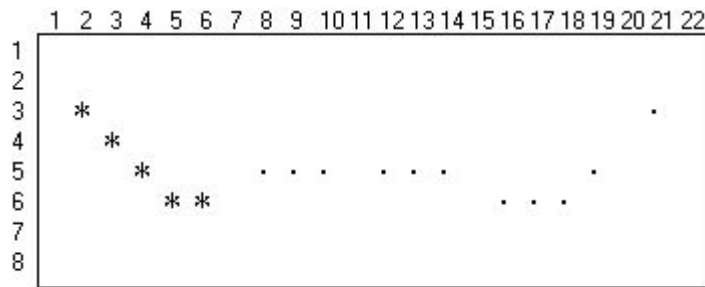
4. Iteration: 4



Iteration	4
Present Peak	(6, 5)

Present Linking Direction :

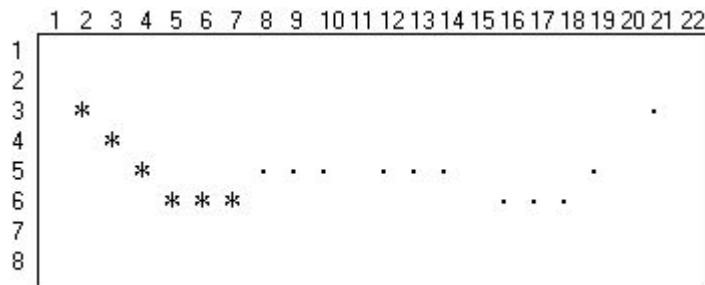
5. Iteration: 5



Iteration	5
Present Peak	(6, 6)

Present Linking Direction : →

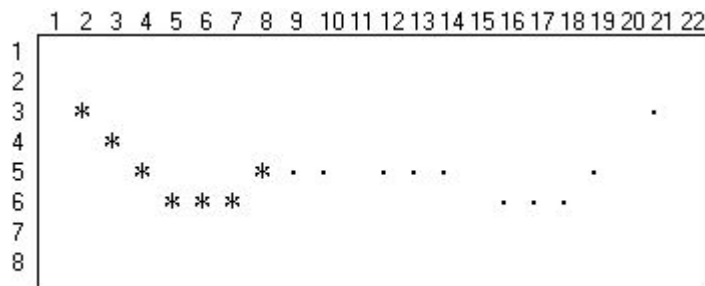
6. Iteration: 6



Iteration	6
Present Peak	(6, 7)

Present Linking Direction : →

7. Iteration: 7

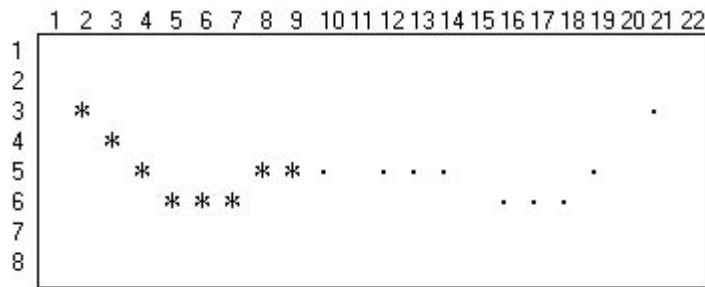


Iteration	7
Present Peak	(5, 8)

Present Linking Direction : ↗



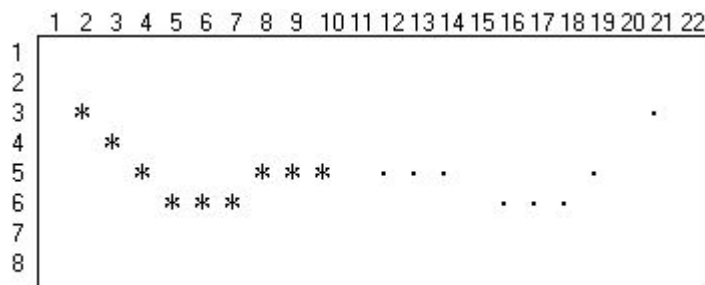
8. Iteration: 8



Iteration	8
Present Peak	(5, 9)

Present Linking Direction : →

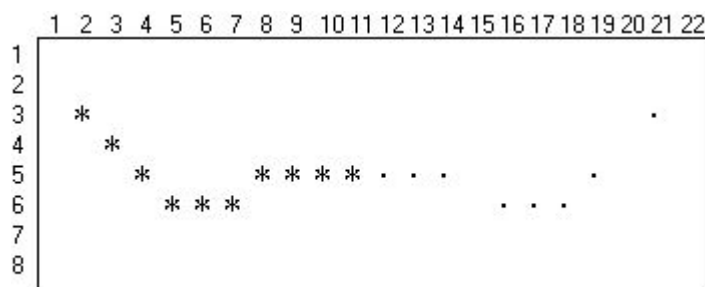
9. Iteration: 9



Iteration	9
Present Peak	(5, 10)

Present Linking Direction : →

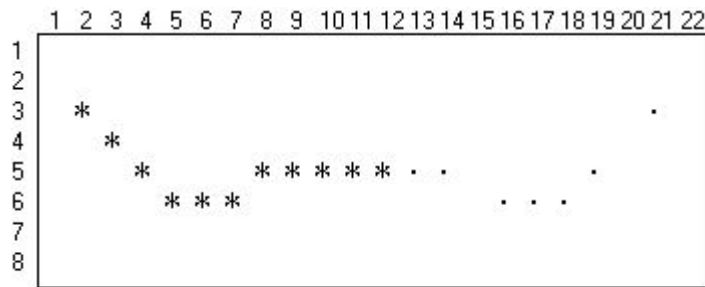
10. Iteration: 10



Iteration	10
Present Peak	(5, 11)

Present Linking Direction : →

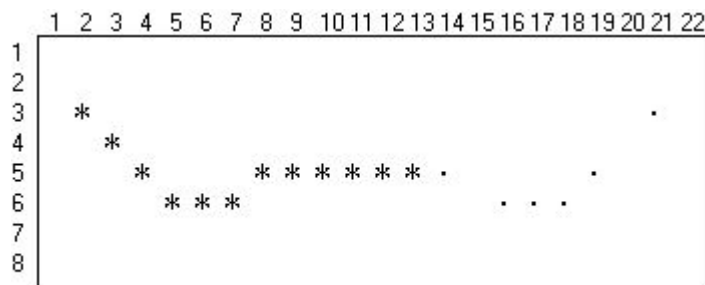
11. Iteration: 11



Iteration	11
Present Peak	(5.12)

Present Linking Direction: →

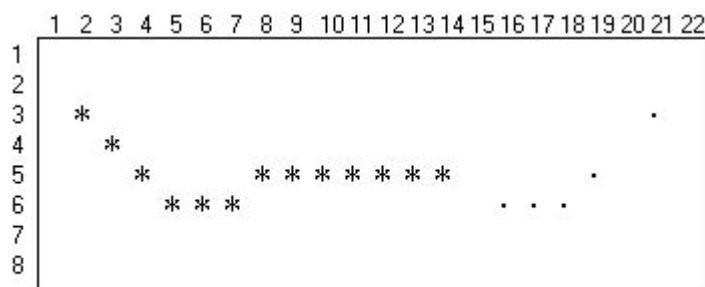
12. Iteration: 12



Iteration	12
Present Peak	(5.13)

Present Linking Direction: →

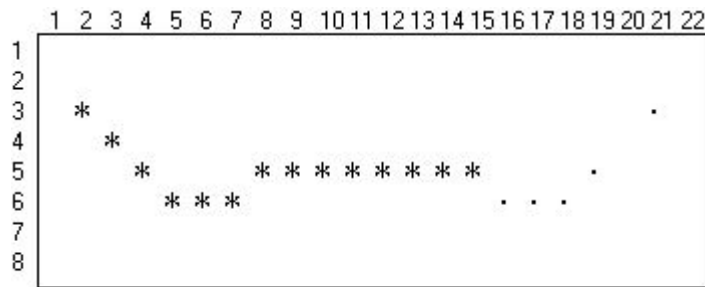
13. Iteration: 13



Iteration	13
Present Peak	(5.14)

Present Linking Direction: →

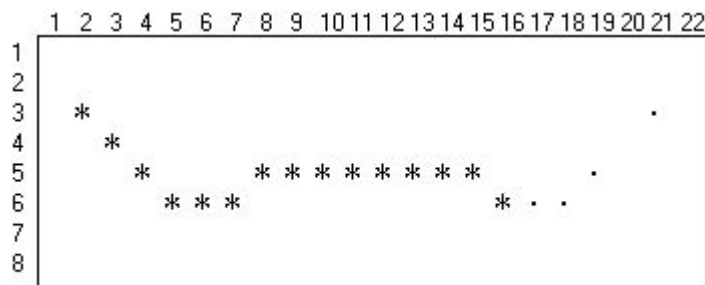
14. Iteration: 14



Iteration	14
Present Peak	(5. 15)

Present Linking Direction : →

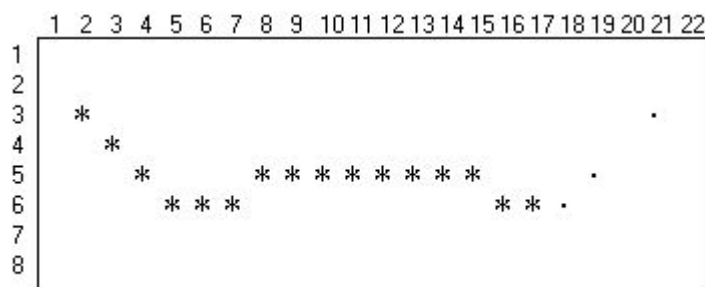
15. Iteration: 15



Iteration	15
Present Peak	(6. 16)

Present Linking Direction : ↘

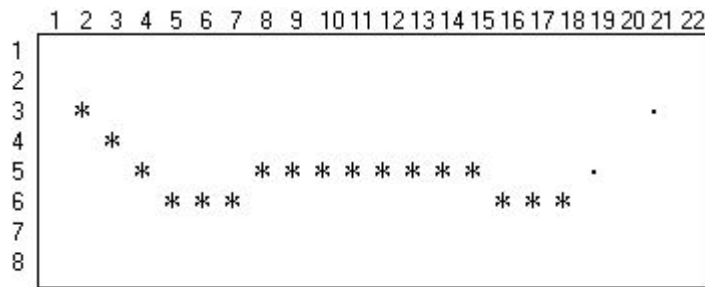
16. Iteration: 16



Iteration	16
Present Peak	(6. 17)

Present Linking Direction : →

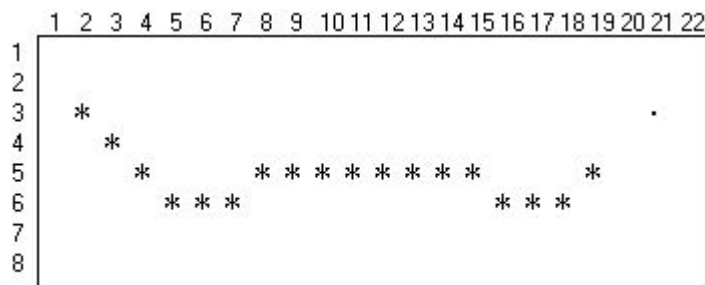
17. Iteration: 17



Iteration	17
Present Peak	(6, 18)

Present Linking Direction : →

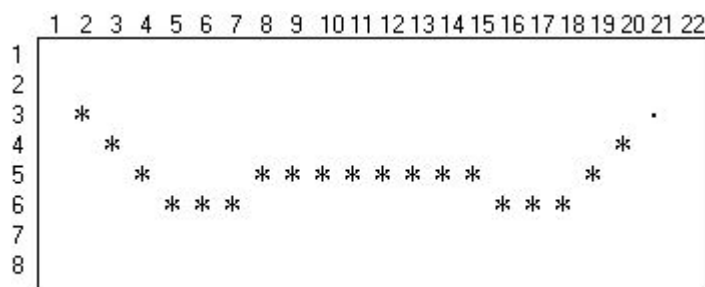
18. Iteration: 18



Iteration	18
Present Peak	(5, 19)

Present Linking Direction : ↗

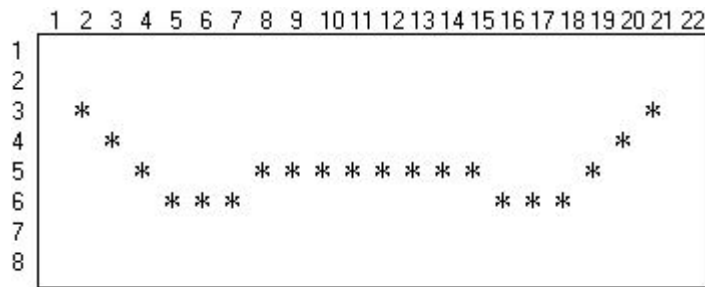
19. Iteration: 19



Iteration	19
Present Peak	(4, 20)

Present Linking Direction : ↗

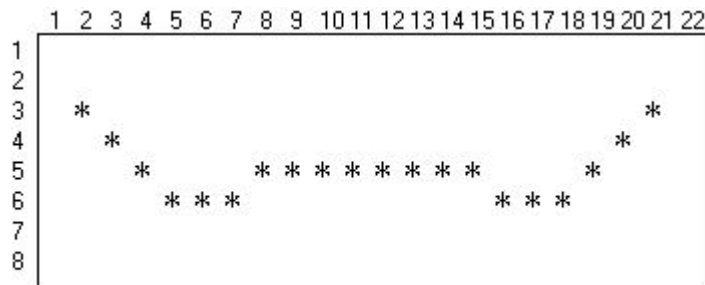
20. Iteration: 20



Iteration	20
Present Peak	(3, 21)

Present Linking Direction : ↗

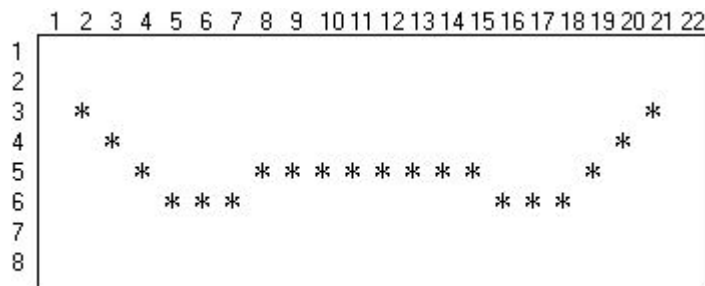
21. Iteration: 21



Iteration	21
Present Peak	(3, 21)

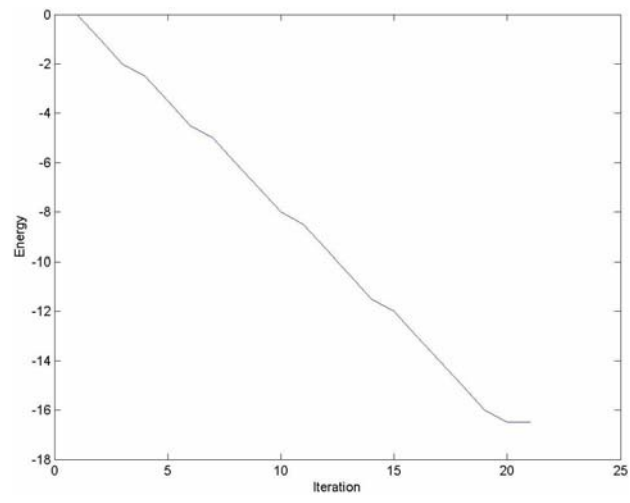
Present Linking Direction : ↗

22. The extracted horizon.



# 1 horizon

Energy curve:



### Experiment 3.

The simulated seismic peak data of bright spot pattern is shown in Fig. 3.19(a), we can show the peaks as solid dots, as Fig. 3.19(b). The size of the input data is  $14 \times 46$ .

We set  $a_1 = 1$ ,  $a_2 = a_3 = 5$ ,  $a_4 = 1$ .

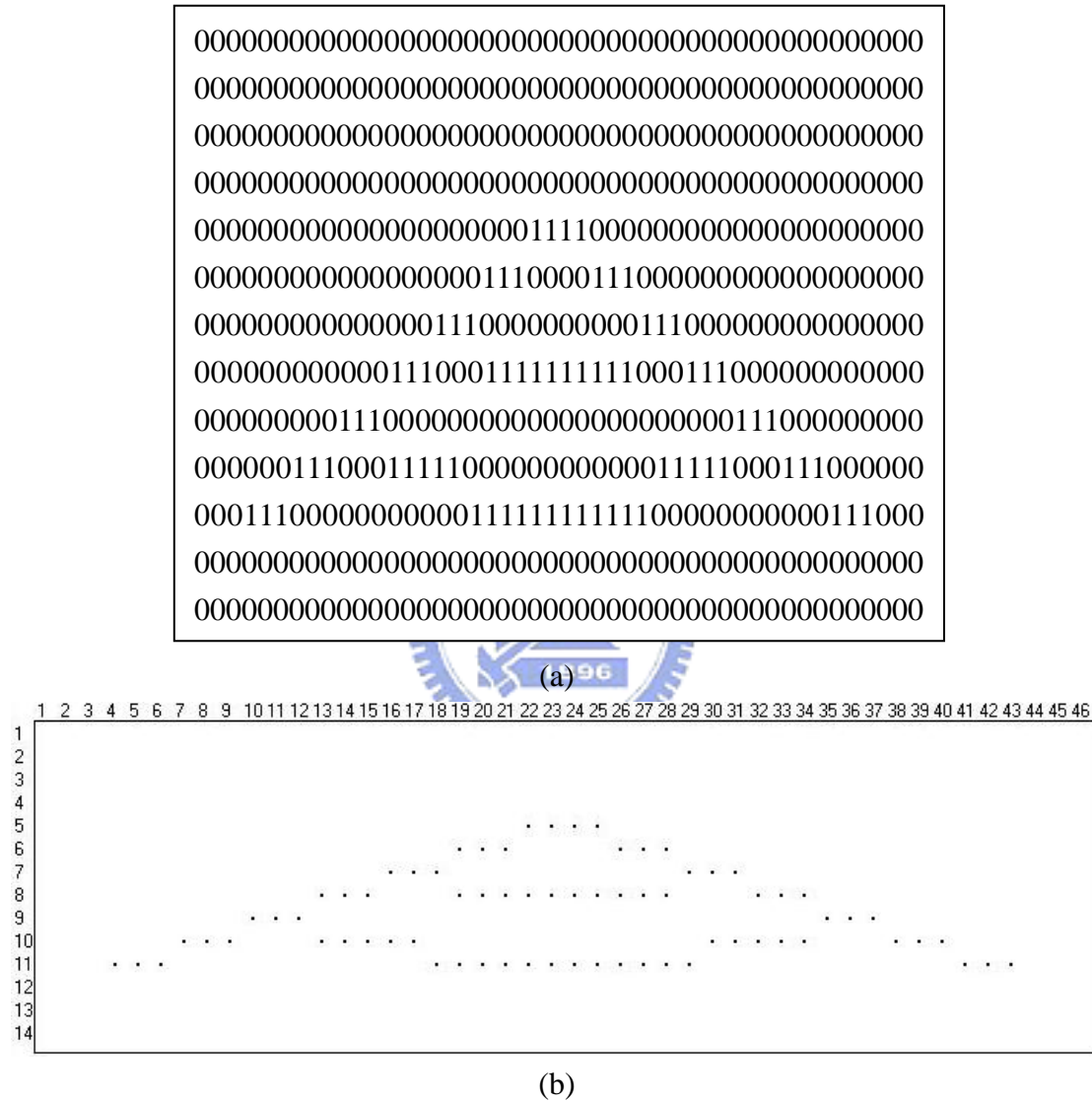
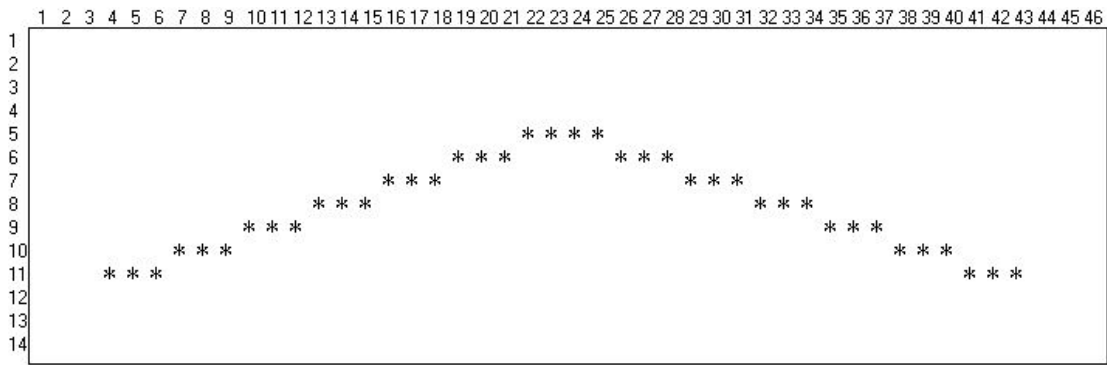


Fig. 3.19 (a) The simulated seismic peak data, (b) The peaks in (a) are shown as solid dots.

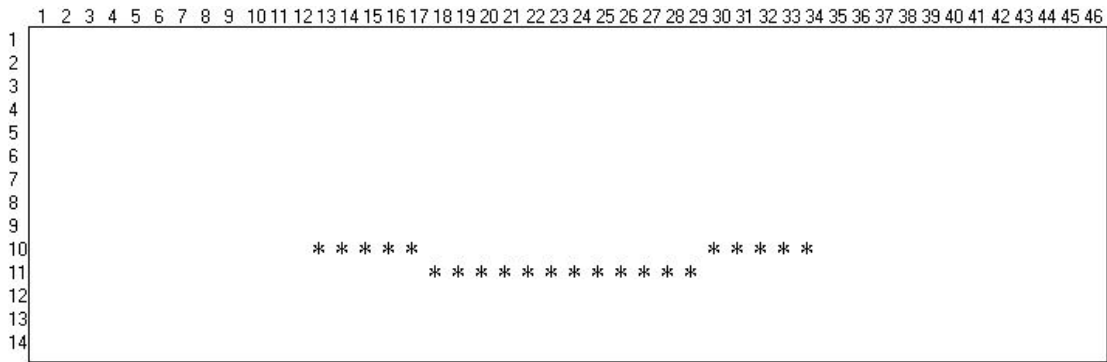
1. The first extracted horizon.



Iteration	41
Present Peak	(11, 43)

Present Linking Direction : →

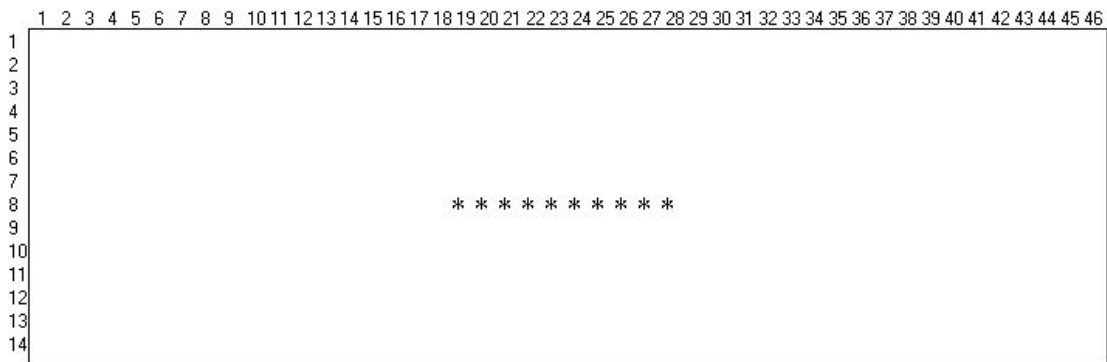
2. The second extracted horizon.



Iteration	64
Present Peak	(10, 34)

Present Linking Direction : →

3. The third extracted horizon.

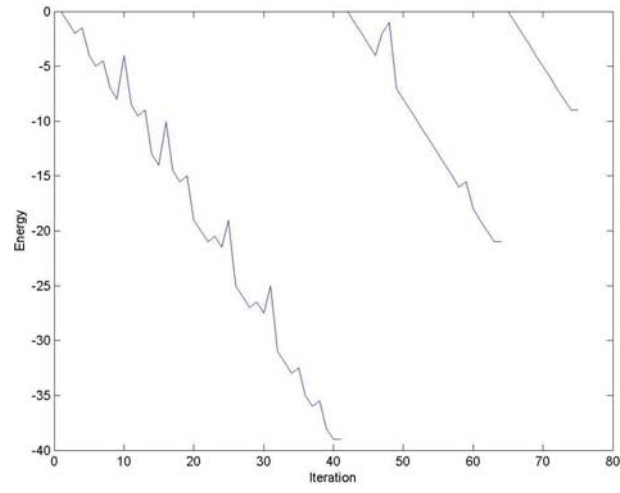


Iteration	75
Present Peak	(8, 28)

Present Linking Direction : →



Energy curve:



#### Experiment 4.

The simulated seismic peak data of bright spot pattern is shown in Fig. 3.20(a), we can show the peaks as solid dots, as Fig. 3.20(b). The size of the input data is  $10 \times 10$ .

We set  $a_1 = 1$ ,  $a_2 = a_3 = 5$ ,  $a_4 = 1$ .

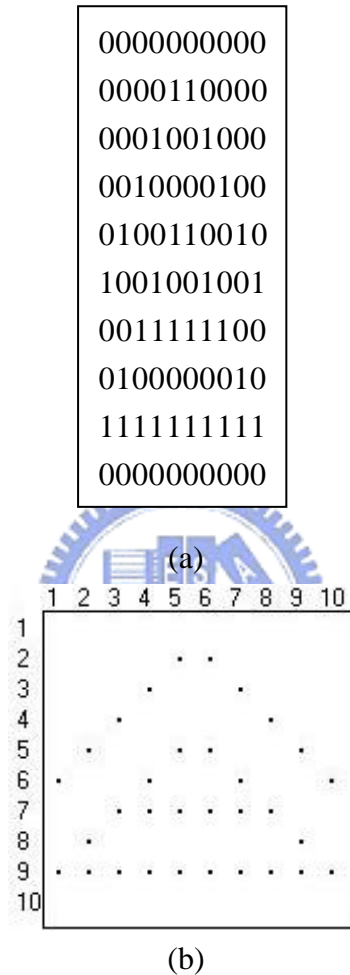
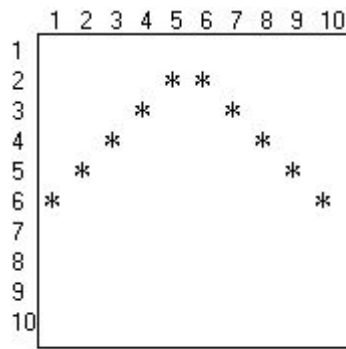


Fig. 3.20 (a) The simulated seismic peak data, (b) The peaks in (a) are shown as solid dots.

1. The first extracted horizon.

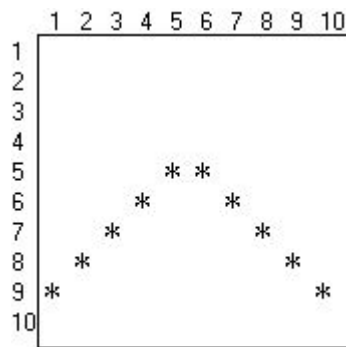


# 1 horizon

Iteration	11
Present Peak	(6, 10)

Present Linking Direction : ↘

2. The second extracted horizon.



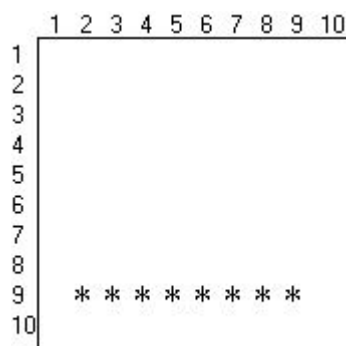
# 2 horizon

Iteration	22
Present Peak	(9, 10)

Present Linking Direction : ↘



3. The third extracted horizon.

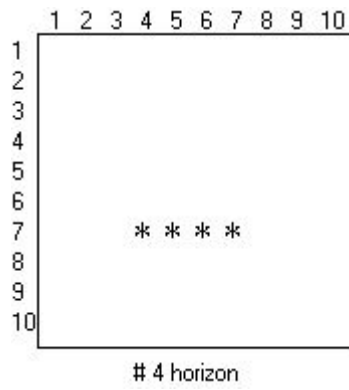


# 3 horizon

Iteration	31
Present Peak	(9, 9)

Present Linking Direction : →

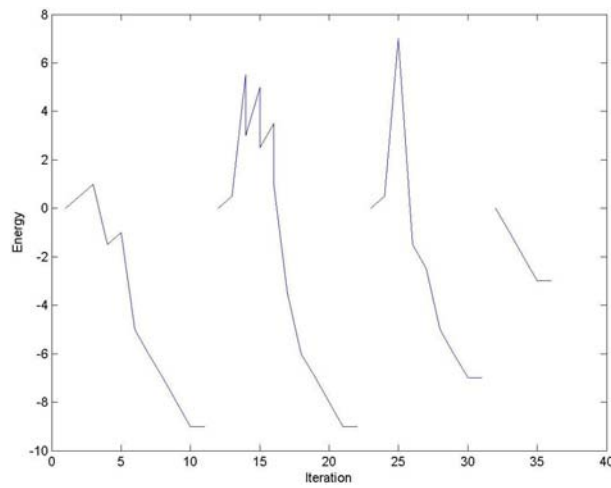
4. The fourth extracted horizon.



Iteration	36
Present Peak	(7, 7)

Present Linking Direction : →

Energy curve:



### Experiment 5.

The simulated seismic peak data of flat spot pattern is shown in Fig. 3.21(a), we can show the peaks as solid dots, as Fig. 3.21(b). The size of the input data is  $15 \times 50$ . We set  $a_1 = 1$ ,  $a_2 = a_3 = 5$ ,  $a_4 = 1$ .

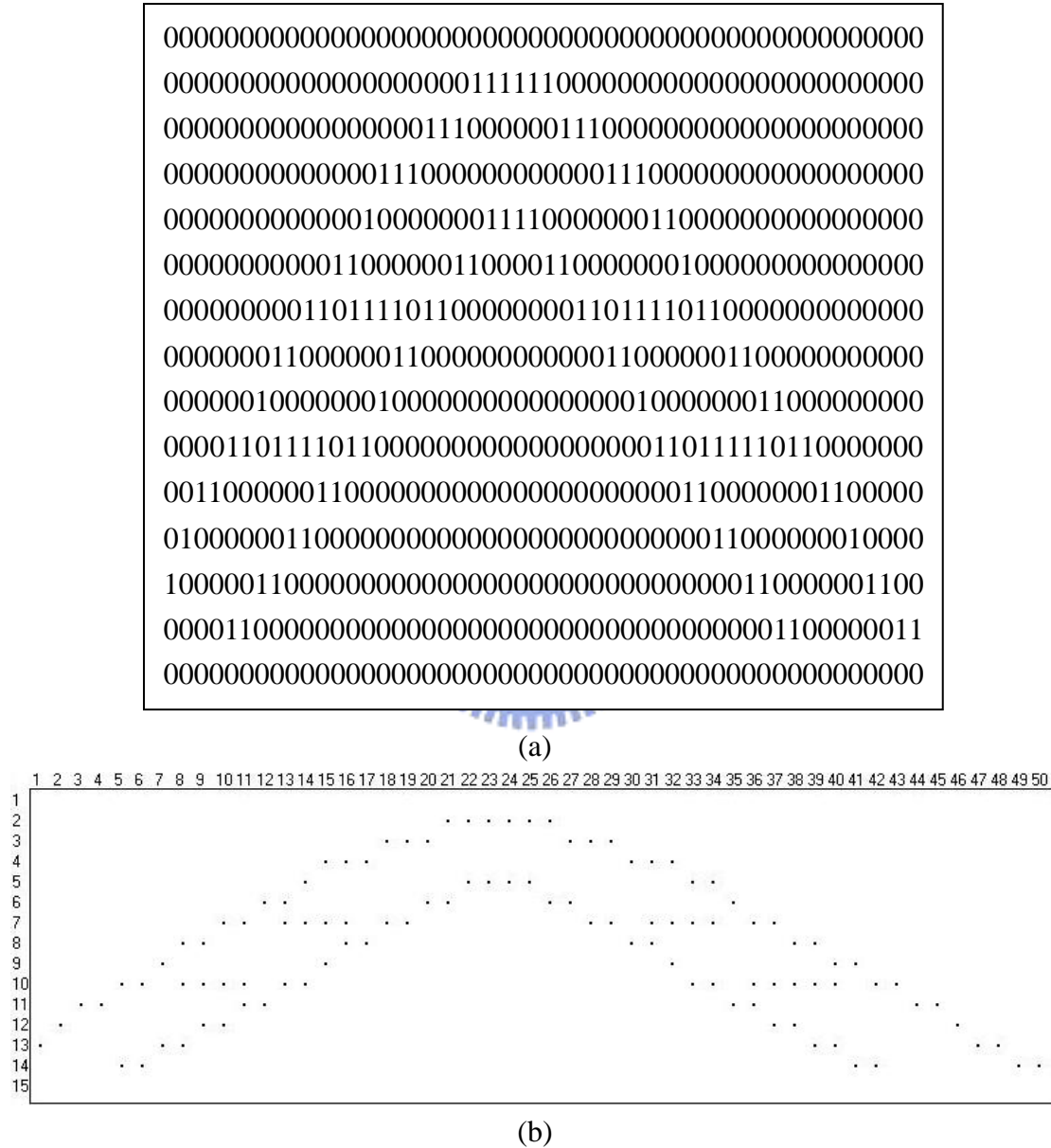
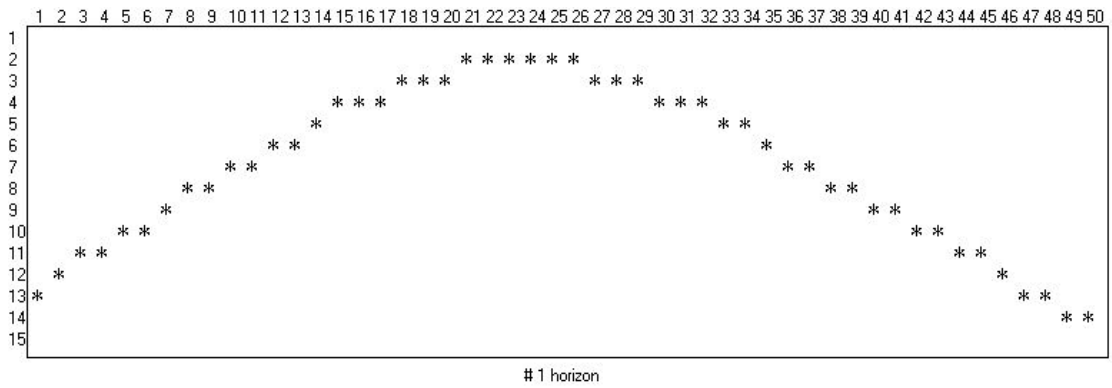


Fig. 3.21 (a) The simulated seismic peak data, (b) The peaks in (a) are shown as solid dots.

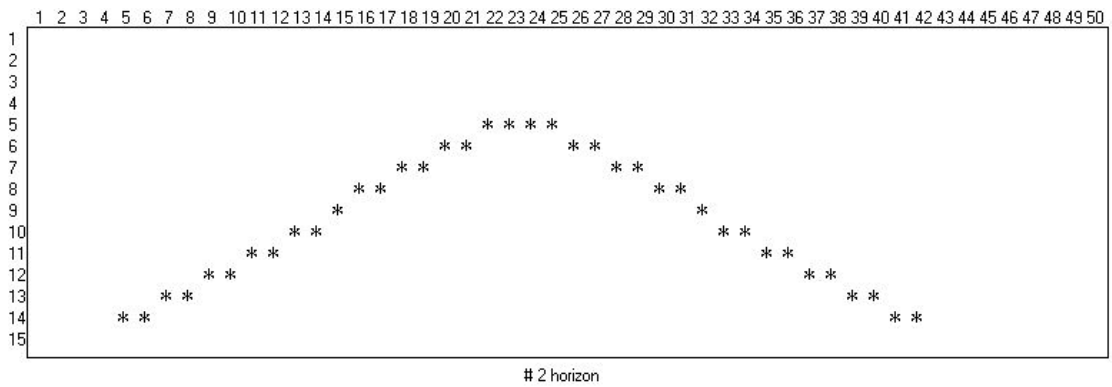
1. The first extracted horizon.



Iteration	51
Present Peak	(14, 49)

Present Linking Direction : ↘

2. The second extracted horizon.



Iteration	90
Present Peak	(14, 41)

Present Linking Direction : ↘

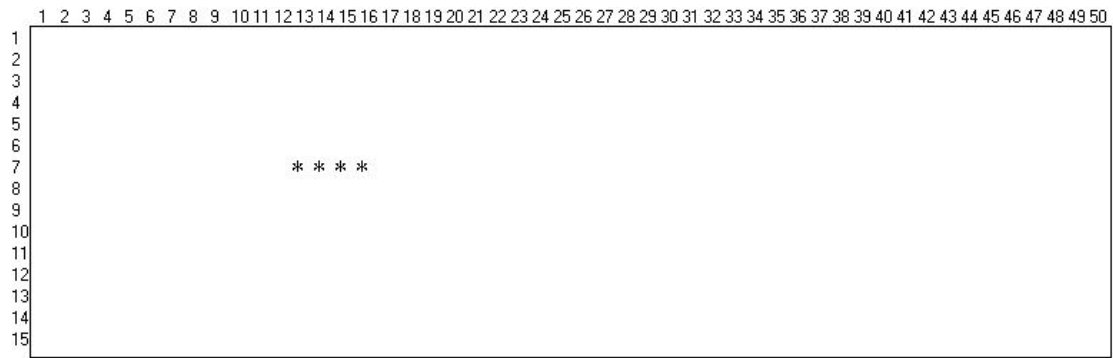
3. The third extracted horizon.



Iteration	95
Present Peak	(10, 11)

Present Linking Direction : →

4. The fourth extracted horizon.

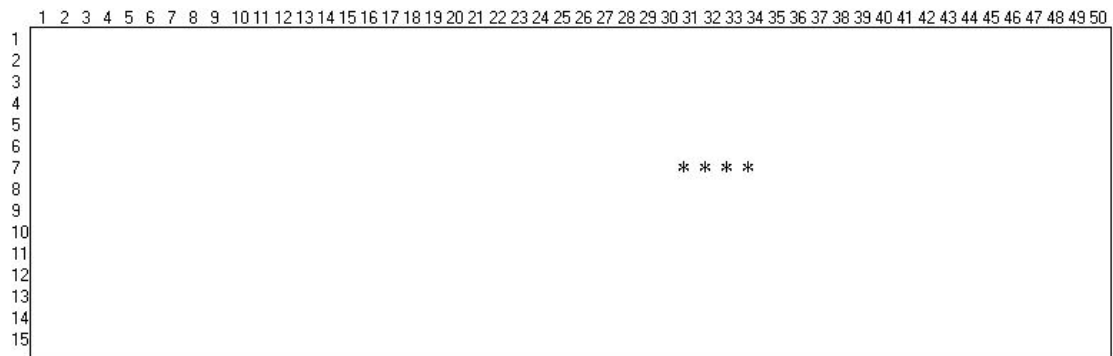


# 4 horizon

Iteration	100
Present Peak	(7, 16)

Present Linking Direction : →

5. The fifth extracted horizon.

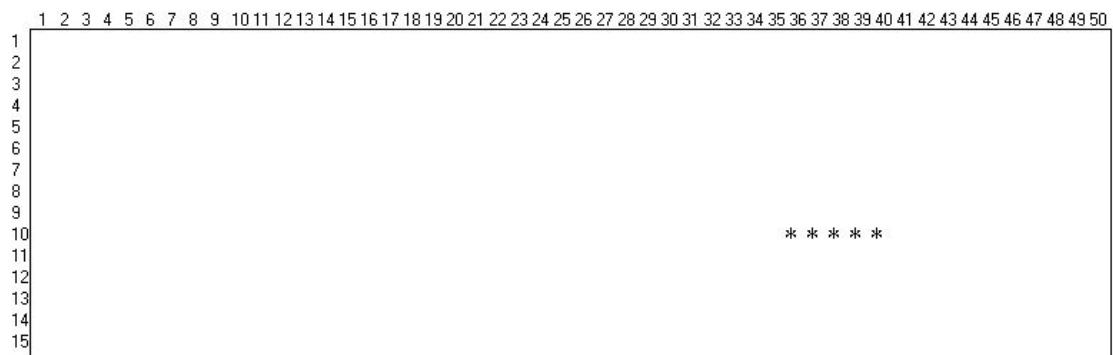


# 5 horizon

Iteration	105
Present Peak	(7, 34)

Present Linking Direction : →

6. The sixth extracted horizon.

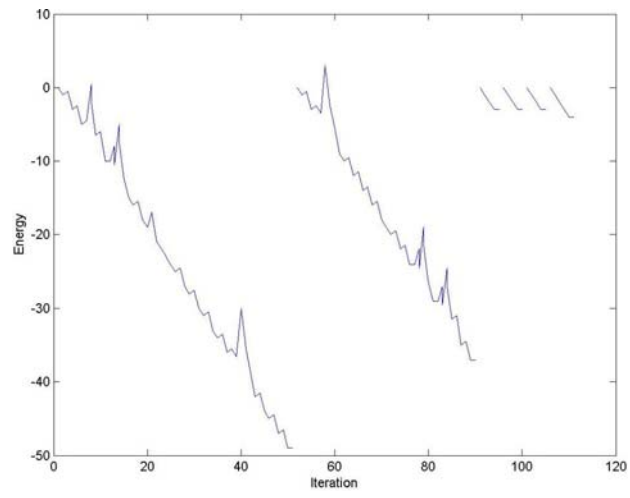


# 6 horizon

Iteration	111
Present Peak	(10, 40)

Present Linking Direction : →

Energy curve:

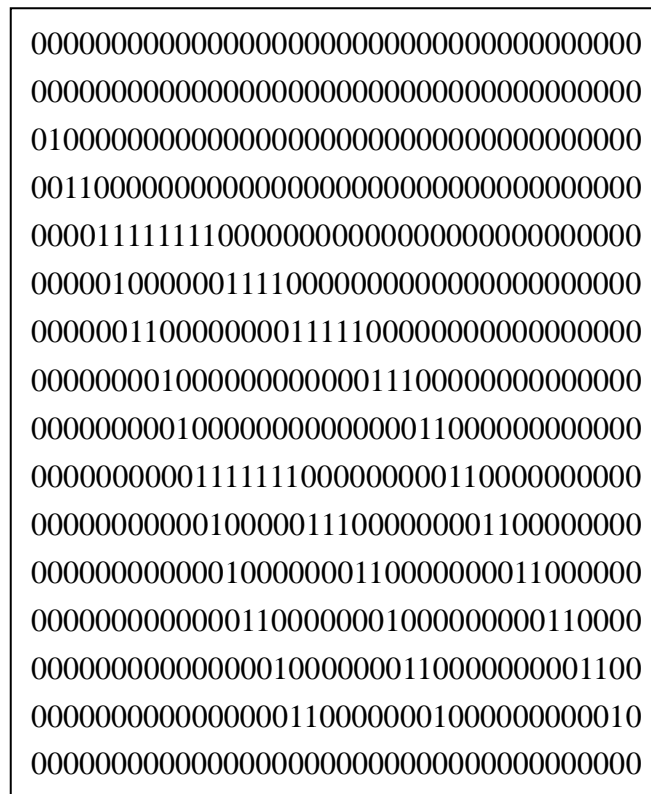




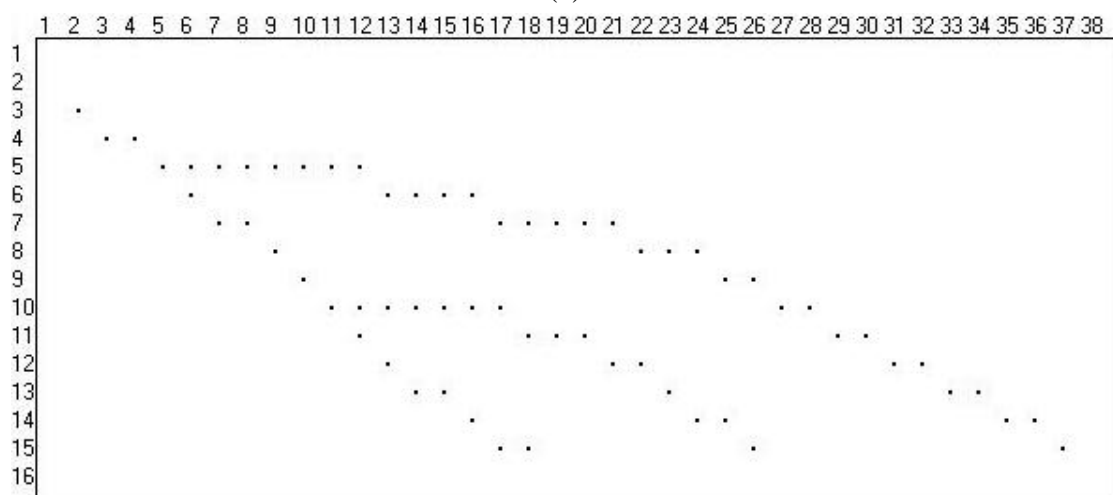
**Experiment 6.**

The simulated seismic peak data of sealevel rise pattern is shown in Fig. 3.22(a), we can show the peaks as solid dots, as Fig. 3.22(b). The size of the input data is  $16 \times 38$ .

We set  $a_1 = 1, a_2 = a_3 = 5, a_4 = 1$ .



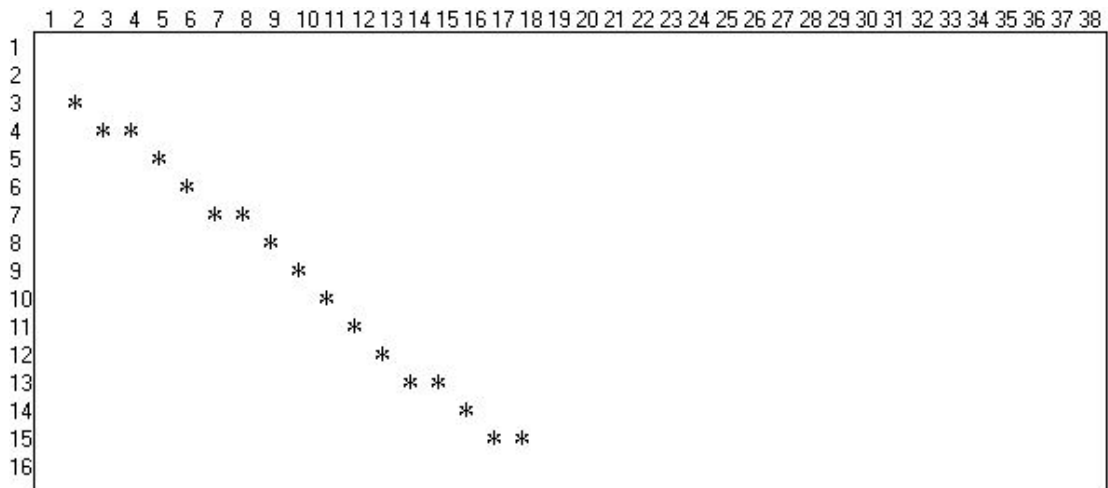
(a)



(b)

Fig. 3.22 (a) The simulated seismic peak data, (b) The peaks in (a) are shown as solid dots.

1. The first extracted horizon.



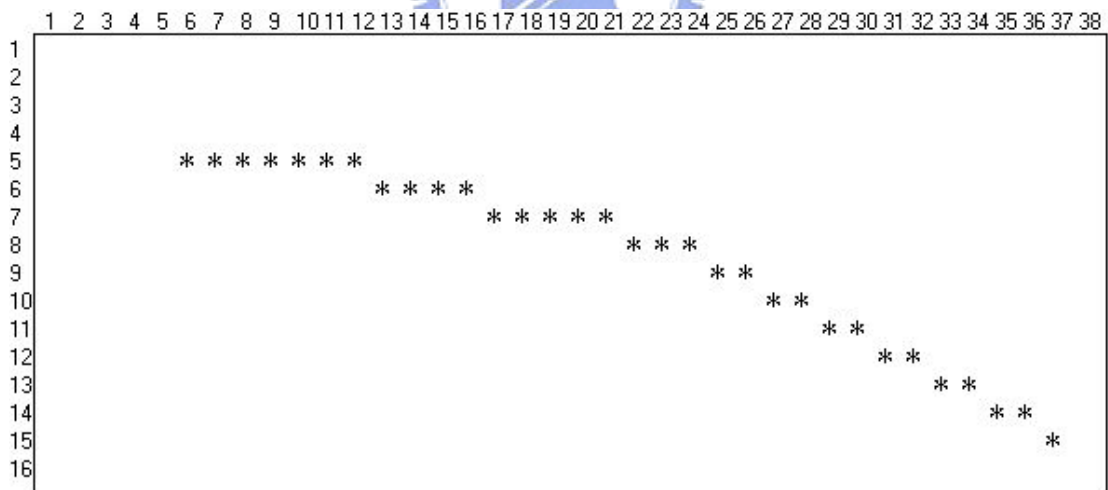
# 1 horizon

Iteration	18
Present Peak	(15, 17)

Present Linking Direction : ↘



2. The second extracted horizon.

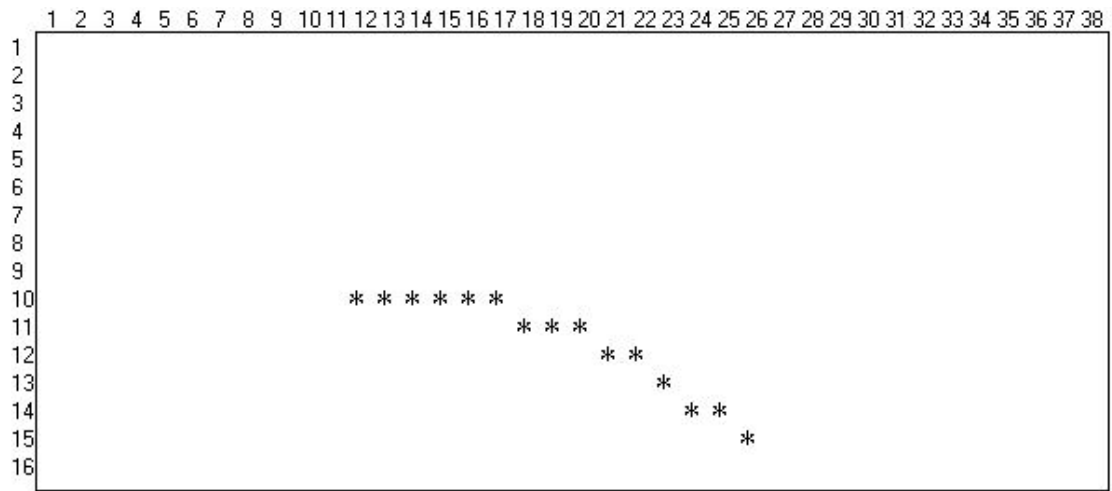


# 2 horizon

Iteration	51
Present Peak	(15, 37)

Present Linking Direction : ↘

3. The third extracted horizon.

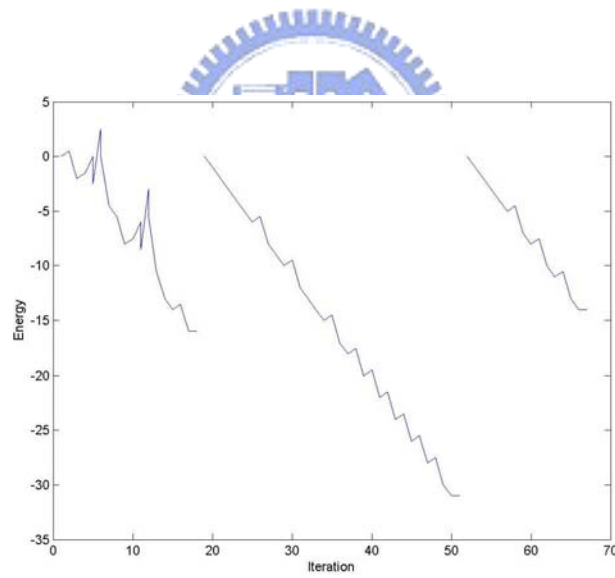


# 3 horizon

Iteration	67
Present Peak	(15, 26)

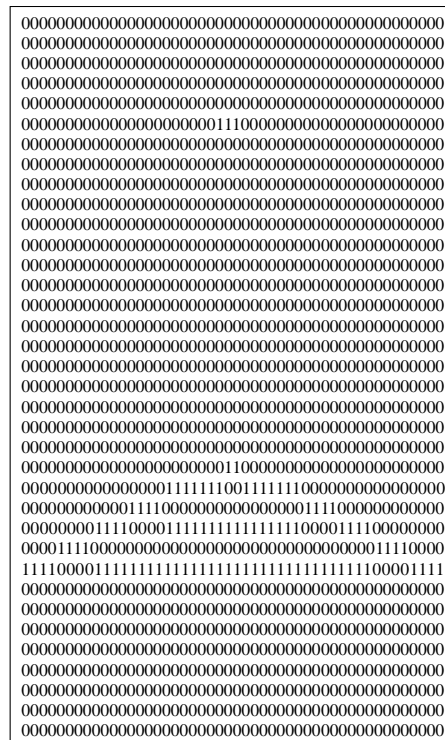
Present Linking Direction : ↘

Energy curve:

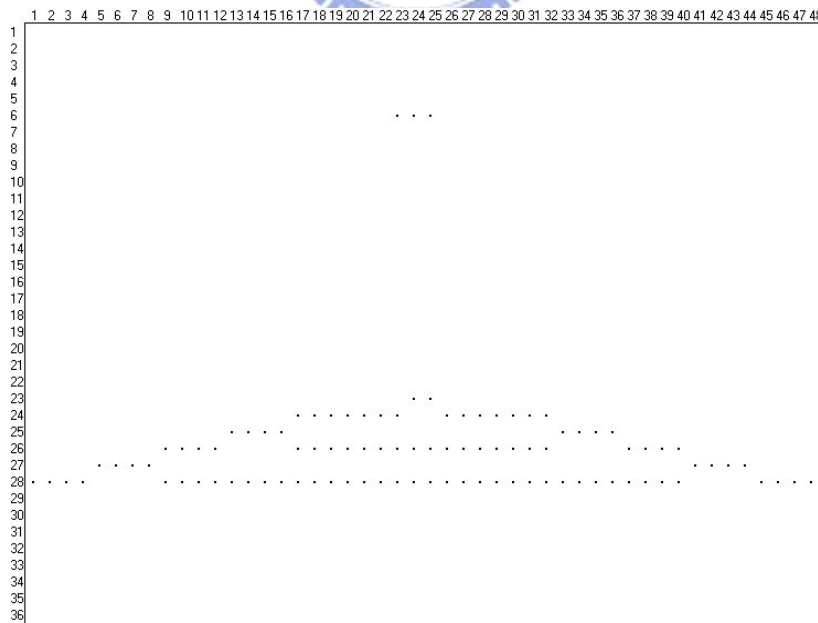


### Experiment 7.

The simulated seismic peak data is shown in Fig. 3.23(a), we can show the peaks as solid dots, as Fig. 3.23(b). The size of the input data is  $36 \times 48$ . We set  $a_1 = 1$ ,  $a_2 = a_3 = 5$ ,  $a_4 = 1$ .



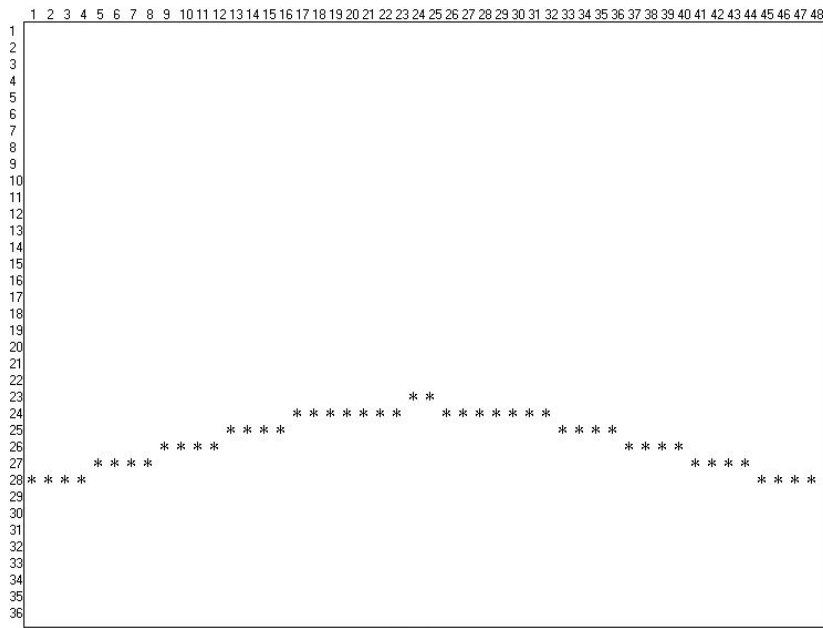
(a)



(b)

Fig. 3.23 (a) The simulated seismic peak data, (b) The peaks in (a) are shown as solid dots.

1. The first extracted horizon.



# 1 horizon

Iteration	49
Present Peak	(28, 48)

Present Linking Direction : →



2. The second extracted horizon.

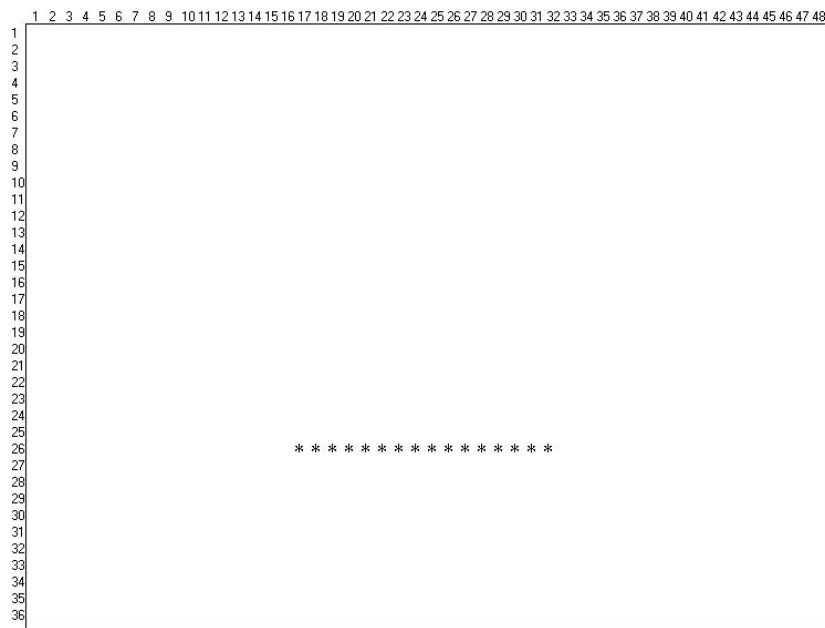


# 2 horizon

Iteration	82
Present Peak	(28, 40)

Present Linking Direction : →

### 3. The third extracted horizon.



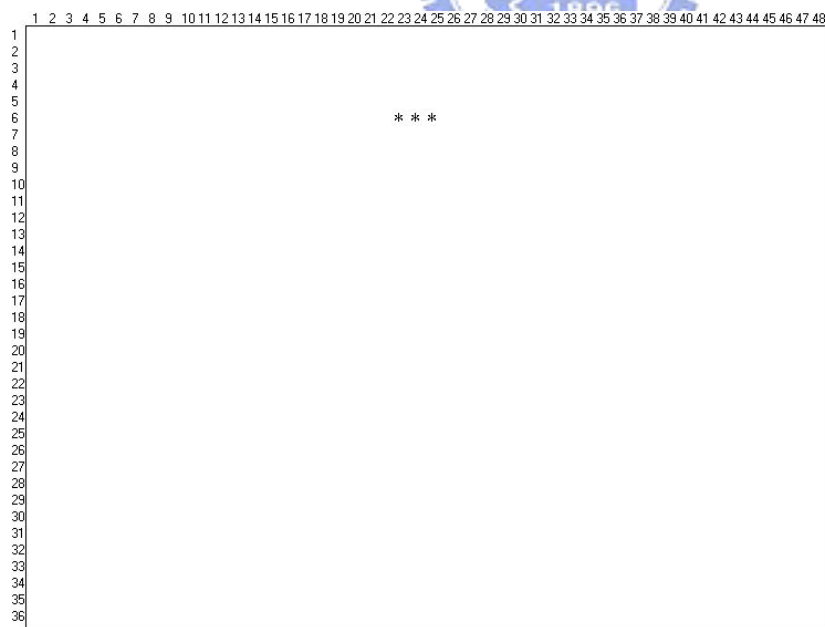
# 3 horizon

Iteration	99
Present Peak	(26, 32)

Present Linking Direction : →



### 4. The fourth extracted horizon.

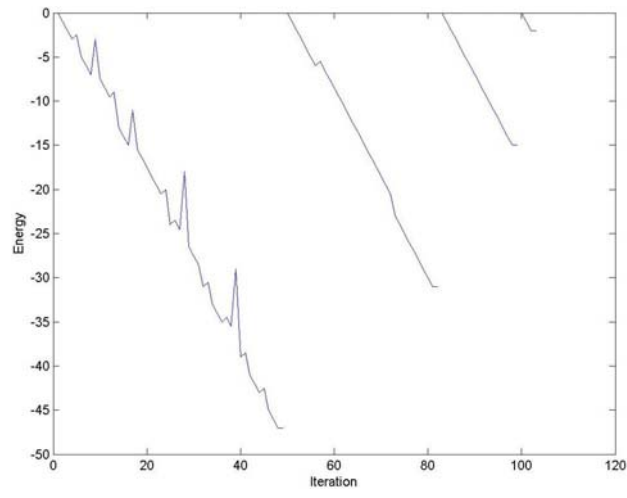


# 4 horizon

Iteration	103
Present Peak	(6, 25)

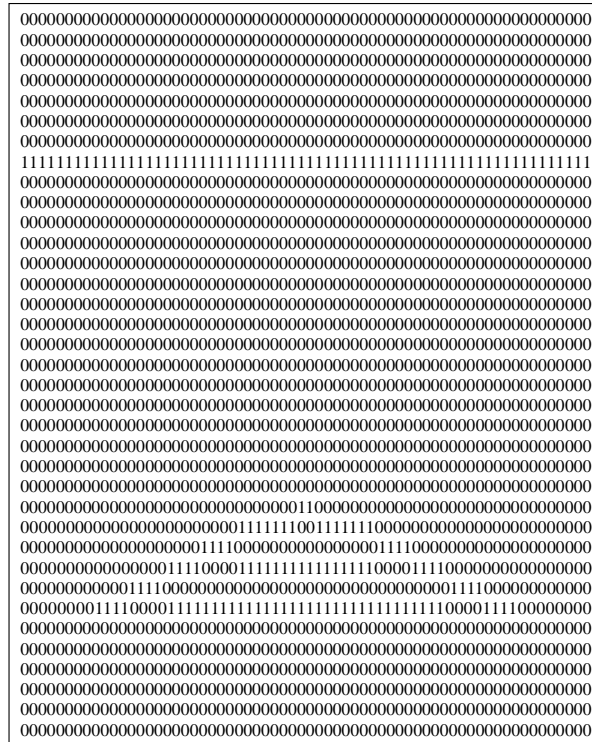
Present Linking Direction : →

Energy curve:

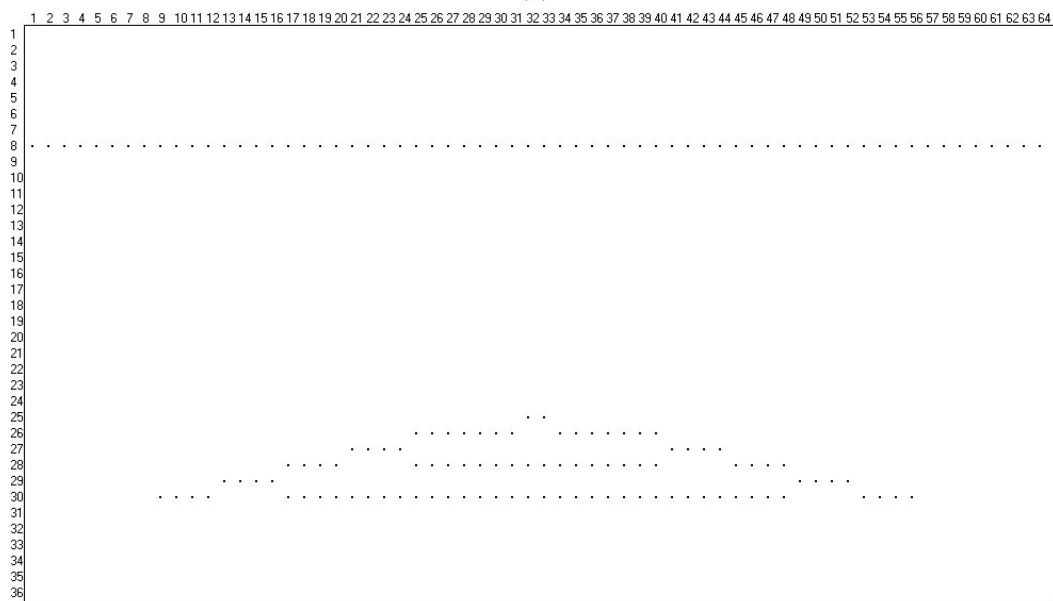


### Experiment 8.

The simulated seismic peak data is shown in Fig. 3.24(a), we can show the peaks as solid dots, as Fig. 3.24(b). The size of the input data is  $36 \times 64$ . We set  $a_1 = 1$ ,  $a_2 = a_3 = 5$ ,  $a_4 = 1$ .



(a)

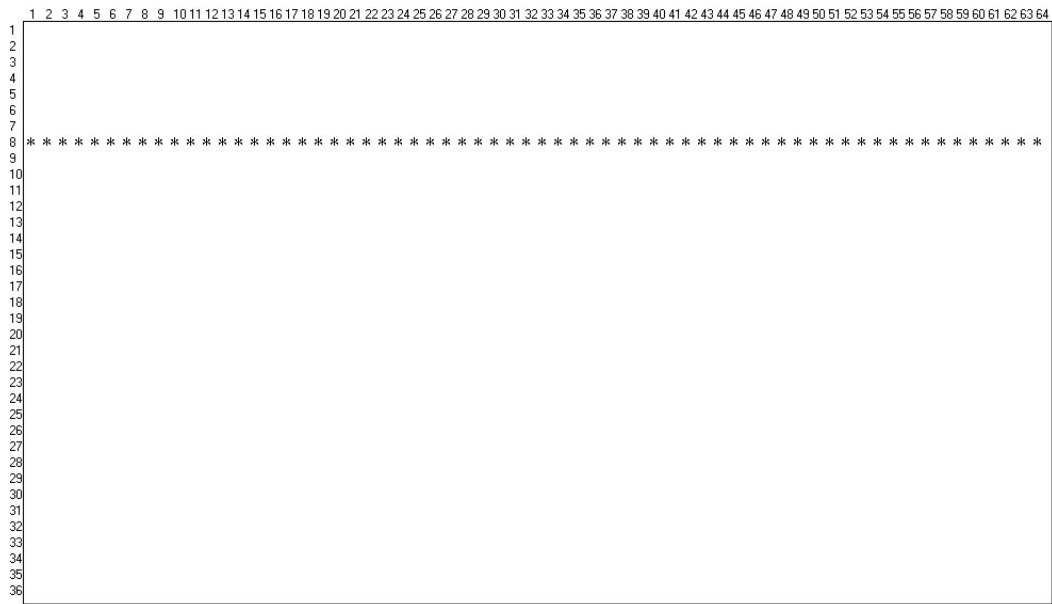


(b)

Fig. 3.24 (a) The simulated seismic peak data, (b) The peaks in (a) are shown as solid dots.



1. The first extracted horizon.



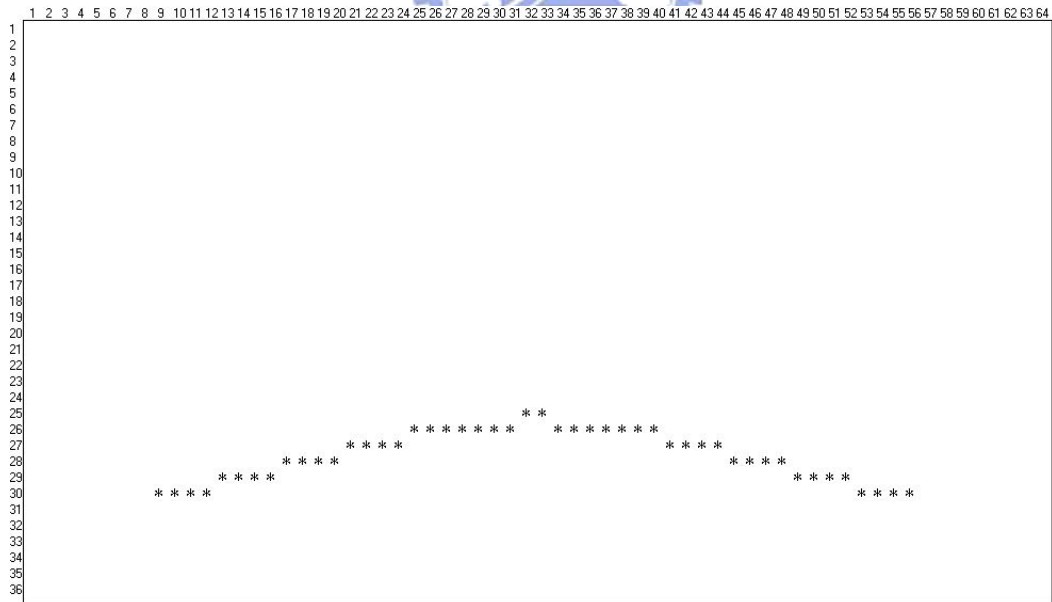
# 1 horizon

Iteration	65
Present Peak	(8, 64)

Present Linking Direction : →



2. The second extracted horizon.

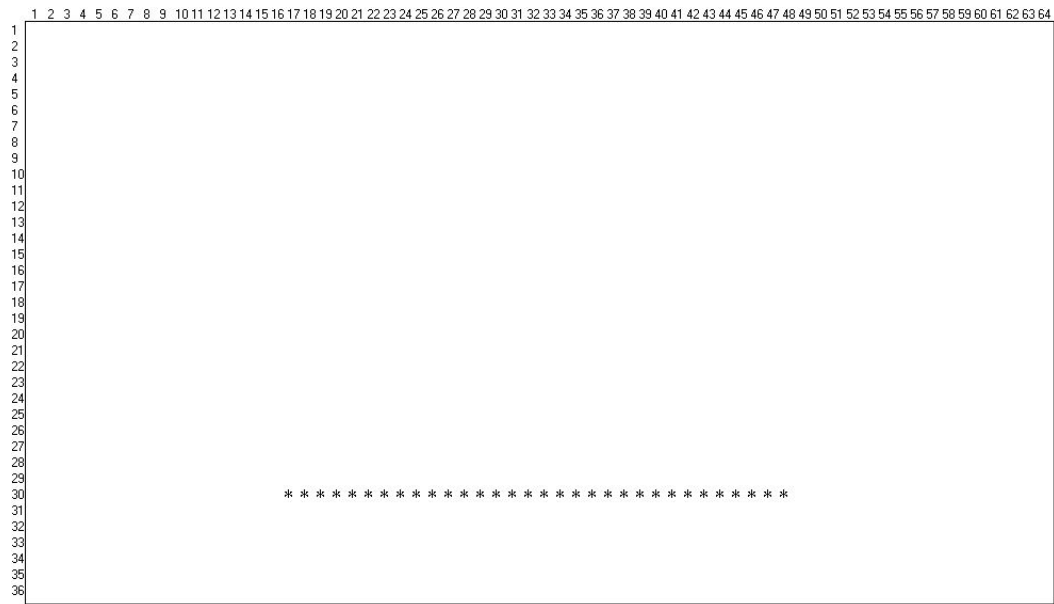


# 2 horizon

Iteration	114
Present Peak	(30, 56)

Present Linking Direction : →

### 3. The third extracted horizon.



# 3 horizon

Iteration	147
Present Peak	(30, 48)

Present Linking Direction : →



### 4. The fourth extracted horizon.

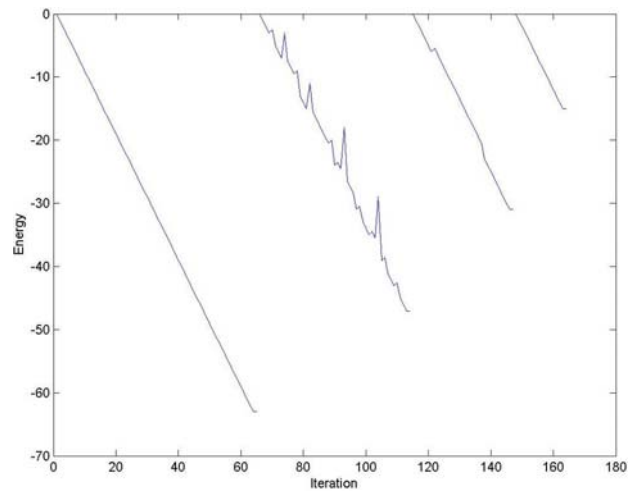


# 4 horizon

Iteration	164
Present Peak	(28, 40)

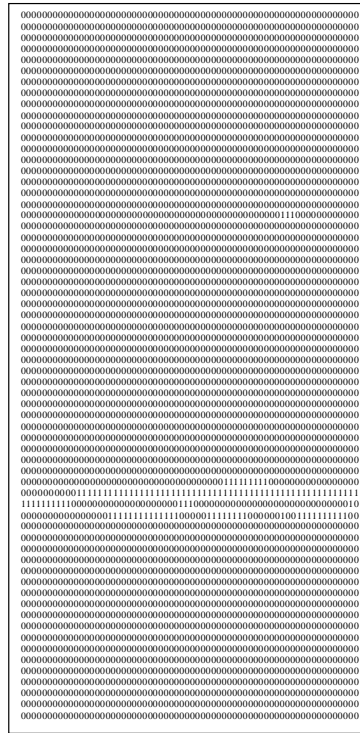
Present Linking Direction : →

Energy curve:

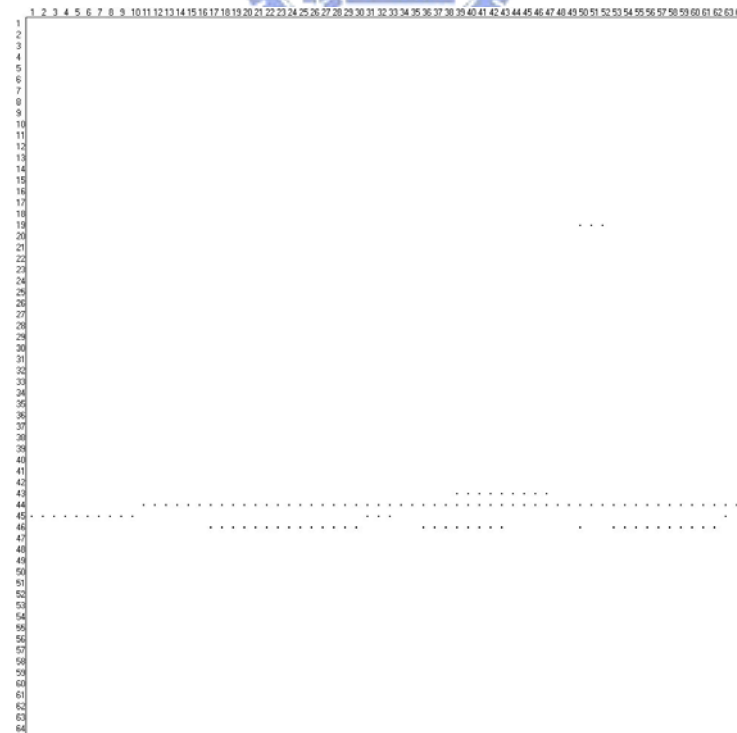


## Experiment 9.

The real seismic peak data is shown in Fig. 3.25(a), we can show the peaks as solid dots, as Fig. 3.25(b). The size of the input data is  $64 \times 64$ . We set  $a_1 = 1$ ,  $a_2 = a_3 = 5$ ,  $a_4 = 1$ .



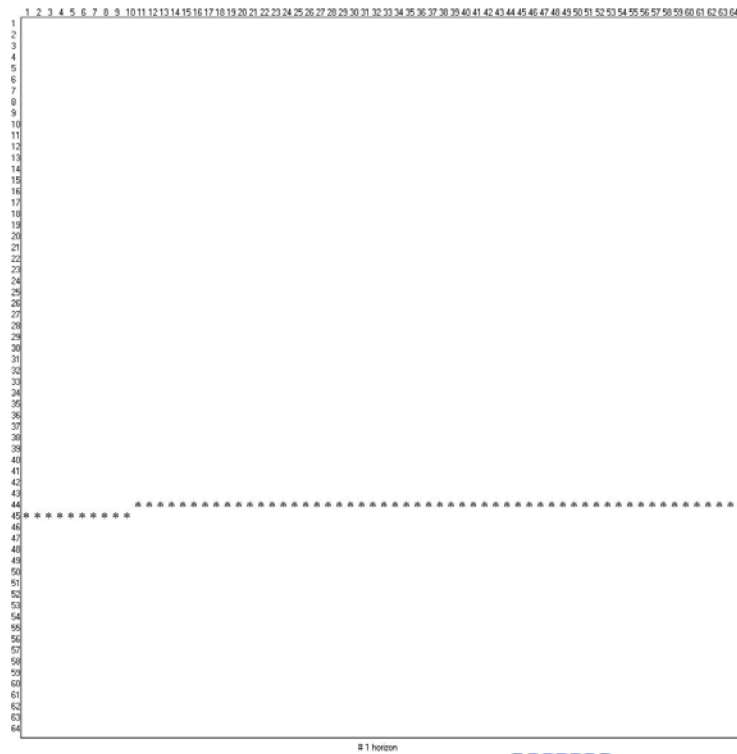
(a)



(b)

Fig. 3.25 (a) The real seismic peak data, (b) The peaks in (a) are shown as solid dots.

1. The first extracted horizon.

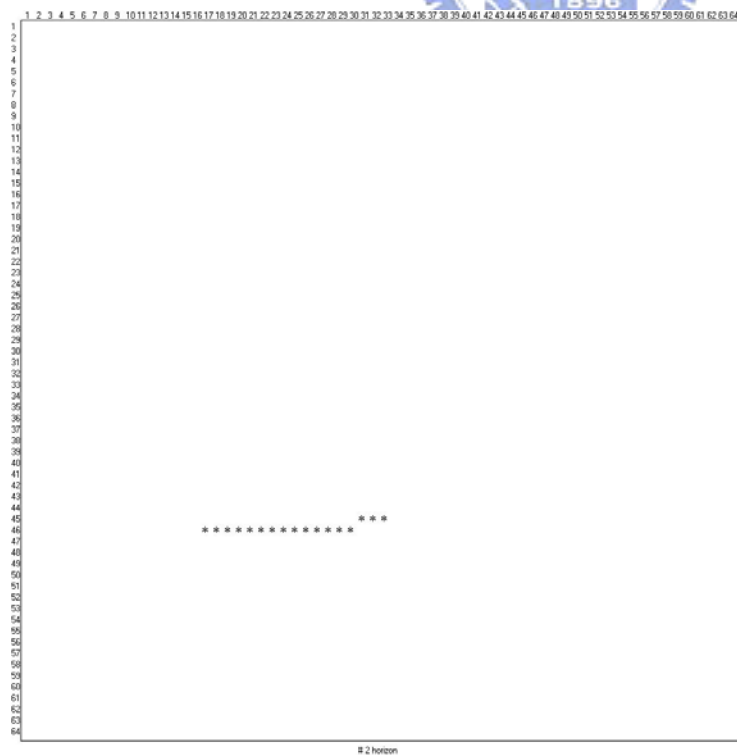


Iteration	65
Present Peak	(44, 63)

Present Linking Direction : →



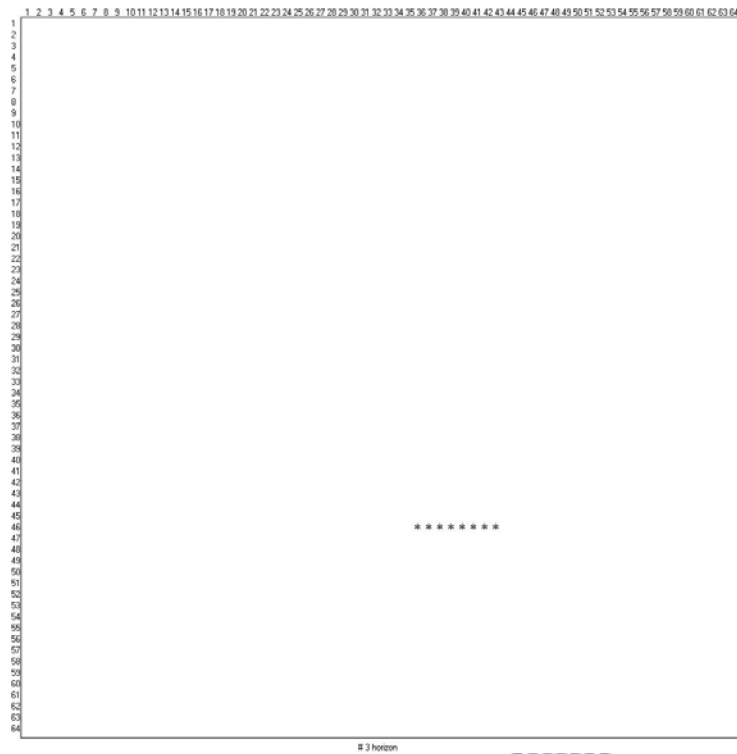
2. The second extracted horizon.



Iteration	83
Present Peak	(45, 33)

Present Linking Direction : →

3. The third extracted horizon.

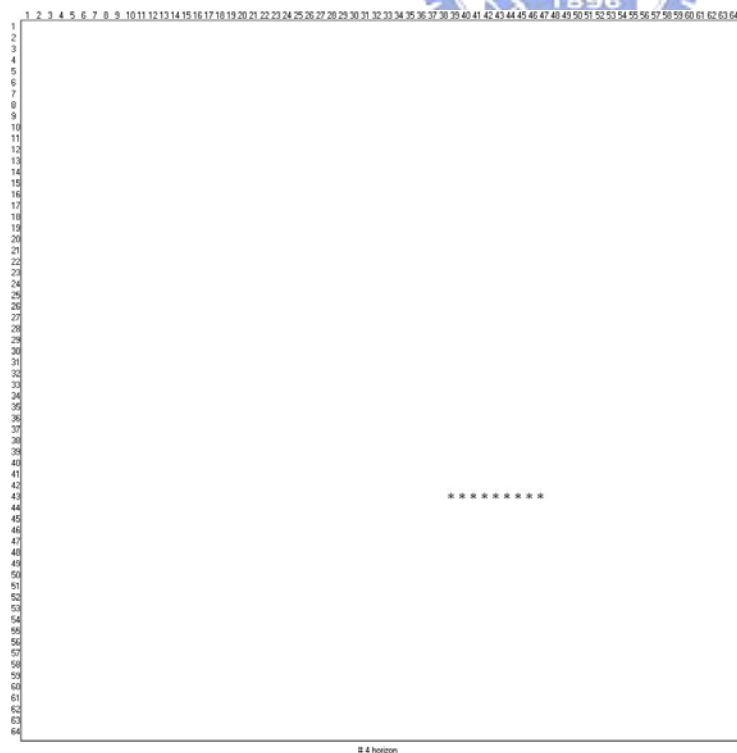


Iteration	92
Present Peak	(46, 43)

Present Linking Direction : →



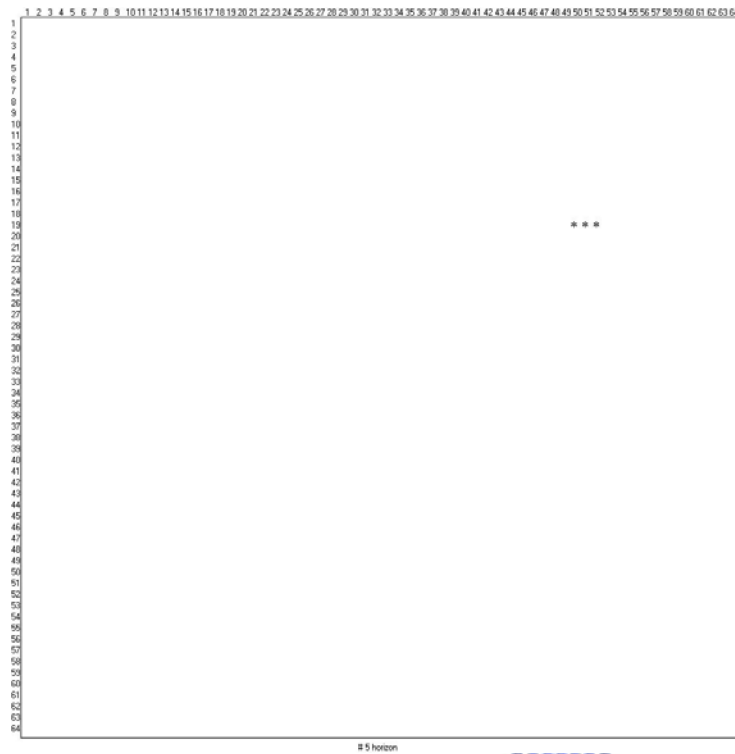
4. The fourth extracted horizon.



Iteration	102
Present Peak	(43, 47)

Present Linking Direction : →

5. The fifth extracted horizon.

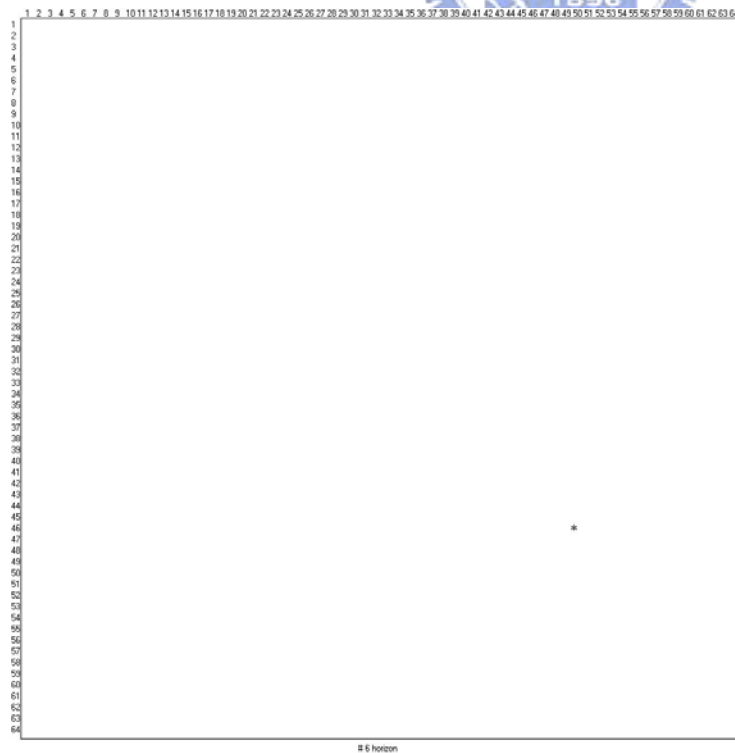


Iteration	106
Present Peak	(19, 52)

Present Linking Direction : →



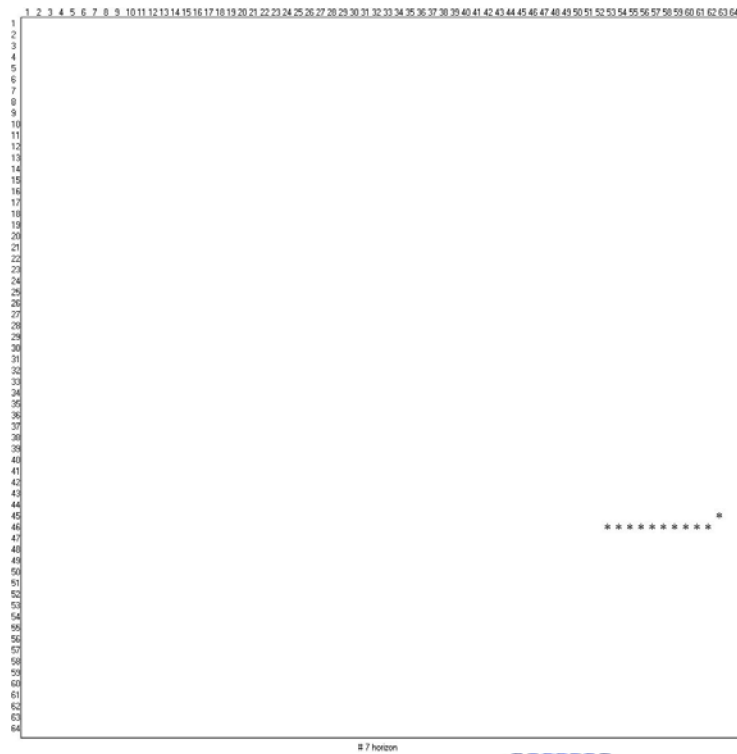
6. The sixth extracted horizon.



Iteration	108
Present Peak	(19, 52)

Present Linking Direction : ↗

## 7. The seventh extracted horizon.

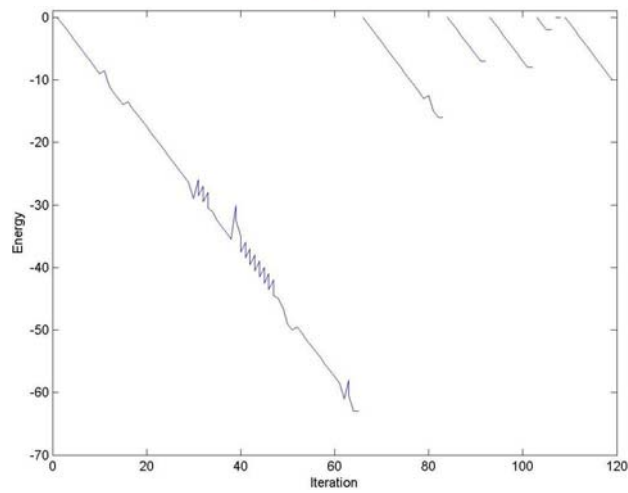


Iteration	120
Present Peak	(45, 63)

Present Linking Direction : ↗



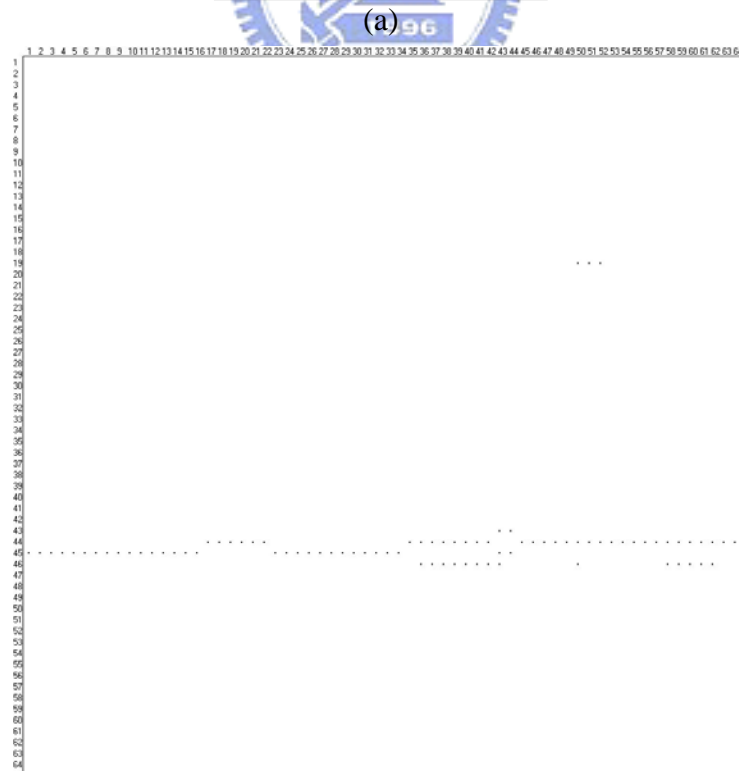
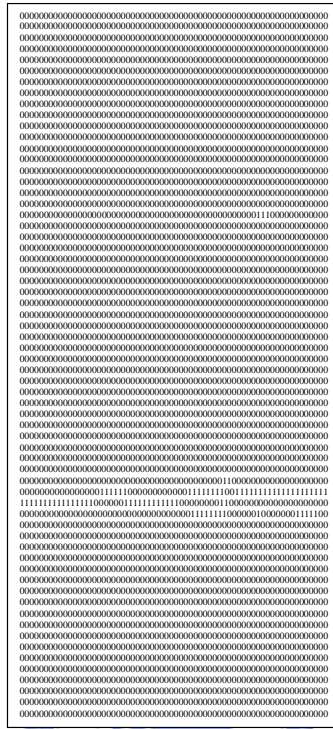
Energy curve:





## Experiment 10.

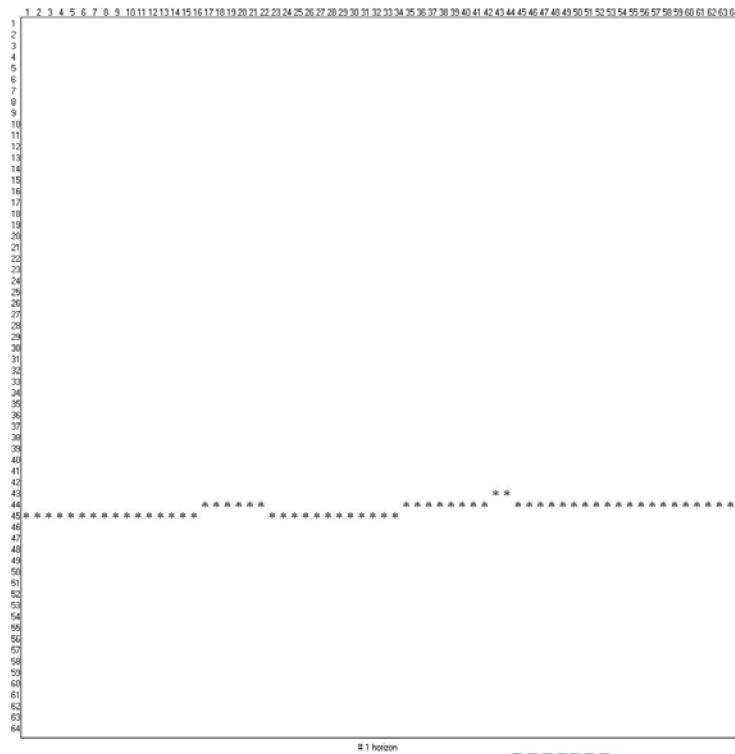
The real seismic peak data is shown in Fig. 3.26(a), we can show the peaks as solid dots, as Fig. 3.26(b) shows. The size of the input data is  $64 \times 64$ . We set  $a_1 = 1$ ,  $a_2 = a_3 = 5$ ,  $a_4 = 1$ .



(b)

Fig. 3.26 (a) The real seismic peak data; (b) The peaks in (a) are shown as solid dots.

1. The first extracted horizon.

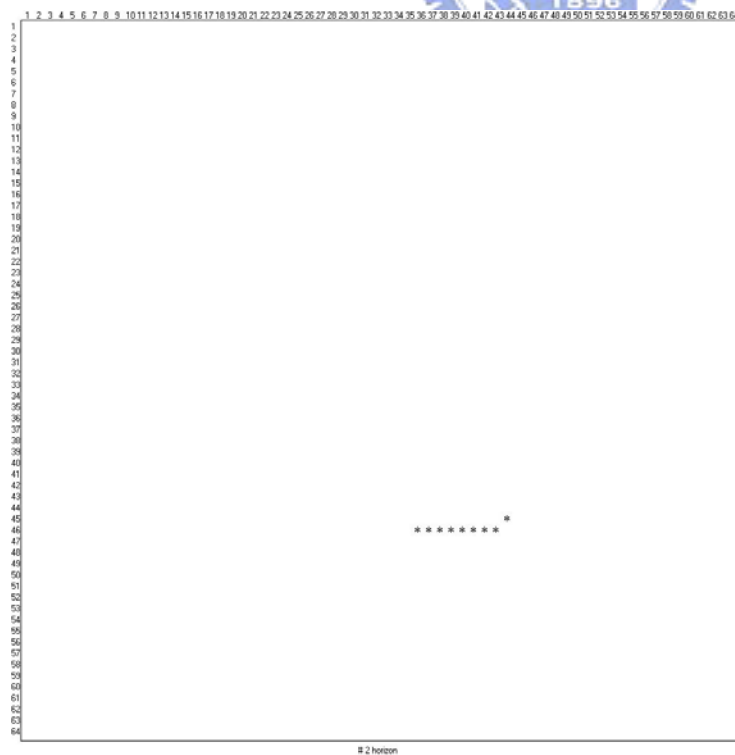


Iteration	65
Present Peak	(44, 64)

Present Linking Direction : →



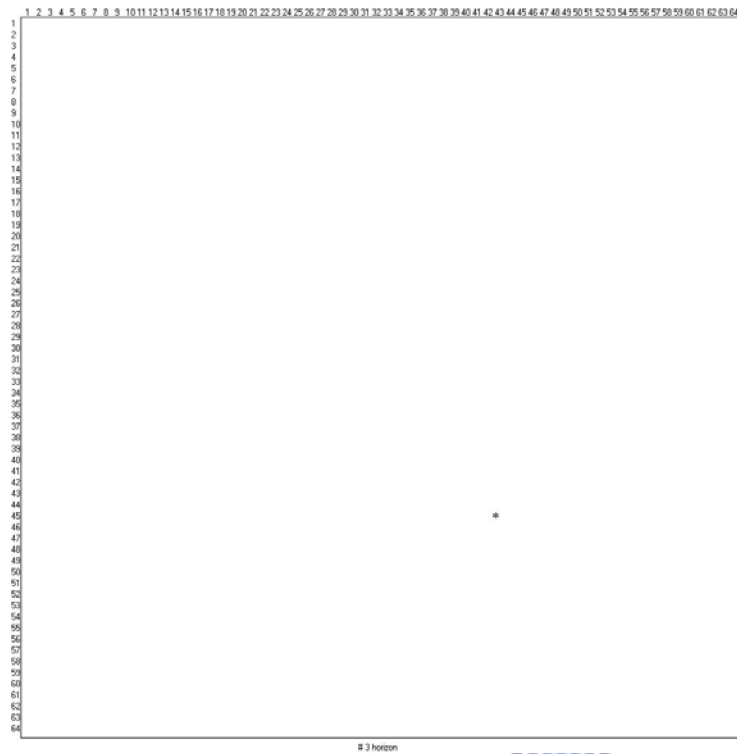
2. The second extracted horizon.



Iteration	75
Present Peak	(46, 43)

Present Linking Direction : →

3. The third extracted horizon.

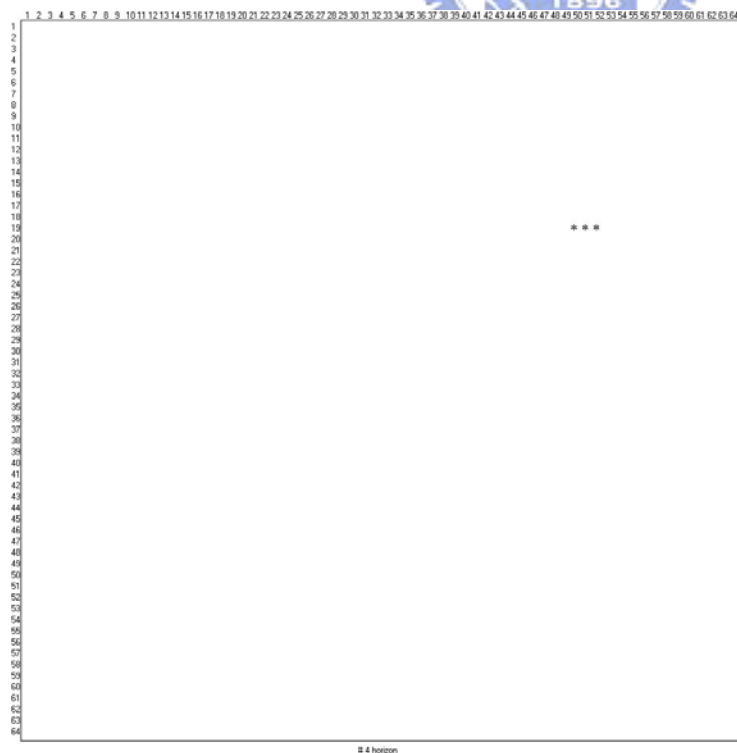


Iteration	77
Present Peak	(46, 43)

Present Linking Direction : ↗



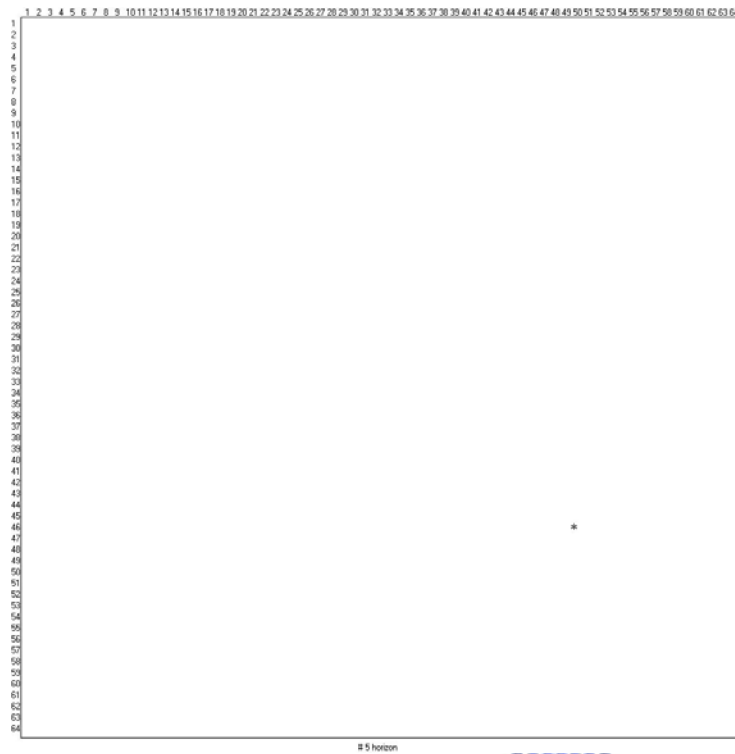
4. The fourth extracted horizon.



Iteration	81
Present Peak	(19, 52)

Present Linking Direction : →

5. The fifth extracted horizon.

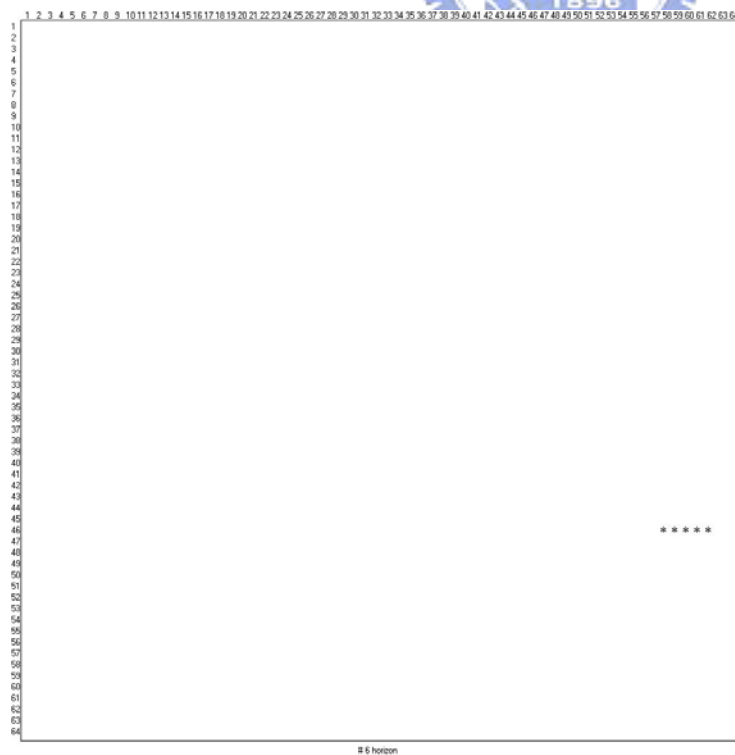


Iteration	83
Present Peak	(19, 52)

Present Linking Direction : ↗



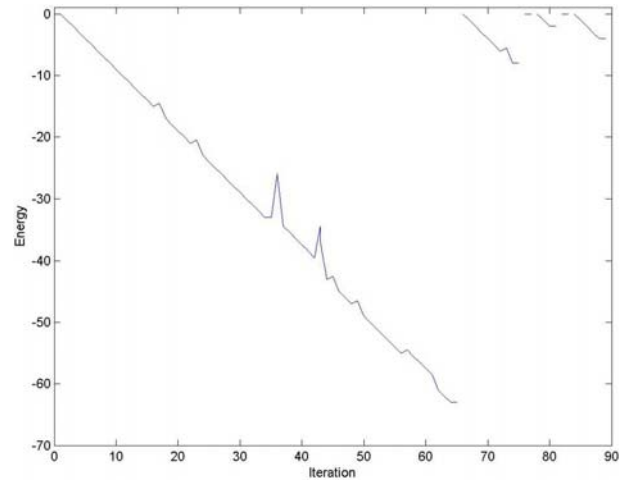
6. The sixth extracted horizon.



Iteration	89
Present Peak	(46, 62)

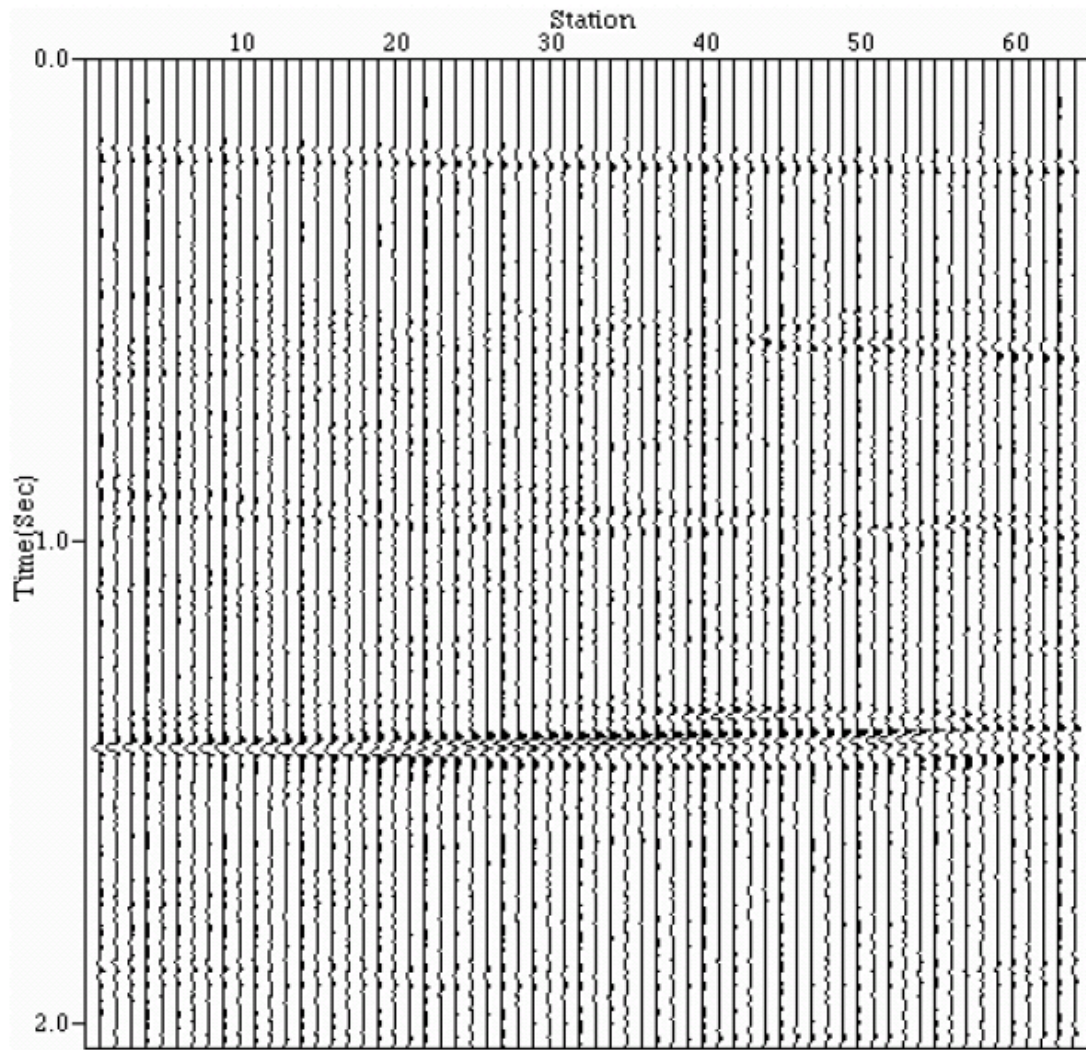
Present Linking Direction : →

Energy curve:



### Experiment 11.

The real seismic data from the Mississippi Canyon is shown in Fig. 3.27(a). After preprocessing, we can get the peak data shown in Fig. 3.27(b). We can show the peaks as solid dots, as Fig. 3.27(c). The size of the input data is  $128 \times 64$ . We set  $a_1 = 1$ ,  $a_2 = a_3 = 5$ ,  $a_4 = 1$ .



(a)



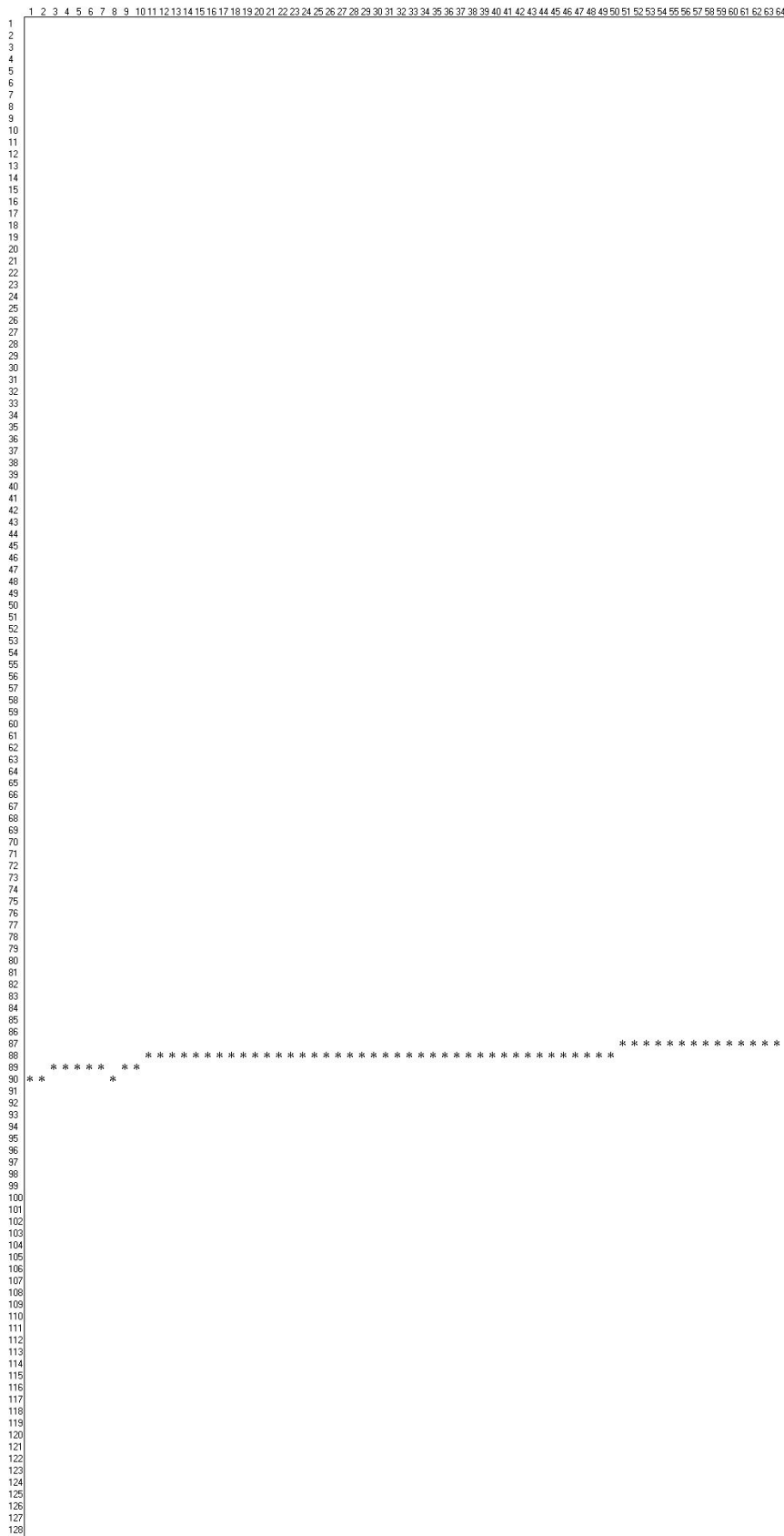


(c)

Fig. 3.27 (a) The seismogram at Mississippi Canyon; (b) The peak data of (a); (c) The peaks in (b) are shown as solid dots.



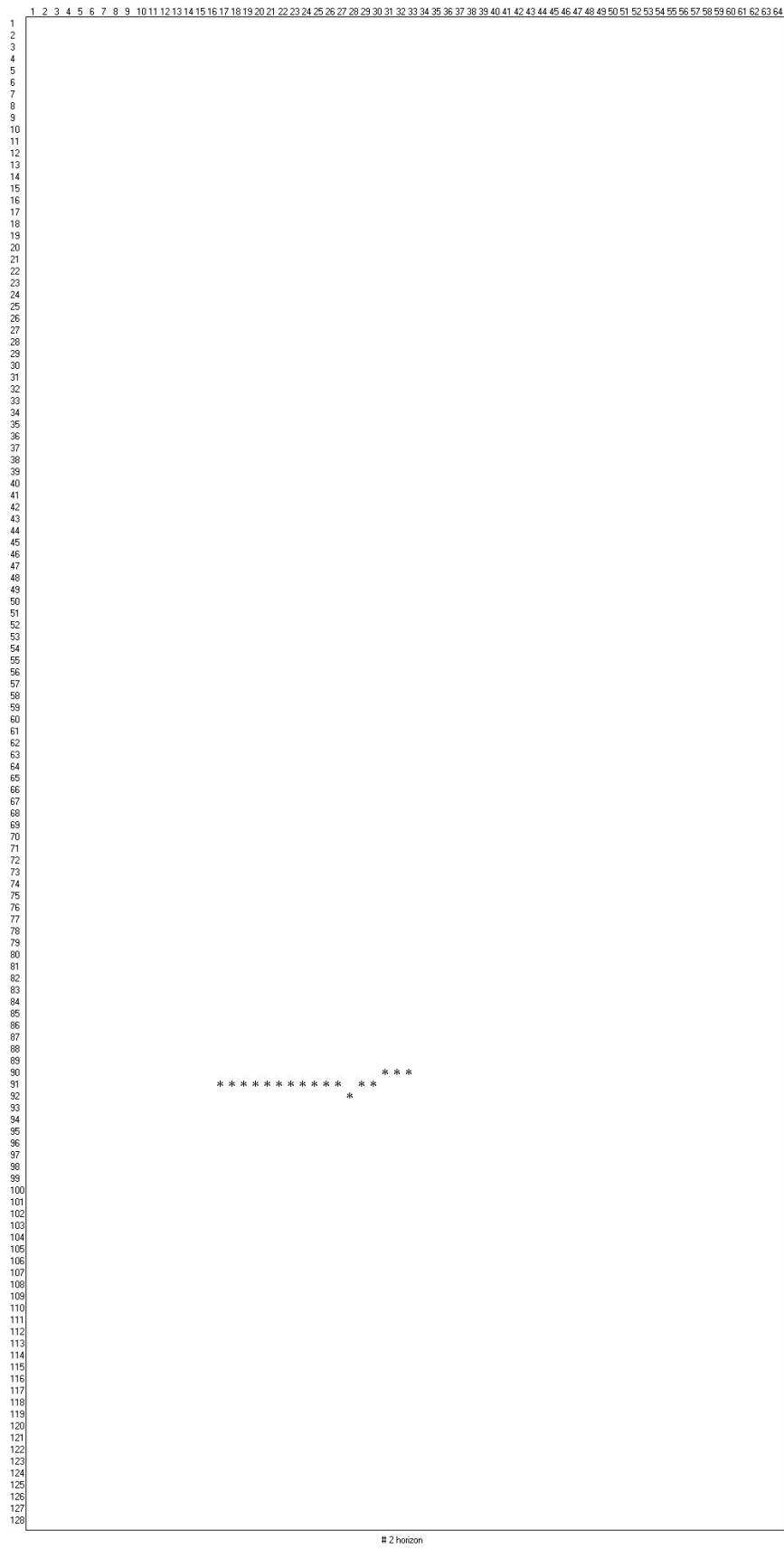
# 1. The first extracted horizon.



Iteration	65
Present Peak	(87, 64)

Present Linking Direction : →

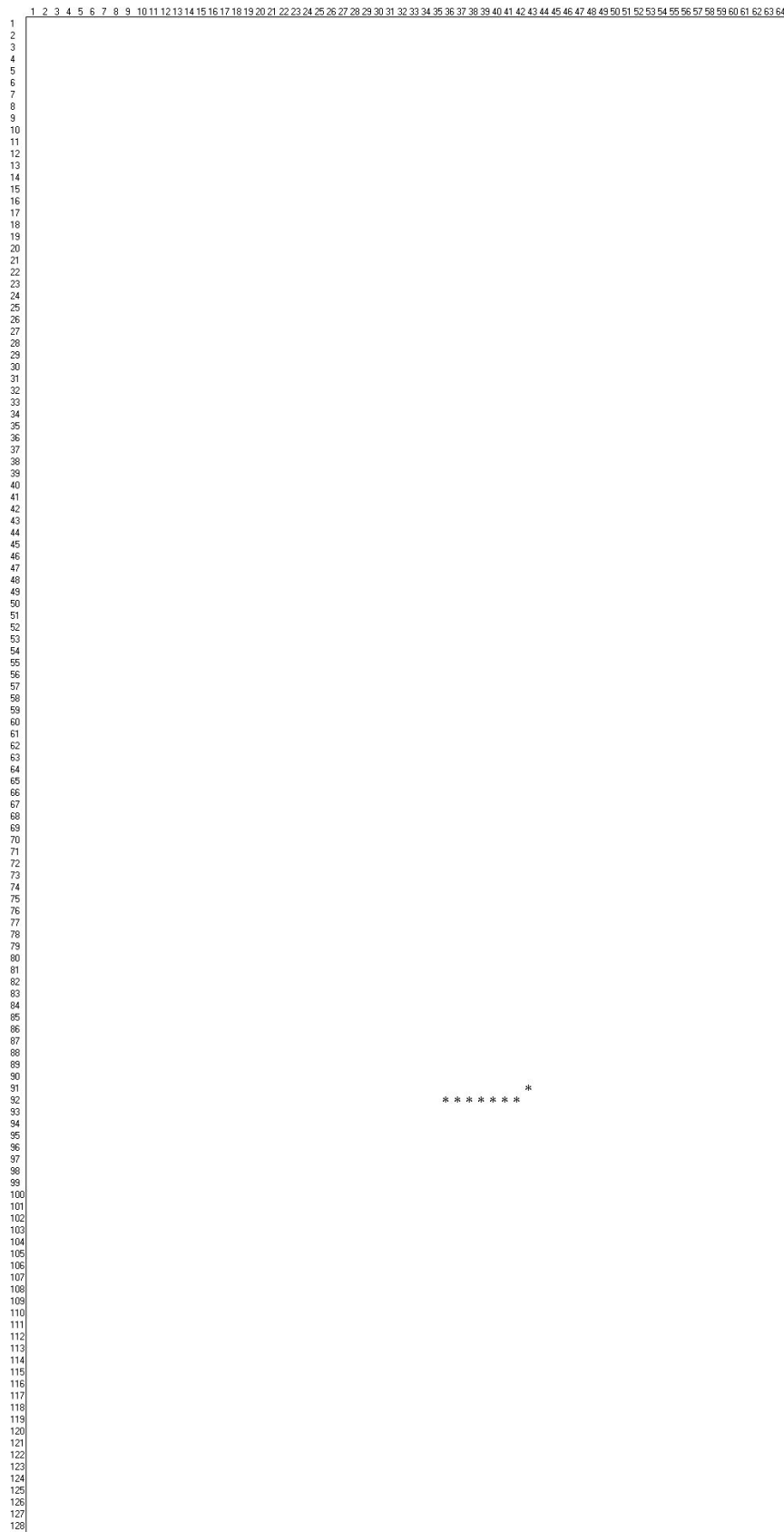
## 2. The second extracted horizon.



Iteration	83
Present Peak	(90, 33)


Present Linking Direction : →

### 3. The third extracted horizon.

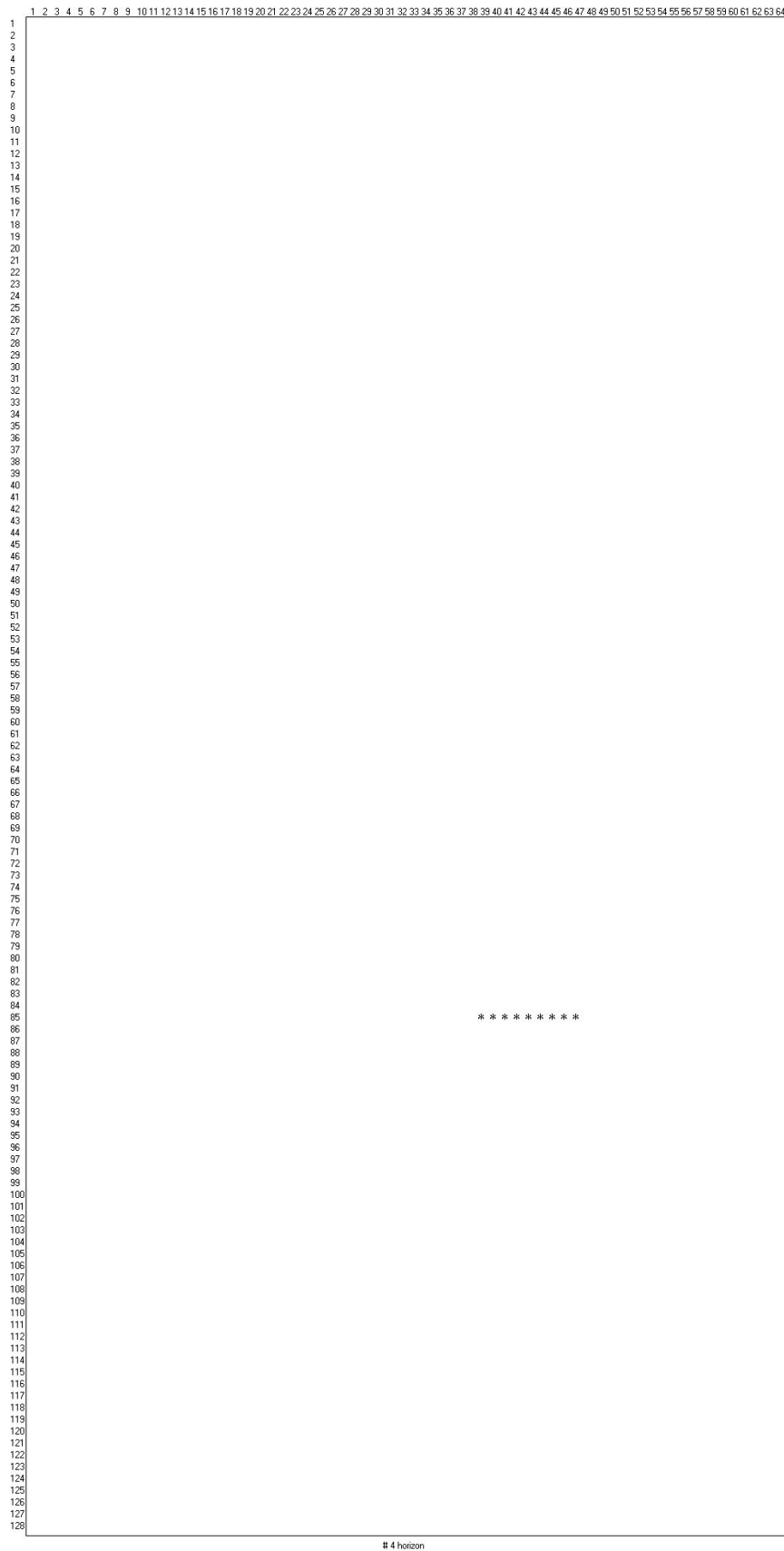


# 3 horizon

Iteration	92
Present Peak	(91, 43)

Present Linking Direction : 

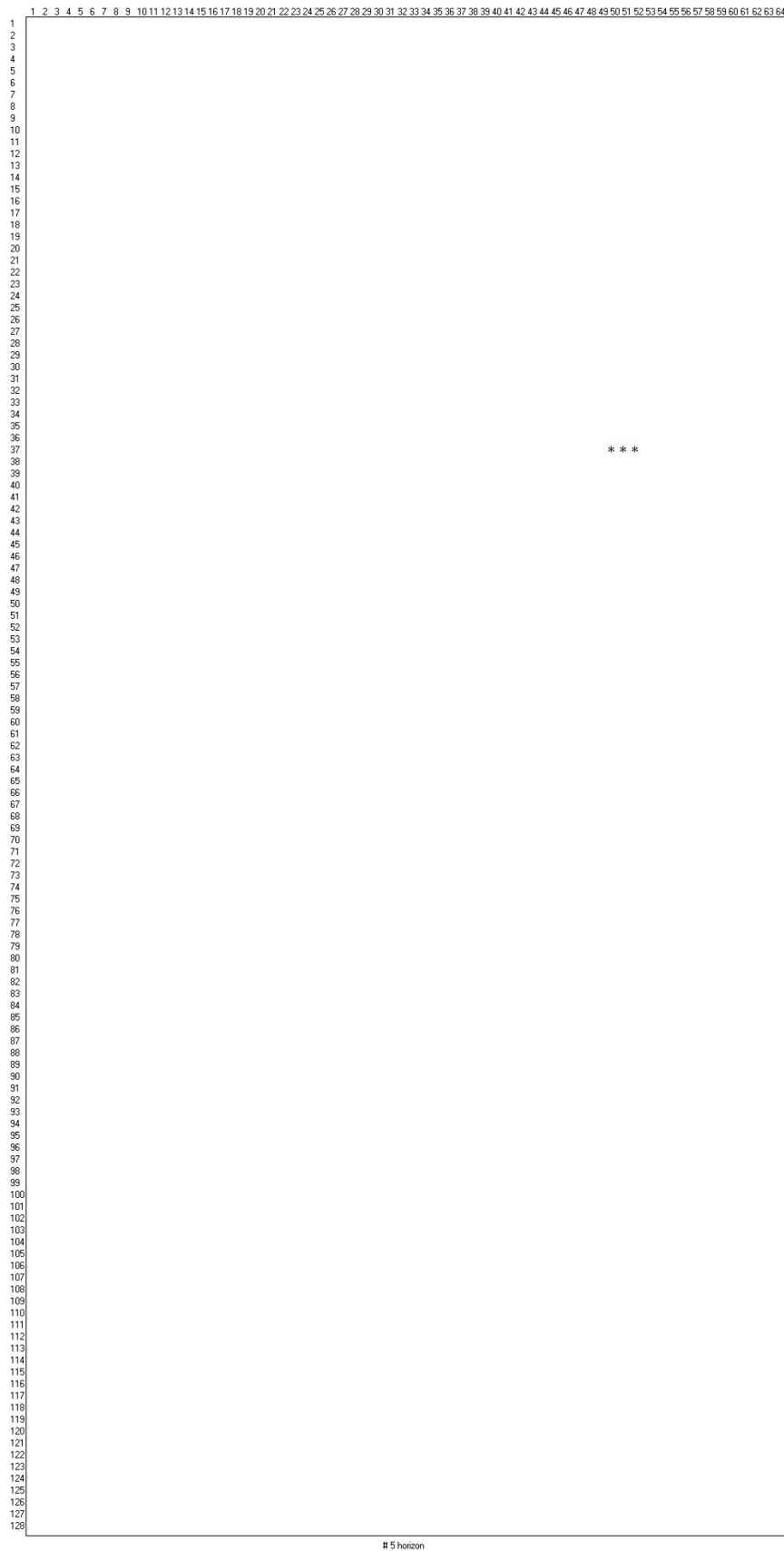
#### 4. The fourth extracted horizon.



Iteration	102
Present Peak	(85, 47)

Present Linking Direction : →

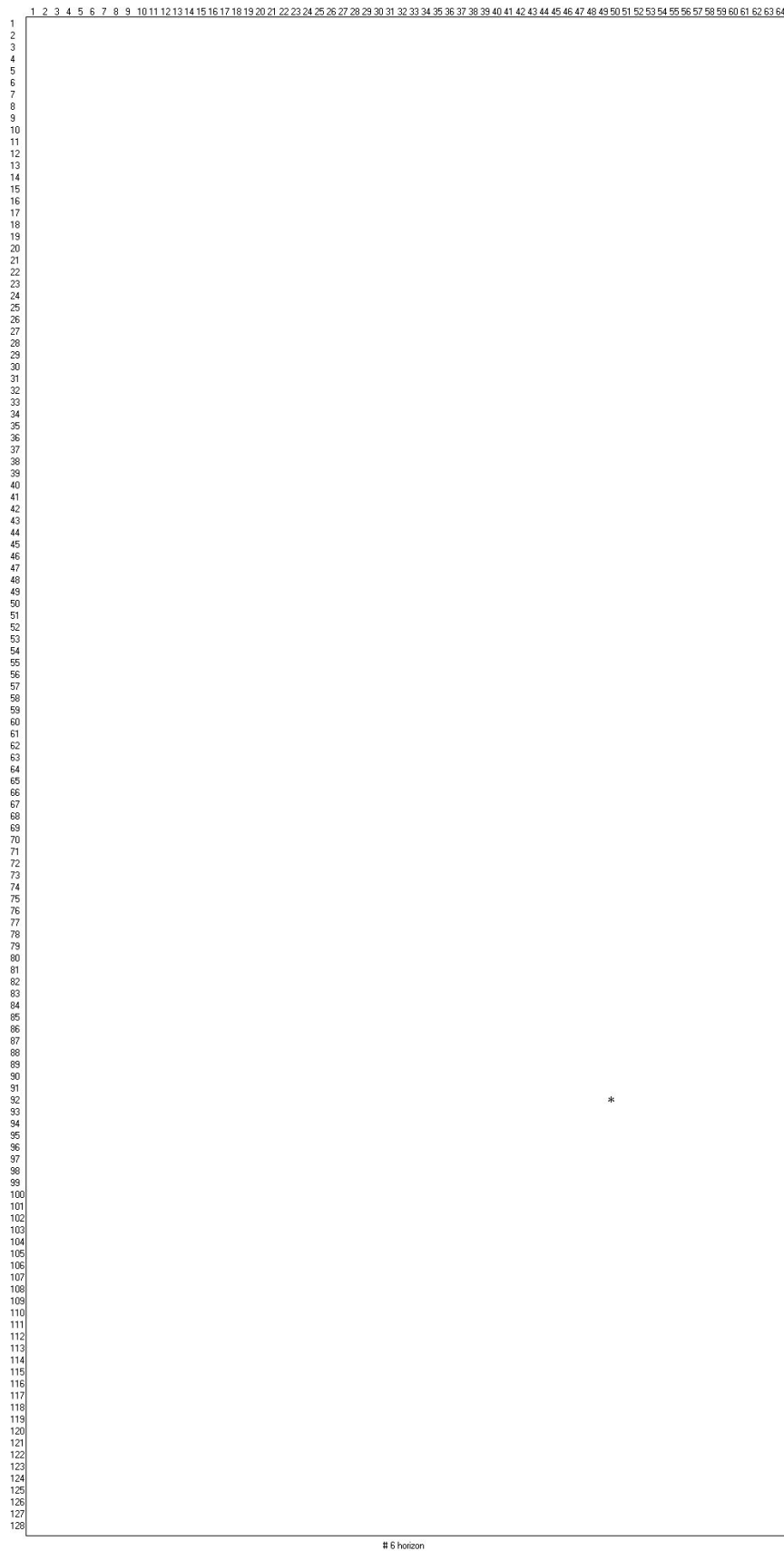
## 5. The fifth extracted horizon.




Iteration	106
Present Peak	(37, 52)

Present Linking Direction : →

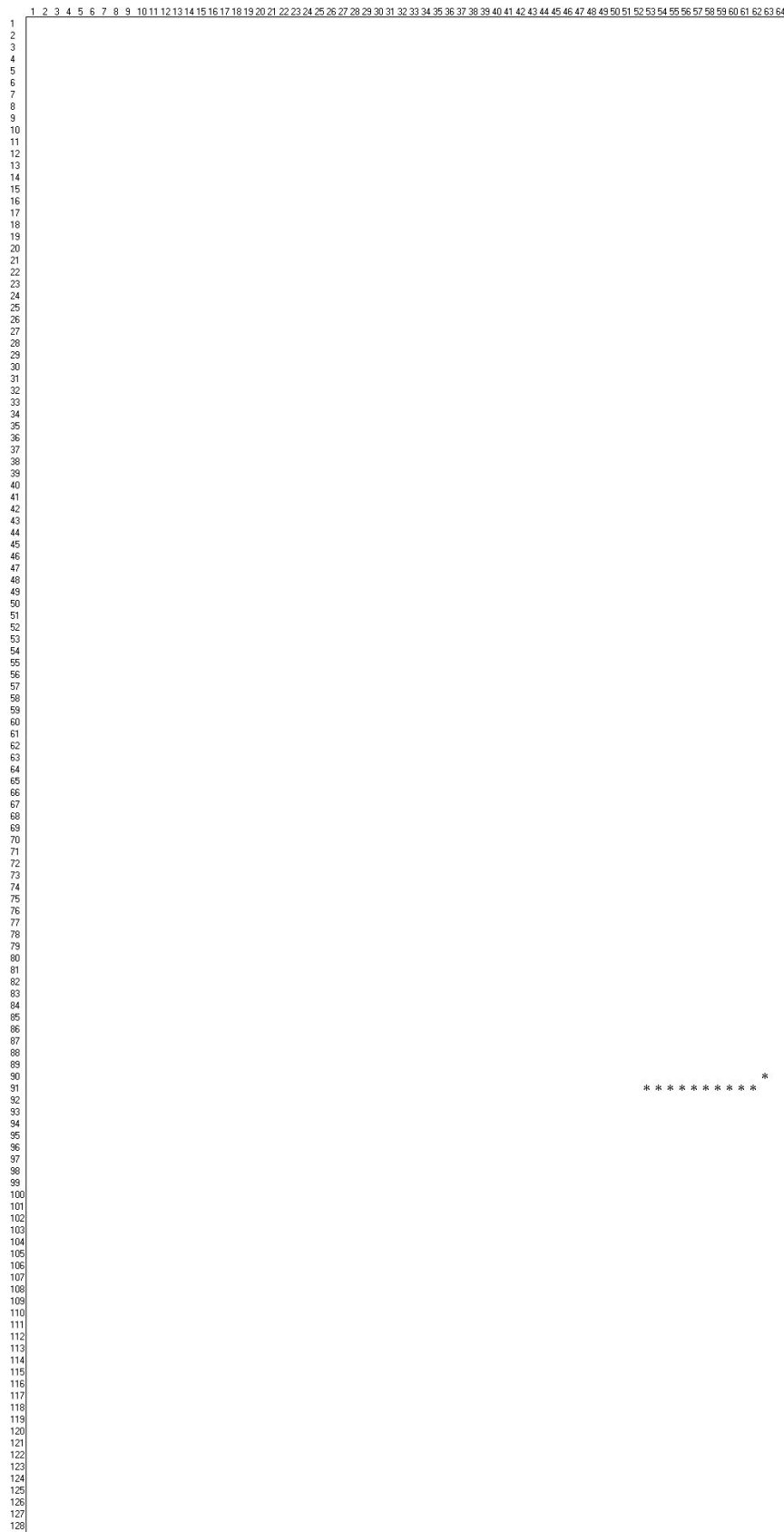
## 6. The sixth extracted horizon.



Iteration	108
Present Peak	(37, 52)

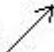
Present Linking Direction : 

## 7. The seventh extracted horizon.

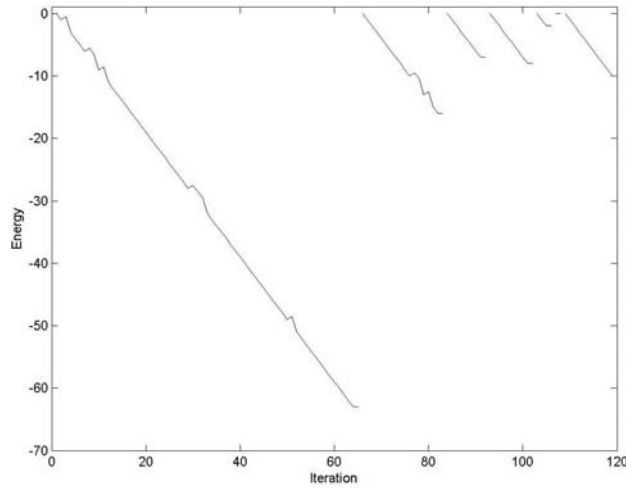


# 7 horizon

Iteration	120
Present Peak	(90, 63)

Present Linking Direction : 

Energy curve:



### 3.7 Conclusions

We have applied cellular neural networks to seismic horizon picking. The first constraint is a local constraint in a  $3 \times 3$  window. It determines the situations of peaks on the same horizon. The second and third constraints are local constraints in a  $7 \times 7$  window. They determine the situations of peaks not on the same horizon and make us get one horizon each time. The fourth constraint is a local constraint in a  $3 \times 3$  window. It links the broken horizons, where the length of each broken part is 2. Here we use less local constraints than Hopfield neural net for seismic horizon linking [8]. This is because the effect of the first constraint is equivalent to the effect of all local constraints used in [8]. All four constraints are local constraints, so it is suited for CNN. We can set up more other constraints to enhance the robustness of the linking algorithm, and then the algorithm can satisfy more kinds of peak data. In addition, we add the consideration of linking direction to the linking algorithm. According to the direction of peak linking, we modify the constraints of the second and third distribution situations for some peaks. This approach can make the linked horizon more smooth and flat.



## References

- [1] N. Keskes and Ph. Zaccagnino, "Image analysis techniques for seismic data," *Society of Exploration Geophysicists 52nd Ann. Int. Meet. Expanded Tech. Prog. Abstr.*, Dallas, TX, 1982, pp.220-221.
- [2] N. Keskes, Ph. Zaccagnino, and P. Mermey, "Automatic extraction of 3-D seismic horizons," *Society of Exploration Geophysicists 53rd Ann. Int. Meet. Expanded Tech. Prog. Abstr.*, Las Vegas, NV, 1983, pp.557-559.
- [3] G. Sibille, N. Keskes, J. M. Fontaine, and J. L. Lequeux, "Enhancement of the perception of seismic facies and sequences by image analysis techniques," *Society of Exploration Geophysicists 54th Ann. Int. Meet. Expanded Tech. Prog. Abstr.*, Atlanta, GA, 1984, pp.447-480.
- [4] S. Y. Lu, "A string-to-string correlation algorithm for image skeletonization," *Proc. Int. Joint Conf. Pattern Recognition*, Munich, Germany, October 1982, pp.178-180.
- [5] Yao-Chou Cheng and Shin-Yee Lu, "The binary consistency checking scheme and its applications to seismic horizon detection," *IEEE Trans. Pattern Anal. Mach. Intell.* 11, April 1989, pp.439-447.
- [6] K. Y. Huang, "Branch and bound search for automatic linking process of seismic horizons," *Pattern Recognition*, Vol. 23, No. 6, 1990, pp.657-667.
- [7] M. B. Dobrin, *Introduction to Geophysical Prospecting*. McGraw-Hill, 1976.
- [8] Kou-Yuan Huang, "Neural network for seismic horizon picking," *IEEE World Congress on Computational Intelligence*, The 1998 IEEE International Joint Conference on. Volume: 3, 1998.